

Abstract

The DNA Mismatch Repair Pathway Affects ATR Activation Upon Temozolomide Treatment in *MGMT*-Promoter Methylated Glioblastoma Multiforme

Sachita Ganesa

2021

In many solid tumors, methylation status of the O⁶-methylguanine methyltransferase (*MGMT*) gene promoter is a prognostic biomarker for treatment with the alkylator, temozolomide (TMZ). In the absence of promoter methylation, the *MGMT* enzyme removes O⁶-methylguanine (O⁶-meG) lesions. However, in the setting of *MGMT*-promoter methylation (*MGMT*-), the O⁶-meG lesion activates the mismatch repair (MMR) pathway which functions to remove the damage. Our group previously reported that *MGMT*-promoter methylation affects activation of the ataxia telangiectasia and RAD3 related protein (ATR) in response to TMZ treatment. Whether or not MMR proteins are involved in ATR activation in the context of *MGMT*-promoter methylation upon alkylation damage remains poorly understood. To investigate the function of mismatch repair in ATR activation, I created isogenic cell lines with knockdowns of the individual mismatch repair proteins MSH2, MSH6, MSH3, MLH1, and PMS2 in both the *MGMT*- and *MGMT*+ backgrounds. Here, I demonstrate that MSH2, MSH6, MLH1 and PMS2 mismatch repair proteins, specifically, are involved in the ATR-CHK1 axis, whereas MSH3 is likely not. This study elucidates a potential mechanistic understanding of how the MMR system is involved in ATR activation by TMZ in glioblastoma cells, which can ultimately be exploited for therapeutic gain in a wide-variety of MMR-mutated cancers.

The DNA Mismatch Repair Pathway Affects ATR Activation Upon Temozolomide
Treatment in *MGMT*-Promoter Methylated Glioblastoma Multiforme

A Dissertation

Presented to the Faculty of the Graduate School

Of

Yale University

In Candidacy for the Degree of

Doctor of Philosophy

By

Sachita Ganesa

Dissertation Director: Ranjit S. Bindra, M.D., Ph.D.

December 2021

© 2021 by Sachita Ganesa

All rights reserved.

Acknowledgements

I would like to acknowledge and offer my deepest gratitude to all who have supported me during my dissertation research and time at Yale. First, I would like to thank my advisor, Dr. Ranjit Bindra, for his guidance and support over the past few years. Next, I would like to thank my committee members, Drs. Yong Xiong, Sandy Chang, and Joerg Bewersdorf for their feedback. Thanks to Dr. Ranjini Sundaram for helping with all the laborious *in vivo* experiments. I would also like to thank all the members of the Bindra lab over the past years for the endless entertainment and friendship. I express my sincerest appreciation for my postdoc mentor and close friend, Dr. Amrita Sule, who believed in me when I did not, challenged me intellectually, and pushed me to excel every day.

On a more personal note, I thank my அம்மா and அப்பா for everything. There are truly no words to express how indebted I am to them for their love and support, their encouragement and motivation, and most importantly the food and laundry. I would be remiss if I did not thank my brother, Chirag, for being not only my biggest critic but also my biggest advocate, and for knowing my own worth more than myself. I also thank my grandparents: my தாத்தா, who taught me to be a dreamer, and both my பட்டினி, who have shown me how powerful and resilient women are. Finally, I am eternally grateful for my co-captain, Mohin, for showing me more love and happiness than I knew was possible.

This thesis is dedicated to my பட்டினி, Lalitha Balasubramanian.

Table of Contents

Acknowledgements.....	iii
Table of Contents.....	iv
List of Figures.....	vii
List of Tables.....	ix
Common Abbreviations.....	ix
Copyright Acknowledgement.....	x
1. Chapter 1: Introduction.....	1
1.1. The role and function of O ⁶ -methylguanine methyltransferase.....	1
1.2. Alkylating agents and temozolomide.....	6
1.3. DNA damage response pathways.....	10
1.3.1. Mismatch repair pathway.....	12
1.4. Ataxia telangiectasia and RAD3 related protein in DNA repair.....	16
1.5. Significance and Innovation.....	20
2. Chapter 2: Materials and Methods.....	21
2.1. Cell culture.....	21
2.2. Mismatch repair knockdown cell line creation.....	21
2.3. Drug compounds.....	22
2.4. Western blot and immunoprecipitation.....	22
2.5. Short-term cell viability and drug synergy assays.....	24
2.6. Clonogenic survival assay.....	25
2.7. Immunofluorescence.....	25

2.8. Flow Cytometry	25
2.9. <i>In vivo</i> studies with temozolomide and ATRi.....	26
2.10. Statistical analysis.....	26
3. Chapter 3: LN229 MGMT- cells show differential ATR activation than MGMT+	27
3.1. Introduction.....	27
3.2. Results.....	29
3.1.1. MGMT- cells are more sensitive to TMZ than MGMT+ cells	29
3.1.2. TMZ and ATR inhibitor synergize in MGMT- cells	32
3.3. Discussion.....	37
4. Chapter 4: Creation of shRNA mismatch repair knockdown cell lines	40
4.1. Introduction.....	40
4.2. Results.....	44
4.2.1. Plasmid preparation and restriction digest	44
4.2.2. Viral production and transfection.....	46
4.2.3. Screening of monoclonal shRNA knockdown cell line clones	49
4.3. Discussion.....	54
5. Chapter 5: Response of mismatch repair knockdown cells to temozolomide and ATR inhibitor.....	57
5.1. Introduction.....	57
5.2. Results.....	60
5.2.1. shMMR cells response to TMZ and ATR inhibitor as monotherapy.....	60
5.2.2. Functional MMR is required for synergy between TMZ and ATR inhibitors.....	63
5.3. Discussion.....	74

6. Chapter 6: Mechanism of DNA repair in mismatch repair knockdown cell lines	78
6.1. Introduction.....	78
6.2. Results.....	82
6.2.1. shMMR cells exhibit dysregulated cell cycling.....	82
6.2.2. shMMR cells exhibit increased DNA replication stress	85
6.2.3. <i>In vivo</i> , MMR is required for synergy between TMZ and ATR inhibitors	88
6.3. Discussion.....	90
7. Chapter 7: Discussion	93
7.1. Conclusions.....	93
7.2. Further exploration of mechanism.....	95
7.3. Other ATR inhibitors, alkylators, and combination therapies	98
7.4. Future directions.....	100
Chapter 8. References	101

List of Figures

Chapter 1

Figure 1.1. Map of the 5' region of the <i>MGMT</i> promoter	2
Figure 1.2. Methylation status of the CpG islands within the <i>MGMT</i> promoter in various cell lines	2
Figure 1.3. Schematic of bisulfite conversion for methylation specific polymerase chain reaction.....	3
Figure 1.4. Temozolomide metabolism.....	9
Figure 1.5. Schematic of eukaryotic mismatch repair	13
Figure 1.6. Temozolomide-induced mismatch repair futile cycling model.....	15
Figure 1.7. Upstream activation pathway of ATR.....	17
Figure 1.8. Structure of ATR inhibitors AZ-20, BAY-1895344, and VX-970.....	18
Figure 1.9. ATR signaling is specific to MGMT- cells and not MGMT+ cells	19

Chapter 3

Figure 3.1. Western blot of LN229 cell line models showing MGMT status	29
Figure 3.2. Short-term cell viability assay with temozolomide in MGMT- and MGMT+ cells.....	30
Figure 3.3. Clonogenic survival assay with temozolomide in MGMT- and MGMT+ cells.....	31
Figure 3.4. Synergy plots of MGMT- and MGMT+ cells with temozolomide and ATR inhibitors	33
Figure 3.5. Attempts at pCHK1 western blot	35
Figure 3.6. Successful CHK1 immunoprecipitation showing earlier ATR activation in MGMT- cells with temozolomide treatment	36

Chapter 4

Figure 4.1. pGIPZ lentiviral vector purchased from Horizon Dharmacon	43
Figure 4.2. Detailed vector map of pGIPZ lentiviral vector purchased from Horizon Dharmacon.....	43
Figure 4.3. Successful restriction digest of shMMR plasmids with SacII after midiprep	45
Figure 4.4. Schematic for lentiviral production with the Lipofectamine 3000 kit.....	47
Figure 4.5. Images of polyclonal populations of LN229 cells with shRNA knockdown of interest	48

Figure 4.6. MGMT+ shMSH2 clone screening through western blot	50
Figure 4.7. Western blot of shRNA mismatch repair cell line models	51
Figure 4.8. Western blot of stability of shMMR proteins and their heterodimeric partner(s)	53

Chapter 5

Figure 5.1. Short-term cell viability assay with temozolomide in MGMT- shMMR cells.....	61
Figure 5.2. Short-term cell viability assay with BAY-1895344 in MGMT- shMMR cells.....	62
Figure 5.3. Synergy plots of shMMR cells with temozolomide and BAY-1895344.....	64
Figure 5.4. Synergy plots of shMMR cells with temozolomide and AZ-20.....	66
Figure 5.5. Synergy plots of shMMR cells with temozolomide and CHK1 inhibitor AZD7762	68
Figure 5.6. Clonogenic survival assay of shMMR cells with temozolomide and BAY-1895344.....	69
Figure 5.7. Synergy plots of MGMT- and MGMT- shMSH2 cells with temozolomide and ATM inhibitor or DNA-PK inhibitor	71
Figure 5.8. U251 shMSH2 glioblastoma cells behave similarly to LN229 MGMT- shMSH2 cells	72
Figure 5.9. U251 shMSH2 cells are resistant to the combination of temozolomide and ATR inhibitor	73

Chapter 6

Figure 6.1. Fluorescence spectra viewer showing minimal overlap between GFP and PI	81
Figure 6.2. Flow cytometry plots of shMMR cells after treatment with temozolomide.....	83
Figure 6.3. Immunofluorescence of pRPA and γ H2AX over time in shMMR cells after temozolomide treatment	86
Figure 6.4. <i>In vivo</i> shMSH6 MGMT- tumors do not respond to treatment with temozolomide and ATR inhibitor VX-970	89

Chapter 7

Figure 7.1. Western blot of MGMT- and MGMT- shMSH2 cells upon temozolomide treatment.....	97
---	----

List of Tables

Table 1. Common abbreviations.	ix
Table 2. shRNA glycerol stock information.	22
Table 3. Antibodies and dilutions for western blot and immunoprecipitation.....	24
Table 4. Restriction digest components to confirm shMMR plasmid preparation.	45

Common Abbreviations

Table 1. Common abbreviations.

Abbreviation	Meaning
ATR	Ataxia telangiectasia and RAD3 related protein
CHK1	CHEK1 – Checkpoint kinase 1
MGMT	O ⁶ -methylguanine methyltransferase
MLH1	Human MutL homolog 1
MMR	Mismatch repair
MSH2	Human MutS homolog 2
MSH3	Human MutS homolog 3
MSH6	Human MutS homolog 6
O ⁶ -meG	O ⁶ -methylguanine
PMS2	Human PMS1 homolog 2
shMMR	Mismatch repair knockdown cells
TMZ	Temozolomide

Copyright Acknowledgement

Data from this dissertation are currently in preparation for submission as:

Ganesa, S., Sule, A.D., Sundaram, R.K., and Bindra, R.S. “The role of mismatch repair in ATR activation upon temozolomide treatment in *MGMT*-methylated glioblastoma.” *In preparation*, 2021.

1. Chapter 1: Introduction

1.1. The role and function of O⁶-methylguanine methyltransferase

The enzyme O⁶-methylguanine methyltransferase (MGMT) removes any alkyl damage at the O⁶ position of guanine. It does this by transferring the methyl group to itself at cysteine-145 through an S_N2 mechanism before degradation by the ubiquitin proteolytic pathway¹⁻⁵. MGMT removes the lesion in a stoichiometric reaction before being degraded as a suicide enzyme^{4,5}. In this way, MGMT does not act as a true enzyme since it is unable to regenerate after removing just one alkyl lesion. MGMT has also been referred to as alkylguanine alkyl transferase, or AGT, but I will refer to both the gene and enzyme as MGMT in this dissertation.

The *MGMT* gene can be found on chromosome 10 at cytogenetic band q26⁶. The expression of the MGMT enzyme is dependent upon its promoter methylation status. The promoter region of MGMT has been extensively studied, and there is an expansive region of CpG islands at the promoter region meaning many cytosine and guanine (CpG) repeats. The 5' region of the *MGMT* promoter consists of 97 CpG islands spanning the minimal promoter and enhancer region, which are important for maximal promoter activity⁷ (**Figure 1.1**). The methylation status of the enhancer element seems to be more crucial in determining the loss of expression of MGMT, based upon data from a luciferase reporter assay where different regions of the methylated promoter were tested across many cell lines; thus, most assays for determining MGMT expression focus on the enhancer region^{8,9} (**Figure 1.2**).

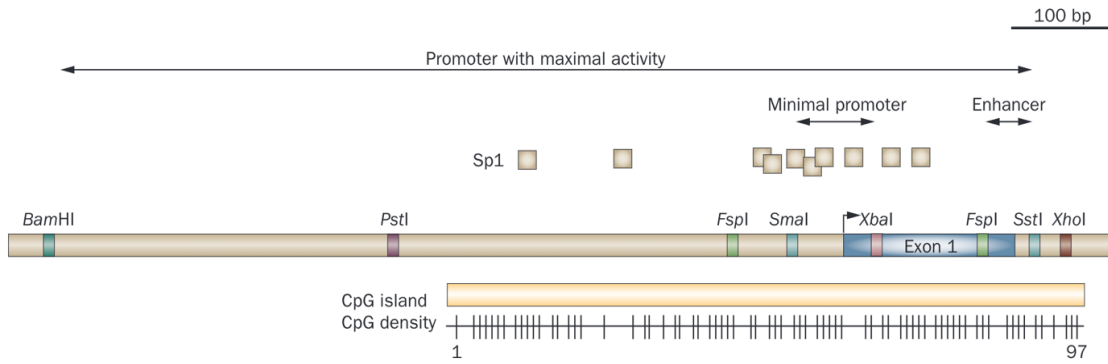


Figure 1.1. Map of the 5' region of the *MGMT* promoter. This map shows the minimal promoter and enhancer regions, as well as binding sites for transcription factors, exons, and restriction enzyme sites. Image from Weller et al., 2010.

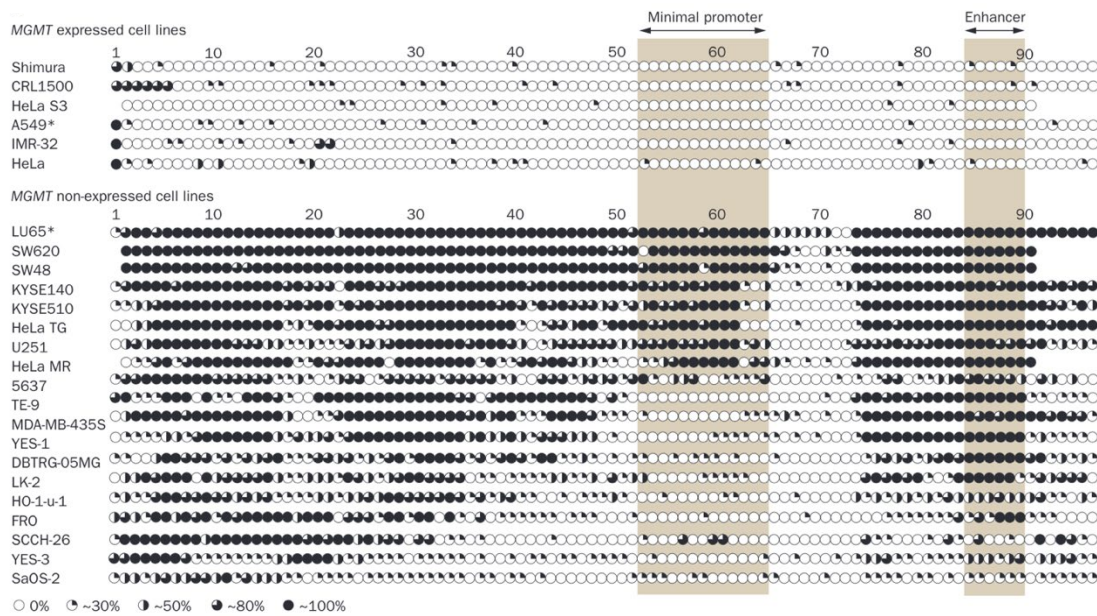


Figure 1.2. Methylation status of the CpG islands within the *MGMT* promoter in various cell lines. Methylation of the enhancer region seems most critical to determine *MGMT* expression. Image from Weller et al., 2010.

There are many methods to test the expression of MGMT in cells and tissues. One of the most common techniques is immunohistochemistry (IHC) for its simplicity and effectiveness^{10,11}. IHC allows the staining and differentiation between tumor cells and surrounding healthy cells; however, this method is only semi-quantitative and does not distinguish to which extent the *MGMT* promoter is methylated. IHC is being phased out as a detection method for MGMT expression as studies have failed to correlate IHC outcomes with more quantitative analysis methods for MGMT expression^{12–15}. Currently, the most common detection method for *MGMT*-promoter methylation analysis is methylation-specific polymerase chain reaction (MSP), where the DNA methylation pattern within CpG islands is analyzed^{6,16–18}. During MSP, DNA is modified and undergoes bisulfite conversion to deaminate unmodified cytosines to uracils⁶. This modification leaves behind methylated cytosine residues. The methylated sequences are then amplified by polymerase chain reaction (PCR) using two different primer sets: one that targets methylated sites and one that targets unmethylated sites. This will reveal the methylation status of every cytosine within the gene specific amplification region⁶. MSP works well for the *MGMT* promoter, as there are 97 CpG islands and thus plenty of cytosine residues to analyze (**Figure 1.3**).

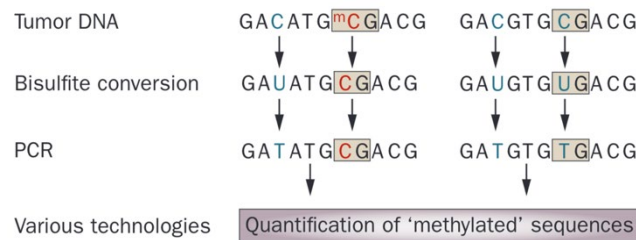


Figure 1.3. Schematic of bisulfite conversion for methylation specific polymerase chain reaction. Image from Weller et al., 2010.

Various tissues can have variable MGMT expression levels, yet tumors typically exhibit higher levels of MGMT expression than the normal, healthy tissue surrounding the region¹⁹. For this reason, MGMT expression has been used as both a predictive and a prognostic biomarker^{20,21}. A predictive biomarker can give information about the effect of a therapeutic agent, whereas a prognostic biomarker can provide information about patients' overall outcome regardless of therapy. It has been shown that *MGMT*-promoter methylation can increase sensitivity to treatment with alkylating agents^{20,22–24}. Tumors with low MGMT expression (and thus *MGMT*-promoter methylation) can take advantage of this sensitivity to eliminate cancer cells. Clinical trials have shown that *MGMT*-promoter methylation status can predict the prognosis of glioma patients through retrospective analysis. Findings showed that patients with *MGMT*-promoter methylation likely have favorable treatment outcomes with the alkylating agent temozolomide (TMZ) but not with radiation therapy^{25,26}. Additional studies showed that patients with anaplastic oligodendroglioma predicted better overall survival and progression-free survival upon treatment with radiation and/or alkylating agents when the tumors were *MGMT*-promoter methylated²⁷. A seminal trial from 2005 showed that glioblastoma multiforme patients who have methylated *MGMT* promoter tumors responded better to treatment with the alkylating agent TMZ than other patients²⁴. About 50% of cancers have low MGMT expression, and so understanding the methylation landscape of the *MGMT* promoter in tumors can be key for a successful treatment regimen²⁴.

Because low expression of MGMT has been shown to be more favorable in the treatment of certain tumors, there have been several approaches in figuring out how to deplete MGMT, using agents such as O⁶-benzylguanine (O⁶-bG)^{6,28}. O⁶-bG is a synthetic

derivative of guanine and acts as a substrate and suicide inhibitor for MGMT. Once O⁶-bG is consumed by MGMT, MGMT is degraded and is not replenished; thus, treating cells with O⁶-bG can decrease MGMT expression. Nonetheless, reports have shown that *in vitro*, O⁶-bG is only effective for a short period of time on the scale of 6 hours²⁹. After 18 hours, MGMT expression was restored suggesting that it is resynthesized²⁹. Clinically, O⁶-bG has been tested in combination with TMZ for MGMT-expressing glioblastoma patients; however, it was reported that the treatment regimen was extremely toxic without providing much benefit to patients³⁰. Another inhibitor, O⁶-(4-bromothienyl) guanine (O⁶-bTG) has 10-fold increased potency than O⁶-bG for inactivating MGMT and has been shown to be orally bioavailable with reduced toxicity²⁸. Clinical data has shown that O⁶-bTG and TMZ combination was effective on advanced solid tumors³¹. Unfortunately, both O⁶-bG and O⁶-bTG have high systemic toxicity due to off-target effects on healthy cells²⁸. Because of the off-target toxicity effects, the use of these MGMT-depleting agents is not quite ready for clinical implementation and additional research needs to be completed to target MGMT more thoroughly.

Overall, *MGMT*-promoter methylation status is critical in determining whether MGMT is expressed or not, and MGMT expression is being explored as a biomarker for response to treatment with alkylators such as the chemotherapeutic agent TMZ. Further studies on safely depleting MGMT may be valuable to improve treatments for patients with MGMT-expressing tumors.

1.2. Alkylating agents and temozolomide

DNA alkylating agents were first discovered in the 1940s and quickly became used for their potential chemotherapeutic value³². Alkylating agents attach an alkyl group (C_nH_{2n+1}) to DNA³³. The most common alkyl adducts are found at the N⁷ position of guanine and N³ position of adenine, though other alkyl lesions can be created on DNA as well³⁴. Before being widely used in the clinic, alkylating agents were better known for their use in chemical warfare during World War I as sulfuric and nitrogenous mustard gas³⁵. In the year 1942 at Yale University, Goodman and Gilman began studying the role of nitrogen mustards to treat tumors in mice. Later that year, these nitrogen mustards were employed to treat humans, showing temporary reduction of tumor mass in Hodgkin's disease lymphosarcoma and leukemia³⁶. Following this discovery, an abundance of new alkylating agents was created over the next few decades for the treatment of cancers.

Alkylating agents are found commonly in the environment and within living cells, and are found in components of air, water, biological byproducts (such as food) and pollutants including tobacco smoke³⁷⁻³⁹. Internally, byproducts of oxidative damage can lead to alkylation damage^{40,41}. We are exposed to the toxicity caused by alkylation damage daily, yet despite these dangers to our health, alkylators are used in the clinic as chemotherapies with the ultimate purpose of killing cancer cells⁴². Alkylating agents seem to be almost paradoxical: they can both induce cancer and be used to treat cancer. However, researchers have been trying to understand the molecular landscape of cancer to target tumors with these alkylating agents more selectively.

There are two main groups of alkylating agents, categorized by the number of reactive sites within the drug: monofunctional alkylators, which have one reactive site, and

bifunctional alkylators, which have two reactive sites. They can further be categorized by their chemical reactivity (S_N1 vs S_N2 nucleophilic substitution), the type of alkyl group (methyl, chloroethyl, etc.), and whether the DNA substrate is single-stranded or double-stranded. Most alkylating agents used in the clinic are S_N1 agents and can be either mono- or bifunctional³⁴. Currently, there are quite a few alkylating agents available in the clinic, but I am interested in studying one of the most used alkylators for glioblastoma, known as temozolomide (TMZ).

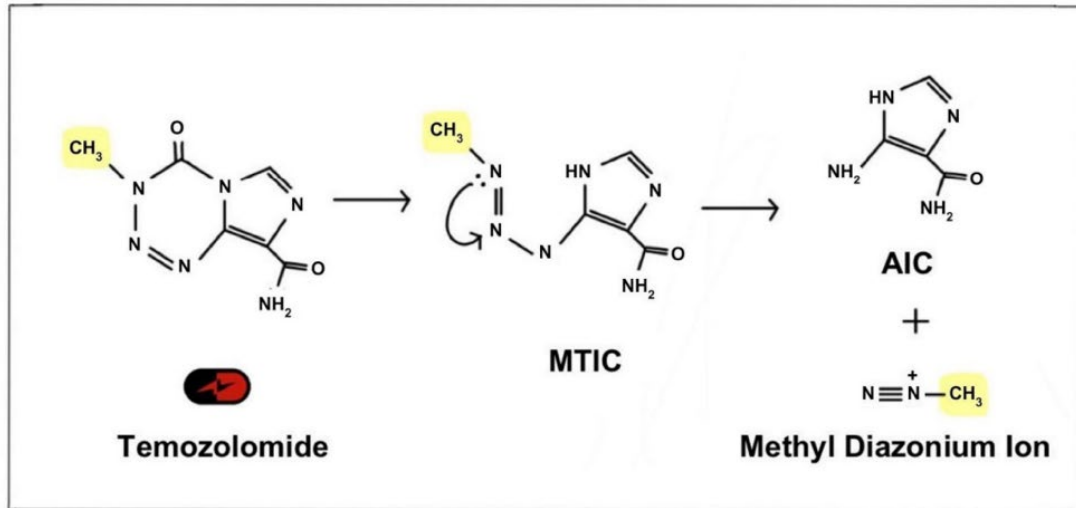
TMZ is a monofunctional S_N1 alkylator and was synthesized in the late 1970s by Malcolm Stevens' group at Aston University in Birmingham, England⁴³. It was approved for clinical use in the early 2000s in both Europe and the USA^{44,45}. In the clinic, TMZ is also referred to as Temodar or Temodal, but I will refer to the drug solely as TMZ in this dissertation. The oral bioavailability and ability of TMZ to cross the blood-brain barrier makes this an attractive choice of chemotherapy for central nervous system cancers, such as glioblastoma multiforme⁴⁴. TMZ is administered as a pro-drug, meaning it needs to be metabolized in the body to activate the otherwise biologically inactive compound. At physiological pH around 7.4, TMZ is activated and converted to the short-lived metabolite 5-(3-methyltriazene-1-yl) imidazole-4-carboxamide (MTIC)⁴⁶. MTIC is hydrolyzed and produces methyl diazonium ions which are electrophilic methylated molecules that can cause DNA damage^{45,47}. Because DNA is negatively charged, it acts as a nucleophile for the positively charged methyl diazonium ions, resulting in the addition of multiple DNA alkyl adducts causing DNA damage (**Figure 1.4**). TMZ is a monofunctional alkylating agent, thus it only affects single stranded DNA instead of double stranded DNA. The most common methylation sites of TMZ include N⁷-guanine and O³-adenine⁴⁸. Additionally,

about 5% of TMZ-induced damage will create alkyl lesions at O⁶-guanine. Even though the O⁶-methylguanine (O⁶-meG) lesions are the least common lesion created by TMZ, they are thought to be the lesion responsible for the overall cytotoxicity of this alkylating agent⁴⁹.

It is well-established that glioblastoma patients with a methylated *MGMT* promoter have better overall survival when treated with the alkylating agent, temozolomide (TMZ)²⁴. As mentioned, this is because lack of *MGMT* allows the O⁶-meG to persist without reversion to guanine causing DNA damage to the cancer cell, ultimately leading to cancer cell apoptosis. Though there has been evidence of low *MGMT* expression in other tumors such as colorectal carcinomas, small-cell lung carcinomas, lymphomas, and head and neck carcinomas, TMZ treatment has been mostly limited to glioblastomas^{17,50,51}. However, resistance to TMZ and tumor recurrence is an issue, even in the *MGMT*-promoter methylated setting. Glioblastomas tend to be very heterogenous and prone to new mutations, making resistance inevitable^{52,53}. Unfortunately, there are not many other predictive markers for response to TMZ besides *MGMT*-promoter methylation status.

In summary, TMZ is commonly used as an alkylator to treat glioblastoma and other cancers. TMZ can take advantage of *MGMT* status in providing better outcomes for those patients with *MGMT*-promoter methylated tumors. However, TMZ resistance can arise and is complicated by new mutations that arise and the lack of knowledge surrounding how those mutations affect response to TMZ. Thus, studying the DNA repair pathways that TMZ recruits can allow us to understand how to mitigate TMZ resistance.

Temozolomide Metabolism



Adduct Formation

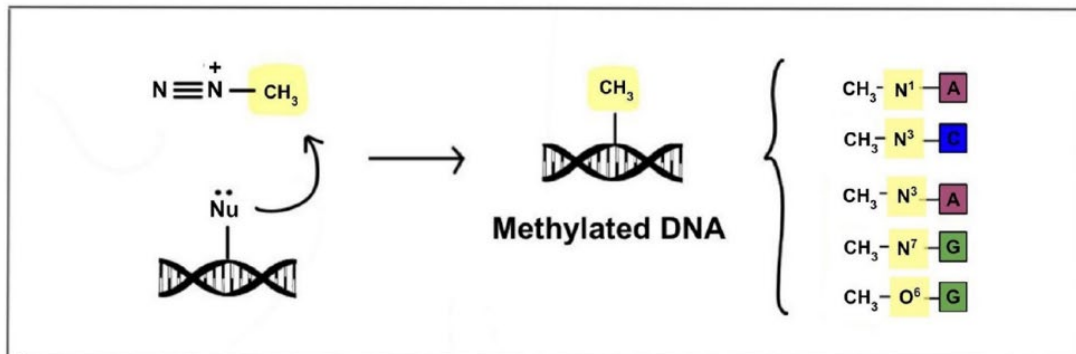


Figure 1.4. Temozolomide metabolism. TMZ forms into the short-lived MTIC before becoming methyl diazonium ions. These positively charged atoms can methylate DNA at various positions. Image from Singh et al., 2021.

1.3. DNA damage response pathways

Our cells are prone to damage that can harm the DNA in our cells, and thus preserving our genomic integrity is required for cellular function. Damage to our genome can arise in multiple ways, including both externally and internally, but the most serious forms of genomic damage affect DNA directly and can cause cancer⁵⁴. For example, extraneous ultraviolet (UV) damage caused from the sun and environmental factors can induce cellular stress and genomic instability which would need to recruit DNA damage response (DDR) pathways to repair the damage⁵⁵. Intracellularly, DNA damage can occur due to DNA replication, reactive oxygen species generated by respiration, and the spontaneous hydrolysis of DNA nucleotides. Given the sheer amount of damage our DNA encounters, which is approximately 10^4 to 10^5 lesions daily, there are many cellular mechanisms in place to repair the damaged lesions and maintain genomic integrity⁵⁴.

In nature, the simplest forms of cellular defense against DNA damage evolved to selectively reverse one type of damage. For example, some types of UV-induced damage can be reversed by special enzymes known as photolyases⁵⁶. Another great example of an enzyme with the ability to selectively reverse one type of damage is MGMT, as discussed above. As an enzyme, MGMT's only function is to remove any O⁶-meG lesions that may arise due to alkylation⁵. However, enzymes with solely one function to remove one specific type of lesions are not common, and there are more complex mechanisms and pathways required to remove more diverse types of DNA damage. Despite a vast amount of research published on the DDR pathways, there are still controversies regarding which pathways are activated by certain types of damage or lesions due to a fair amount of overlap between these mechanisms.

DDR pathways can be vaguely categorized into single-strand break repair and double-strand break repair. Within these categories, there are a plethora of other smaller repair pathways. Some of the common pathways in single-strand break repair are base excision repair (BER) or nucleotide excision repair (NER). During BER, bases that have small chemical alterations (such as those due to alkylation) that do not disturb the structure of the DNA double-helix are repaired^{57,58}. First, DNA glycosylases that are specific to the lesion will identify and eliminate the damaged base from the sugar-phosphate backbone of the DNA. The removal of the base will leave an abasic (AP) site exposed for AP-endonuclease to cleave before DNA polymerase β will replace the base, and XRCC1/ligase III will seal any breaks in the DNA. A special type of BER will involve the nuclear protein, poly(ADP-ribose) polymerase (PARP) which will parylate single-strand breaks recruiting XRCCI/ligase III again⁵⁹⁻⁶¹. NER is more complex than BER as it requires excision and replacement of an entire nucleotide that can destabilize the DNA helix, instead of simply removing a base^{62,63}. There are many proteins involved in NER depending on the type of nucleotide lesion, but notably replication protein A (RPA) will prevent single-strand DNA from reannealing, and polymerase β and ligase III can both be recruited to replace and ligate the lesion^{64,65}. Double-strand break repair is more complex than BER or NER and is usually split into the 2 distinct pathways of homologous recombination and nonhomologous end-joining, which involve a plethora of additional proteins⁶⁶⁻⁶⁸. As mentioned prior, there is plenty of overlap between these pathways, which is why it is important to acknowledge them. The one pathway I am particularly interested in studying is the DNA mismatch repair pathway.

1.3.1. Mismatch repair pathway

The mismatch repair (MMR) pathway can be categorized as one of the mechanisms of single-strand break repair and is a highly conserved pathway that plays a critical role in maintaining and preserving our genome⁶⁹. MMR is typically recruited upon mismatches between bases or upon insertions and deletion mismatches that occur during replication⁶⁹. This system is particularly important in preventing mutations from becoming permanent and passed down through cells that are dividing, making MMR imperative in both the short-term and long-term.

Escherichia coli (*E. coli*), yeast, and human MMR all have very similar functions, further exemplifying its importance as it is conserved across many organisms⁷⁰⁻⁷². In eukaryotes, MMR consists of two families of proteins which are heterodimers: MutS and MutL, which are homologs from *E. coli*. In the first step of the MMR pathway, the mismatch is recognized by either MutS α or MutS β . MutS α is a heterodimer composed of the proteins MSH2 and MSH6, and MutS β is composed of MSH2 and MSH3⁷¹⁻⁷³. Whereas MutS α is responsible for recognizing base-base mispairs and small indels on the order of 1 to 2 nucleotides, MutS β is responsible for recognizing indels of 1-15 bases^{69,74}. The binding of MMR proteins to the mismatch then allows the conversion of ADP to ATP, converting these heterodimers into sliding clamps that can glide along the DNA to look for additional mismatches^{74,75}. The sliding of these heterodimers will then allow for the interaction with the MutL α heterodimer, composed of proteins MLH1 and PMS2⁷⁶. Upon MLH1 recruitment, excision occurs where the MMR proteins must excise the error from the newly synthesized strand that has the error, as opposed to the template strand. In a 5' reaction, MutS α activates the exonuclease EXO1⁷⁷. MutL α has been found not necessary

for all 5' repair, though when present can modulate excision^{74,76}. In the event of a 3' mismatch which is less studied and understood, MutL α activity has been shown to be essential^{76,78}. After excising the lesion, a DNA polymerase will replace the lesion, and DNA ligase I will fill the gap of the DNA duplex⁷⁴ (**Figure 1.5**).

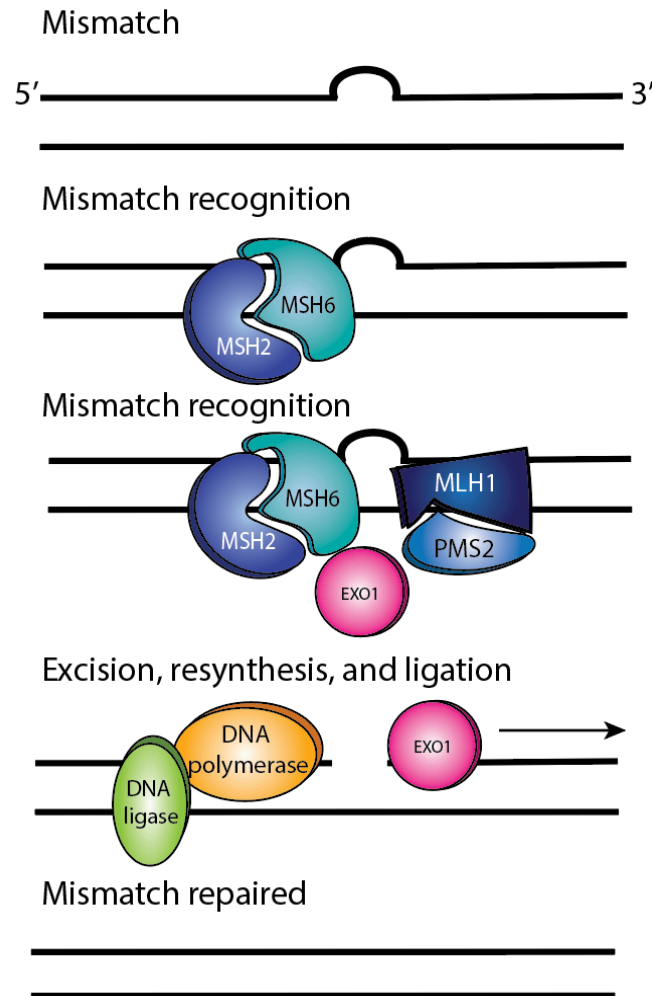


Figure 1.5. Schematic of eukaryotic mismatch repair. Upon recognition of the mismatch by MutS α or MutS β , MutL α is recruited along with EXO1 to excise the mismatch. Then DNA polymerase and DNA ligase resynthesize and ligate the DNA, respectively.

Upon alkylation damage from TMZ, O⁶-meG lesions will mispair with thymine instead of cytosine⁷⁹. In the absence of the MGMT enzyme to remove the O⁶-meG lesion, MMR will be recruited to excise the thymine mismatch. However, in this case, the MMR proteins will fail to replace thymine with cytosine and will continually add another thymine. This iterative replacement of thymine with itself will result in a phenomenon known as futile cycling, ultimately leading to additional DNA breaks and cell death⁷⁹. The model of futile cycling is heavily debated as many believe that it is the primary method of TMZ toxicity while others consider that there are other mechanisms at play for TMZ-induced cell death⁸⁰ (**Figure 1.6**).

Understanding the role of MMR is important for its clinical significance. Mutations in MMR can affect genomic stability, resulting in a phenotype known as microsatellite instability (MSI)⁸¹. Microsatellites are repeated sequences of DNA, though the most common is with the cytosine and adenine nucleotides⁸². When MMR mutations are unable to repair a replication error, an MSI region is created⁸³. Adding MSI regions that should not originally exist can result in frame-shift mutations, leading to a slew of issues within the cell and creating a higher predisposition to cancer⁸³. MMR mutations and MSI are associated with cancers ranging from colon cancer to gastric, ovarian, and brain cancers including glioblastoma⁸⁴. Further, germline MMR mutations can lead to Lynch syndrome, which increases the risk of being diagnosed with any of the cancers previously mentioned^{85,86}. There have also been documented cases of glioblastoma patients developing resistance to TMZ and acquiring new mutations within the MMR pathway⁸⁷⁻

89.

To conclude, studying the intricacies of the MMR pathway is fundamental in understanding how to maintain genomic integrity, and how to take advantage of the system in the setting of cancer. MMR is relevant pertaining to the clinic; being able to dissect this complex pathway as it relates to TMZ-induced alkylation in the context of *MGMT*-promoter methylation may enlighten physicians and scientists to develop new chemotherapies for patients.

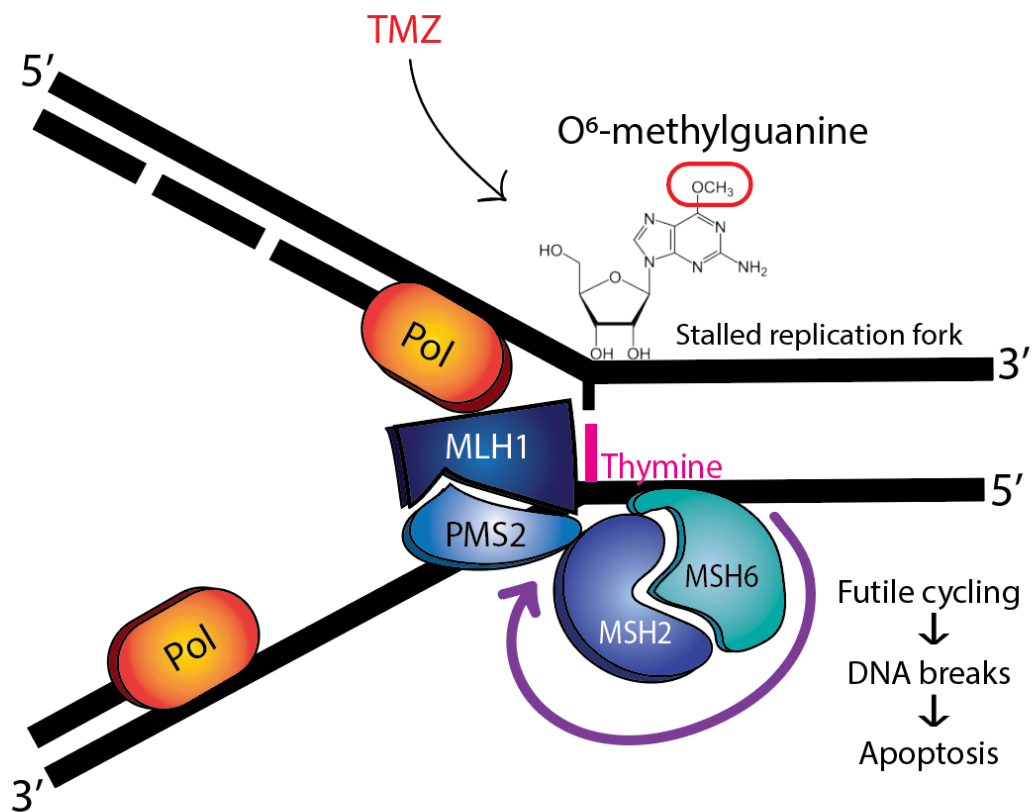


Figure 1.6. Temozolomide-induced mismatch repair futile cycling model. MMR proteins will continually replace thymine with itself, and iterative cycles of this will lead to futile cycling, DNA breaks, and cell death through apoptosis.

1.4. Ataxia telangiectasia and RAD3 related protein in DNA repair

Ataxia telangiectasia and RAD3 related protein (ATR) is a crucial protein in regulating genomic stability, much like the other DDR pathways and proteins mentioned previously⁹⁰. ATR, ataxia telangiectasia mutated (ATM) and DNA-dependent protein kinase (DNA-PK) are members of the PI3K-like kinase (PIKK) family. All three of these kinases play a role in DNA damage signaling, though ATM and DNA-PK are activated by double-stranded breaks and ATR is mostly activated by single-strand breaks^{91,92}. Though these kinases have all been well-studied for their distinct roles, there is still quite some overlap between these pathways upon certain types of DNA damage, which remains understudied and controversial. Specifically, it is still unknown how ATR is activated by DNA damage and replication stress⁹³.

ATR is an essential protein unlike the other kinases, as its absence has been shown to lead to embryonic lethality. The activation of the ATR pathway begins with a single-strand break. Replication protein A (RPA) will coat the single-stranded DNA to prevent it from reannealing onto itself. ATR-interacting protein (ATRIP) then directly binds to RPA, allowing the ATR-ATRIP complex to recognize the DNA damage site or stressed replication, and recruits RAD17⁹⁴. The pathway continues as the 9-1-1 complex (RAD9, RAD1, and HUS1), and Topoisomerase Binding Protein I (TopBP1) are also recruited to the site of damage. This mechanism is thought to be one of the pathways by which ATR is activated⁹⁵⁻⁹⁷ (**Figure 1.7**). Upon activation of ATR, it can phosphorylate its downstream substrate, CHK1⁹⁴. The phosphorylation of CHK1 at serine 317 and serine 345 are often used as well-characterized markers for ATR activation, as ATR is the sole kinase to phosphorylate these serine residues⁹⁸. Including the phosphorylation of CHK1, further

downstream of ATR signaling continues to be complex. CHK1 phosphorylation has been known to activate the CHK1 protein, which will then phosphorylate CDC25, a regulator of cell cycle phases^{99,100}. ATR activation has also been shown to induce G₂/M arrest¹⁰¹.

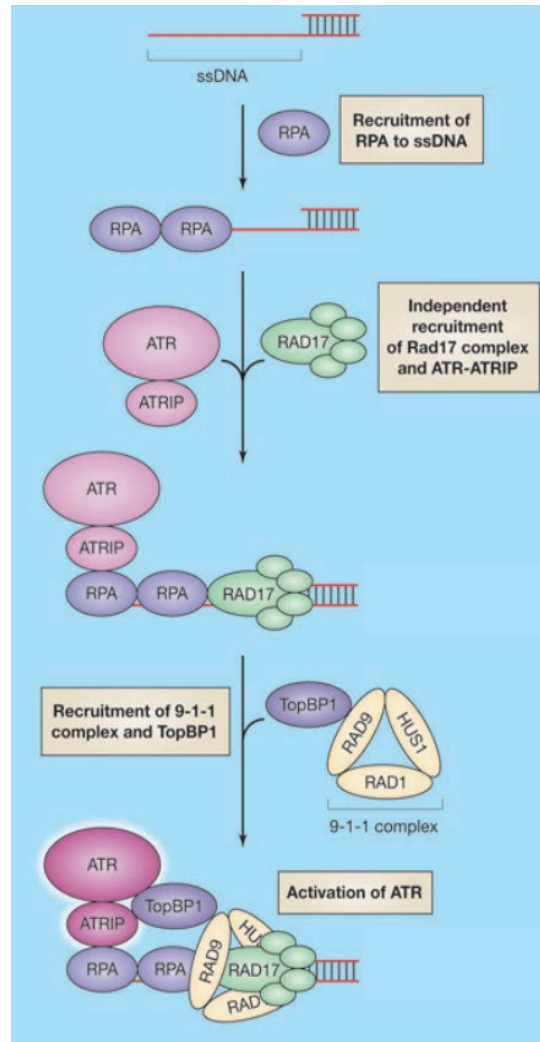


Figure 1.7. Upstream activation pathway of ATR. RPA is recruited to single-strand DNA (ssDNA) before the recruitment of ATRIP and RAD17. Then, the 9-1-1 complex and TopBP1 are recruited, all assembling to activate ATR. Image from Shiotani and Zou, 2009.

ATR appears to serve a greater purpose in tumor cells than in normal cells⁹⁹. ATR is involved in an entire signaling cascade with many moving parts, and tumor cells tend to be dysregulated in various parts of this pathway and have higher levels of replication stress. Studies have shown that inhibiting the ATR pathway can be selectively toxic in cancer cells, leading to the development of ATR inhibitors. The first ATR inhibitor identified was caffeine, as it disrupts cell-cycle arrest caused by DNA damage and sensitizes cells to DNA damage¹⁰². Caffeine is not selective for ATR alone and also targets ATM, requiring high toxic doses for clinical effect in cancer cells^{99,102}. For this reason, there has been the development of other ATR inhibitors. In 2011, the first potent and selective ATR inhibitor was created by Vertex Pharmaceuticals, VE-821, and a few years later its improved analog VE-822 (also known as VX-970 to be used later in **Chapter 6** was created^{103,104}. VX-970 was the first ATR inhibitor to enter clinical trials, making its use in the *in vivo* studies of this dissertation relevant. AstraZeneca and Bayer Pharmaceuticals have also created structurally unique, highly selective, and potent ATR inhibitors, AZ-20 and BAY-1895344, respectively, with sub-micromolar concentrations required for cancer cell kill^{105,106} (**Figure 1.8**).

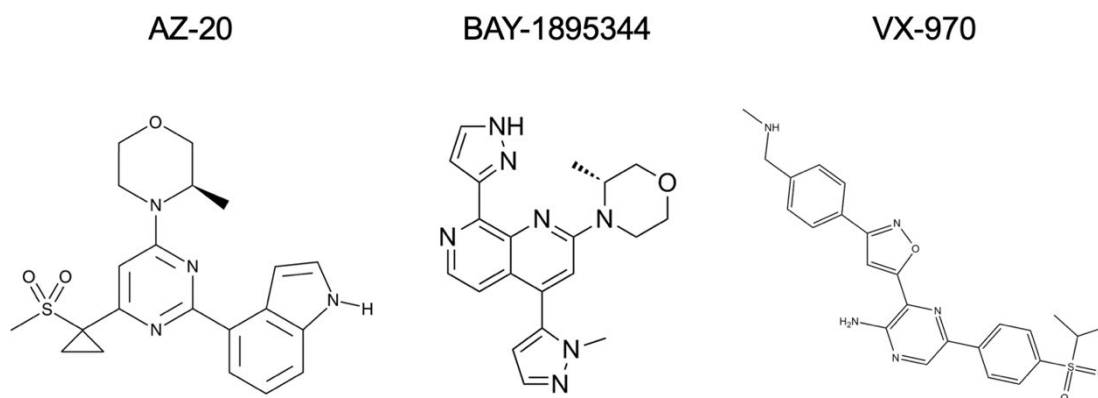


Figure 1.8. Structure of ATR inhibitors AZ-20, BAY-1895344, and VX-970.

CHK1 is a downstream substrate of ATR, and thus there have also been CHK1 inhibitors in development. It is possible that these inhibitors do not differ significantly from ATR inhibitors due to their close relation, though CHK1 inhibitors are in clinical trials as well. It appears ATR inhibition may have a wider clinical range than CHK1 inhibitors, making ATR inhibitors a better choice for study^{107,108}.

Recently, work published from our laboratory showed that ATR is activated in *MGMT*-promoter methylated cancers upon treatment with TMZ. Western blotting showed earlier ATR activation through pCHK1 levels in *MGMT*-promoter methylated cells (MGMT-) vs. cells with *MGMT* (MGMT+)¹⁰⁹. Additionally, TMZ sensitizes MGMT- cells to ATR inhibitors as seen from synergy plots. This data led us to believe that perhaps MMR futile cycling is not the only method of TMZ toxicity, but that TMZ can also lead to replication stress, ATR signaling, and subsequently cell death (**Figure 1.9**).

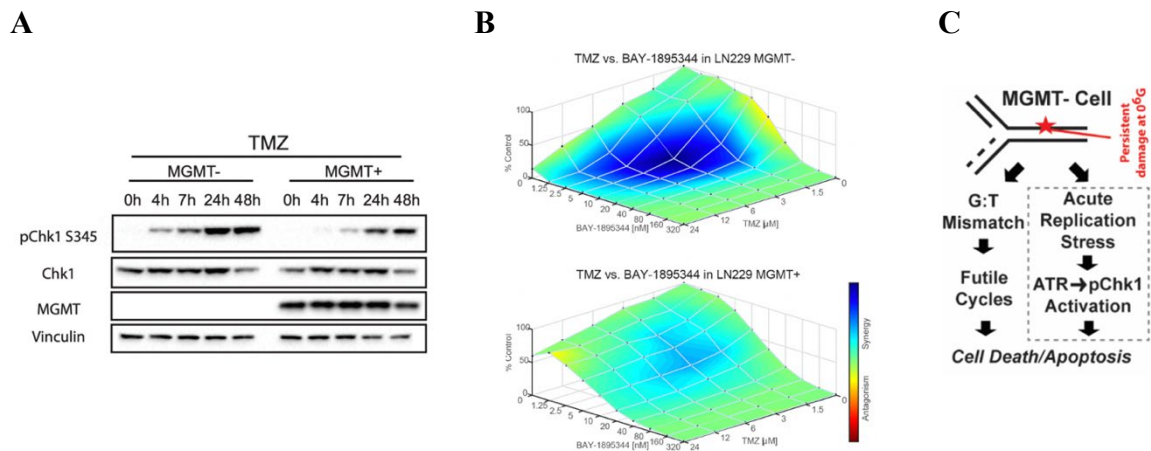


Figure 1.9. ATR signaling is specific to MGMT- cells and not MGMT+ cells. (A) Western blot with TMZ-treated MGMT- and MGMT+ cells over 48 hours shows earlier activation of ATR in MGMT- cells. (B) There is exquisite synergy with TMZ and ATR inhibitor in only MGMT- cells. (C) TMZ may activate ATR signaling, not only MMR. Images from Jackson et al., 2019.

1.5. Significance and Innovation

Given that canonically TMZ-induced damage leads to MMR, and that a publication from our lab previously showed that TMZ causes ATR activation occurs in MGMT- cells, the next logical step is to understand if and how MMR affects ATR signaling¹⁰⁹. Previously, it has been published that MMR plays a role in ATR signaling but the specific proteins involved have not been teased out¹¹⁰. In this dissertation, I sought to investigate the role of the DNA mismatch repair system as it relates to ATR activation upon TMZ treatment in glioblastoma multiforme. This study is novel and data pertaining to this research question has not been published to the best of my knowledge.

To ensure that I thoroughly study each MMR protein for its individual and unique roles, I started by creating shRNA knockdown cell lines of all the MMR proteins in both the MGMT- and MGMT+ context. These isogenic cell line models are unique in allowing me to isolate one specific protein in the context of *MGMT*-promoter methylation. Using these cell lines, I then investigated the role of TMZ-induced ATR activation upon loss of the MMR protein in assays ranging from *in vitro* western blots to *in vivo* mouse studies. If ATR signaling was affected in the MMR knockdown cell lines compared to the parental MMR-proficient cell lines, then I would be able to conclude that that individual MMR protein is associated with ATR signaling.

Understanding how MMR is involved in ATR signaling upon TMZ-induced damage has significant clinical implications. Many cancers have MMR deficiencies, so studying the molecular landscape of these cancers can allow for more targeted therapies with combinations of TMZ and ATR inhibitor. Overall, the data presented here can ultimately be helpful to target and treat a wide-variety of MMR-mutated cancers.

2. Chapter 2: Materials and Methods

2.1. Cell culture

Human glioblastoma LN229 MGMT- and MGMT+ cell lines were obtained from Bernd Kaina (Johannes Gutenberg University Mainz, Mainz, Germany). U251 cells were purchased from Horizon. All cells were confirmed negative of *Mycoplasma* using qPCR. Cells were cultured in DMEM with 10% FBS.

2.2. Mismatch repair knockdown cell line creation

The pGIPZ™ shRNA lentiviral vectors for mismatch repair proteins MSH2, MSH3, MSH6, MLH1 and PSM2, were purchased as glycerol stocks from Horizon Dharmacon™ (**Table 2**). Nontargeting GIPZ lentiviral shRNA particles were purchased from Horizon Dharmacon™. From the glycerol stock, the shRNA plasmids were prepared and confirmed by restriction digest with SacII. To generate lentiviral particles, HEK293T cells were transfected with the shRNA lentiviral plasmid of interest, a packaging plasmid (psPAX2, 12260 from Addgene), and an envelope plasmid (pCMV-VSV-G, 8454 from Addgene) using Lipofectamine™ 3000 Transfection Reagent (Invitrogen, L3000001). Viral particles were harvested from the cell media after 48h. To create the cell lines, LN229 MGMT- and MGMT+ cells were infected with a high titer of shRNA lentivirus of interest and 8 µg/mL of polybrene. 48 hours later, cells were selected with 1 µg/mL of puromycin for 3-4 days before use. Cells were harvested as a polyclonal population and confirmed for the protein knockdown with western blotting before proceeding with limiting dilution to create monoclonal cell populations which were then confirmed by western blotting.

Table 2. shRNA glycerol stock information.

Protein	shRNA information	shRNA sequencing primer
MSH2	Entrezgene 4436, RHS4430-200305416	5' - GCATTAAAGCAGCGTATC - 3'
MSH3	Entrezgene 4437, RHS4430-200158125	5' - GCATTAAAGCAGCGTATC - 3'
MSH6	Entrezgene 2956, RHS4430-200281418	5' - GCATTAAAGCAGCGTATC - 3'
MLH1	Entrezgene 4292, RHS4430-200268977	5' - GCATTAAAGCAGCGTATC - 3'
PMS2	Entrezgene 5395, RHS4430-200253216	5' - GCATTAAAGCAGCGTATC - 3'

2.3. Drug compounds

All drug compounds were purchased from SelleckChem. Compounds were resuspended as a stock concentration in DMSO, aliquoted, and stored at -20C: temozolomide (S1237), AZ-20 (S7050), BAY-1895344 (S9864), VX-970, AZD7648 (S8843), AZD0156 (S8375), and AZD7762 (S1532).

2.4. Western blot and immunoprecipitation

Cells were treated with drug where indicated, trypsinized and pelleted for use immediately or placed in storage at -80C. Cells were lysed on ice with 1X RIPA buffer (Cell Signaling Technology, 9806S) and 1X Halt™ Protease and Phosphatase Inhibitor Single-Use Cocktail (ThermoFisher Scientific, 78442). The lysed cell pellets remained on ice for 30 minutes while briefly vortexing every 5 minutes for 10 seconds. Lysed cell pellets were centrifuged for 10m at 4C. The remaining lysates were quantified using the Bradford protein assay.

For immunoprecipitation (IP), cells were lysed in lysis buffer (50 mM HEPES, 250 mM NaCl, 1% NP-40, 5 mM EDTA, and 1X Halt cocktail). The lysed cell pellets were sonicated 5 seconds on/10 seconds off for 15 seconds at 100% and then centrifuged for 25m at 4C. The lysates were quantified using the Bradford protein assay. Equal concentrations of protein lysates were bound to 0.5 mg of magnetic Protein G Dynabeads (Invitrogen, 10003D) along with 1.5 µg of CHK1 antibody and incubated on a rotator overnight at 4C. The following day, beads were collected and washed once with wash buffer (50 mM HEPES, 250 mM NaCl, 0.1% NP-40, 5 mM EDTA, and 1X Halt cocktail), once with high-salt wash buffer (50 mM Tris pH 7.5, 1 M NaCl, 1% Triton X-100, 1 mM DTT, 10% glycerol, and 1X Halt cocktail), and once more with wash buffer. Protein was eluted from the beads by resuspending in 2X Laemmli in wash buffer before boiling for 5m at 70C.

For both western blot and IP, protein was separated using NuPAGE™ 4 to 12%, Bis-Tris gels and transferred to a PVDF (polyvinylidene fluoride) membrane at 90 volts for 90 minutes. After 1 hour of blocking in 5% BSA or 5% non-fat dry milk in 1X TBS-T, membranes were incubated at 4C overnight in primary antibody.

The following primary antibodies were used as indicated in **Table 3**. The following day, membranes were washed in 1X TBS-T and incubated with peroxidase-conjugated secondary antibodies at room temperature at 1:5000 in 1X TBS-T for 1-2 hours before visualizing the signal with the Clarity ECL kit (BioRad, 1705061).

Table 3. Antibodies and dilutions for western blot and immunoprecipitation.

Antibody	Company	Catalog	Blocking	Dilution
pCHK1 S317	Cell Signaling Technologies	12302	5% BSA	1:666
pCHK1 S345	Cell Signaling Technologies	2348	5% BSA	1:666
pCHK1 S296	Cell Signaling Technologies	2349	5% BSA	1:666
CHK1	Cell Signaling Technologies	2360	5% milk	1:1000
CHK1	SantaCruz	SC-8408	5% milk	1:500
MGMT	Cell Signaling Technologies	2379	5% BSA	1:1000
MSH2	Cell Signaling Technologies	2850	5% milk	1:1000
MLH1	Cell Signaling Technologies	4256	5% BSA	1:1000
MSH3	BD Biosciences	611390	5% BSA	1:666
MSH6	BD Biosciences	610918	5% BSA	1:1000
PMS2	ProteinTech	66075-1-Ig	5% milk	1:1000
GAPDH	ProteinTech	HRP-60004	1X TBS-T	1:10000

2.5. Short-term cell viability and drug synergy assays

Cells were seeded at 1,000 cells per well in a 96-well plate. The following day, cells were treated with various concentrations of drugs as indicated. After drug treatment of 3 days, or 6 days with temozolomide, cells were washed once in 1X PBS, fixed in 4% paraformaldehyde, and stained with Hoescht at 1 μ g/mL. Plates were imaged on Cytation 3 (BioTek) and counted using cell profiler (<http://cellprofiler.org>). For synergy assays, synergy was calculated using Combenefit ¹¹¹.

2.6. Clonogenic survival assay

Cells were pretreated with temozolomide in culture for 72h. Cells were then seeded in fresh media without drug in 6-well plates in triplicate, at a 3-fold dilution ranging from 9,000 to 37 cells per well. After seeding, cells were treated with ATRi and placed plates in the 37C incubator. After 14 days, plates were removed, washed with 1X PBS, and stained with crystal violet for 1 hour. Colonies were counted by hand and counts were normalized to the plating efficiency of corresponding drug treatment condition.

2.7. Immunofluorescence

Cells were seeded in clear bottom, black 96-well plates at 10,000 cells/well (Grenier, 655866). At the stated times, cells were treated with drug. The pRPA32 S33 protocol was described previously⁹³. Cells were incubated with primary antibodies at 4C overnight, at 1:1000 dilution of pRPA32 S33 (Bethyl, A300-246A) and 1:500 dilution of anti-phospho-histone H2A.X Ser139 clone JBW301 (Millipore Sigma, 05-636). Secondary antibodies dilutions were 1:500, and Hoescht 33342 at 1 µg/mL. Cells were imaged on a Keyence BZ-X800 and foci were analyzed using the Focinator¹¹².

2.8. Flow Cytometry

For propidium iodide (PI) staining, cells were seeded in 6-well dishes 24-48h before drug treatment. After drug treatment, cells were harvested by trypsinization before being fixed with 70% ethanol. Cells were then stained with RNase/PI buffer (BD Biosciences, 550825) 30 minutes before analysis on a CytoFLEX Flow Cytometer. All experiments were performed in triplicate and analyzed using FlowJo software.

2.9. *In vivo* studies with temozolomide and ATRi

Female athymic nu/nu mice (Hsd: Athymic Nude-Foxn1nu, Envigo) were used for *in vivo* studies. LN229 MGMT- or LN229 MGMT- shMSH6 cells were injected subcutaneously into the right and left flank at a concentration of approximately 5 million cells per 100 μ L of Matrigel (Corning, 354234). Prior to treatment, mice were randomized into four groups of 8-9 animals, where each group was similar in average starting tumor volume. Mice were treated and tumors were measured as described previously¹⁰⁹. All studies were approved through the Institutional Animal Care and Use Committee at Yale School of Medicine (New Haven, CT).

2.10. Statistical analysis

Data are presented as mean \pm SD for flank studies or SEM. Student's *t* test or 2-way ANOVA (xenograft studies) were used to make comparisons. Statistical analyses were carried out using GraphPad PRISM. Asterisks indicate levels of significance and p-value (* \leq 0.05, ** \leq 0.01, *** \leq 0.001, **** \leq 0.0001).

3. Chapter 3: LN229 MGMT- cells show differential ATR activation than MGMT+

3.1. Introduction

Using relevant cell line models is key in any rigorous scientific experiment, especially when trying to gain mechanistic insight. Because my work focuses on understanding the mechanisms underlying temozolomide treatment in glioblastoma multiforme, I wanted to use an established glioblastoma multiforme cell line. Thus, I chose to use adherent human LN229 glioblastoma cells, which were established from a 60-year-old female Caucasian patient with right frontal parieto-occipital glioblastoma in 1979. These cells have been used in a wide range of studies previously and can form tumors in nude mice which will be useful as discussed in **Chapter 6**. Additional characteristics of these cells are that they have p53 with a proline to leucine mutation at residue 98, are wild-type for PTEN, and have a deletion of p16¹¹³.

The LN229 cells are *MGMT*-promoter methylated as the wild-type, parental cell line meaning that they do not express the MGMT enzyme (MGMT-). Though I am interested in studying the mismatch repair system in the MGMT- setting, it is important to also perform experiments in a cell line that expresses MGMT (MGMT+) as a control. My goal is to have an isogenic pair of cell lines to identify how MGMT-status affects DNA repair in the context of MMR and TMZ-treatment. To this end, the lab previously obtained an LN229 MGMT+ cell line from Johannes Gutenberg University Mainz, Mainz, Germany. The LN229 MGMT- cells were transfected with human MGMT cDNA cloned

into a mammalian expression vector (pSV2MGMT), and were selected with G418, allowing the expression of the MGMT enzyme¹¹⁴.

In 2005, a seminal trial published results that glioblastoma patients with *MGMT*-promoter methylated tumors responded more favorably to treatment with the alkylating agent TMZ than patients with an unmethylated *MGMT* promoter^{24,49}. This finding sparked many investigations into understanding how TMZ-induced damage is repaired by the MGMT enzyme, and how damage accrues in the MGMT- setting^{22,26,27,48}. Most studies revealed that in the MGMT- context, TMZ-induced O⁶-meG lesions remain unrepaired causing more deleterious damage. This accumulated damage ultimately leads to cell death through many debated hypotheses, which is why it is believed that the MGMT- tumor cells respond better to TMZ treatment. One of these hypotheses proposes that the unrepaired O⁶-meG lesions will recruit the proteins in the MMR pathway¹¹⁵. These MMR proteins will attempt to repair the mismatch between O⁶-meG and thymine but will iteratively replace thymine with itself, ultimately leading to cell death after numerous cycles of futile cycling⁸⁰. This is only one proposed mechanism of TMZ-induced toxicity in the MGMT-setting, but not the only one.

Previously, our group published that upon TMZ treatment, MGMT- cells activate the ATR/CHK1 axis earlier than MGMT+ cells as seen through the phosphorylation of CHK1¹⁰⁹. Additionally, we reported that TMZ can sensitize MGMT- cells to treatment with ATR inhibitors. This finding opened a new hypothesis that perhaps futile cycling is not the only mechanism of TMZ toxicity. Thus, as a first step, I wanted to verify the MGMT-status of my cell lines and confirm that they are responding to TMZ treatment as expected. Then, it was important for me to recapitulate the findings from our publication that ATR is

activated earlier in MGMT- cells upon TMZ treatment than MGMT+ cells through western blotting and synergy assays as presented in this chapter. These first experiments are crucial in creating a strong foundation for the rest of the data presented in this dissertation.

3.2. Results

3.1.1. MGMT- cells are more sensitive to TMZ than MGMT+ cells

To verify the MGMT status of my cells, I first completed a western blot on whole cell lysates probing for MGMT. I observed that the promoter methylated *MGMT* cells do not express MGMT, whereas the cells with the overexpression construct of MGMT do express the protein in high quantities (**Figure 3.1**). The cell lines were acquired as mentioned prior.

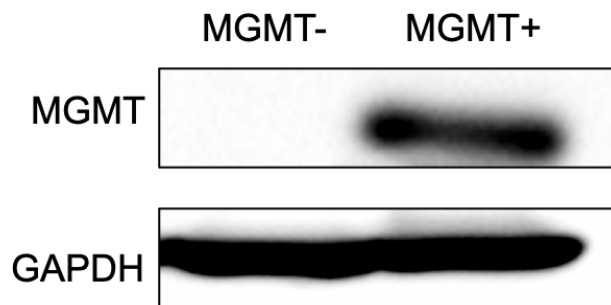


Figure 3.1. Western blot of LN229 cell line models showing MGMT status.

It is known that MGMT- patients respond better to TMZ treatment than MGMT+ patients²⁴. Thus, the same principle should apply in MGMT-/MGMT+ cell lines, and has been shown previously by work published from our laboratory. I performed a short-term cell viability assay assessing whether I could recapitulate the known phenotype that MGMT- cells are more sensitive to TMZ than MGMT+ cells. Upon increasing doses of TMZ over a 6-day treatment, the MGMT- cells are sensitive and do not survive at high concentrations of the drug, whereas the MGMT+ cells are resistant to TMZ treatment even at the highest concentrations (**Figure 3.2**).

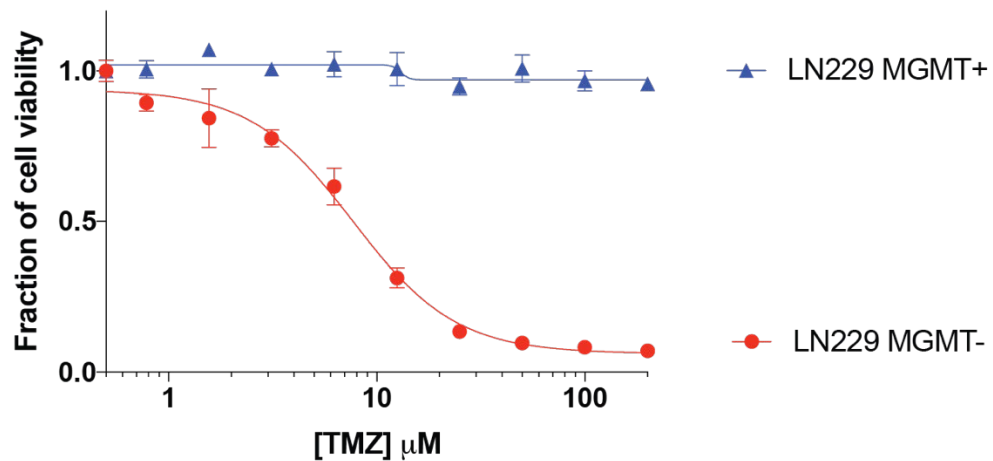


Figure 3.2. Short-term cell viability assay with temozolomide in MGMT- and MGMT+ cells. After treatment with TMZ at high concentrations, the MGMT+ cells (top, blue line) remain resistant compared to MGMT- cells (bottom, red line).

Additionally, the clonogenic survival assay (CSA) has been the gold-standard of determining drug sensitivity¹¹⁶. The CSA measures drug sensitivity in cells after either constant drug treatment or the prolonged effect of drug pre-treatment, for 10-16 days before fixing, staining, and quantifying cell colonies. Thus, I performed a CSA in these cell lines with TMZ and found striking results that MGMT- cells are more sensitive to TMZ whereas the MGMT+ cells remain resistant to treatment, consistent with what we have reported previously (**Figure 3.3**).

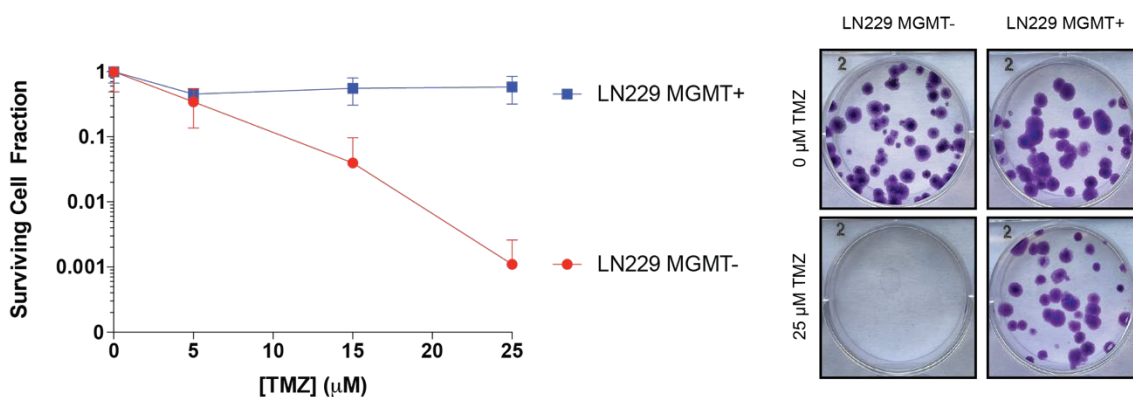


Figure 3.3. Clonogenic survival assay with temozolomide in MGMT- and MGMT+ cells. After pre-treating cells with indicated concentrations of TMZ for 72 hours, I seeded cells in triplicate in 6-well plates and allowed cells to incubate for 14 days without additional drug before fixing and staining. The MGMT+ cells (top, blue line) remain resistant to TMZ compared to MGMT+ cells (bottom, red line) after prolonged exposure to TMZ.

3.1.2. TMZ and ATR inhibitor synergize in MGMT- cells

Published work from our laboratory previously detailed that TMZ can further sensitize MGMT- cells to ATR inhibitors¹⁰⁹. The information gained from that novel study could potentially be used as a new avenue to selectively treat MGMT- patients with the combination of TMZ and ATR inhibitors. As has already been shown in Jackson, et al. 2019, the MGMT- cells exhibit synergy upon treatment with TMZ and ATR inhibitors, whereas the MGMT+ do not. This suggests that MGMT status plays a role in the synergistic interaction of this drug combination. I repeated this experiment to once again confirm the MGMT status of my cells, expecting synergy in the MGMT- cells upon TMZ and ATR inhibitor treatment, which is what I observed with 2 structurally unique ATR inhibitors, BAY-1893455 and AZ-20 (**Figure 3.4**).

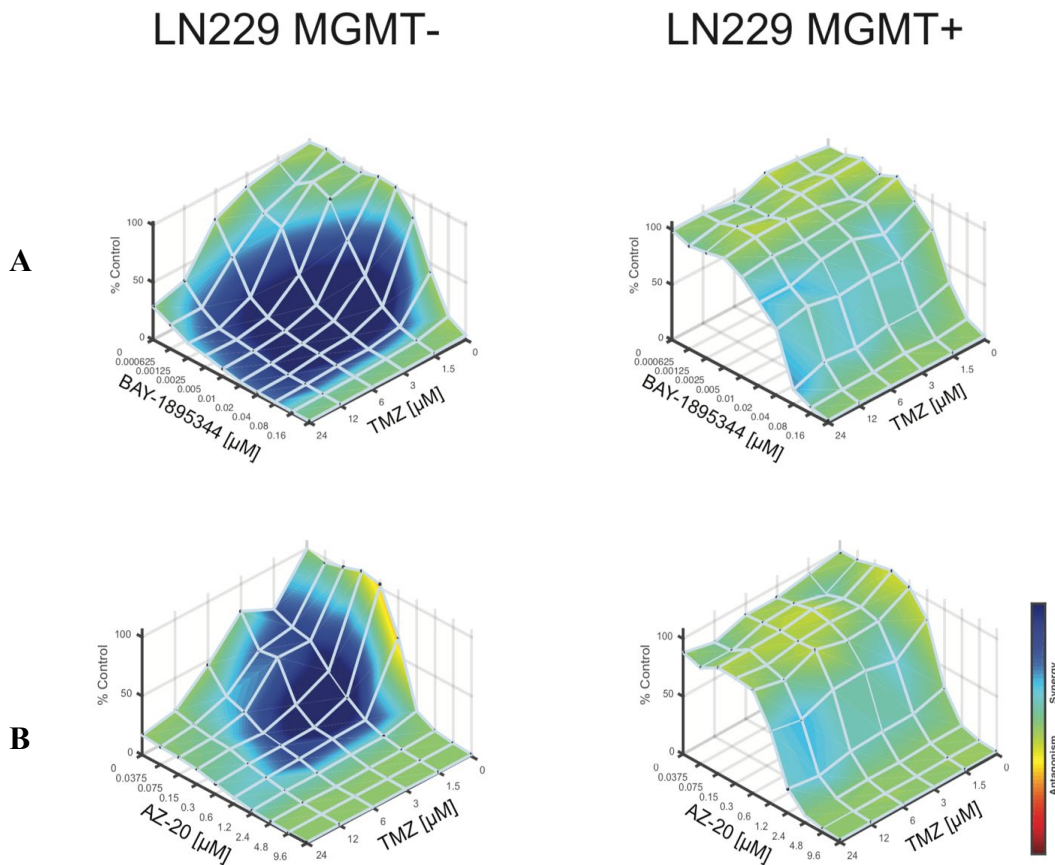


Figure 3.4. Synergy plots of MGMT- and MGMT+ cells with temozolomide and ATR inhibitors. (A) MGMT- cells treated with TMZ and the combination of ATR inhibitor BAY-1895344, or **(B)** AZ-20. Synergy is defined as the combination of 2 drugs causing increased cell killing more than each drug individually. The deep blue color on the two left-sided graphs indicates synergy and increased cell kill. The MGMT+ cells do not show synergy or increased cell kill, as indicated by the light green area on graphs.

Because the entirety of this thesis is based on understanding the underlying mechanisms of why MGMT- cells activate ATR earlier than MGMT+ cells, it was imperative to be able to recapitulate the phenotype observed through western blotting. Previously published data in the laboratory showed an increase in phosphorylated CHK1 levels, a direct downstream substrate of ATR¹⁰⁹ (**Figure 1.9**). However, when first attempting to repeat these western blots, I was met with great difficulty despite attempting the western blot numerous times and changing various conditions (**Figure 3.5**). This led me to extensively optimize a protocol for a CHK1 immunoprecipitation (IP), allowing me to pull-down with CHK1 and probe for pCHK1. The development of this novel protocol would also ensure a greater signal and decreased noise, to enhance the signal to noise ratio compared to a whole cell lysate western blot.

After many attempts with multiple protocols and minute changes, I optimized the CHK1 immunoprecipitation as detailed in Section 2.4 (**p. 22**). After seeding cells in 15 cm dishes and waiting to harvest until confluent, I was left with sizable cell pellets for lysis. The initial lysis volume was kept low at 200 μ L per pellet to increase the concentration of the lysate. The protein lysates were bound at equal concentrations, no less than 1 mg of protein per sample, to increase the signal of pCHK1 expression. Before the overnight binding step, I increased the volume of lysates, beads, and antibody to 1 mL in wash buffer to allow greater surface area for the binding to occur. After many attempts, a successful IP showed increased and earlier ATR activation through pCHK1 levels in MGMT- cells after various concentrations of TMZ treatment (**Figure 3.6**).

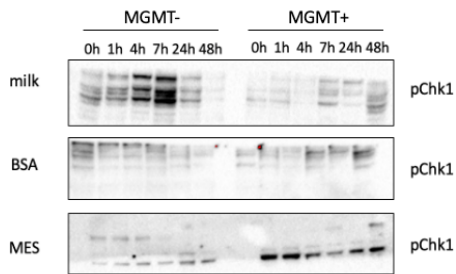
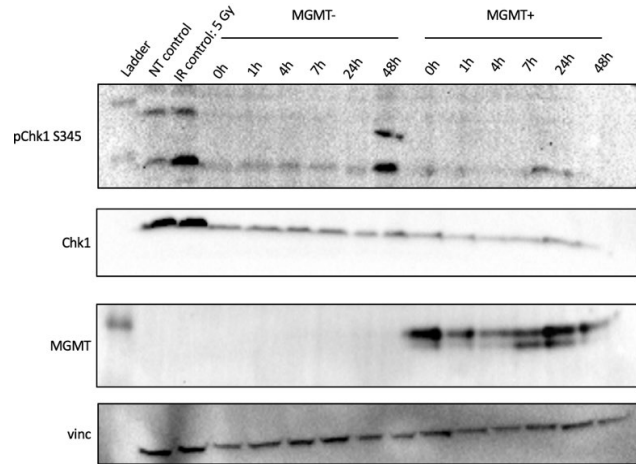
A**B**

Figure 3.5. Attempts at pCHK1 western blot. Failed attempts at probing for pCHK1 after (A) changing blocking conditions from 5% milk to 5% BSA, to using a MES gel instead of the typical MOPS gel, and (B) setting up the experiment multiple times without success. This led me to develop a very optimized CHK1 immunoprecipitation protocol.

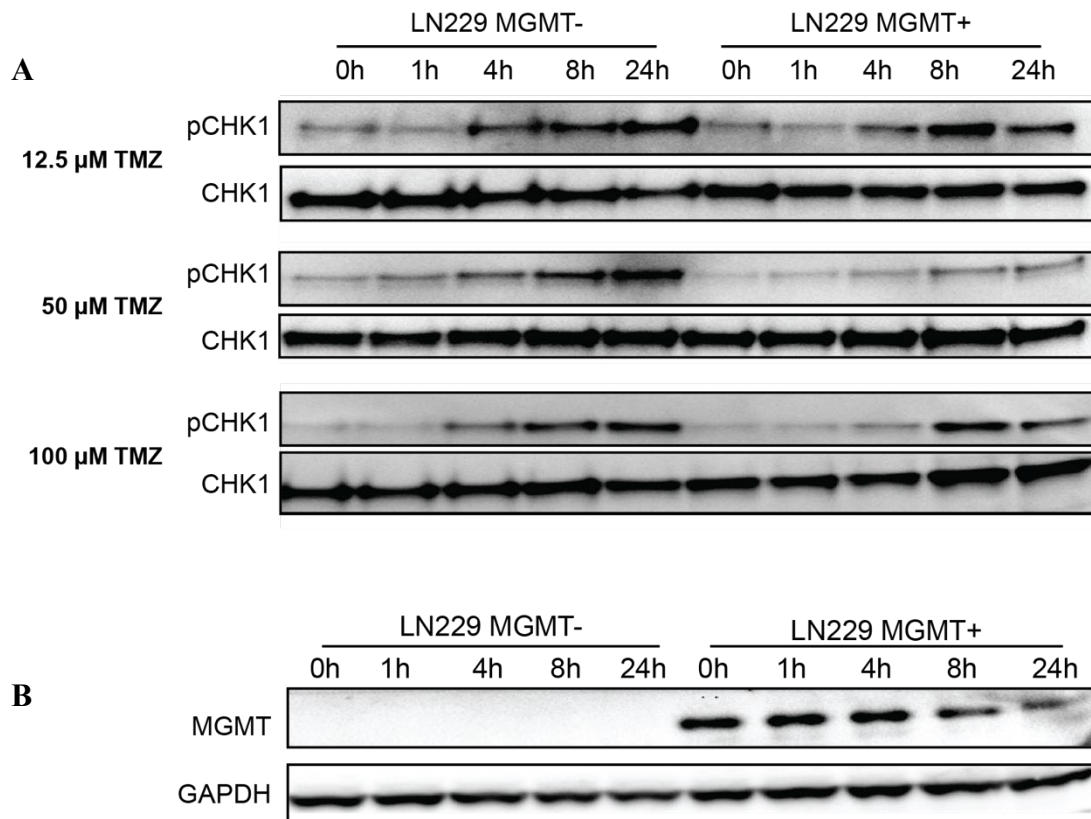


Figure 3.6. Successful CHK1 immunoprecipitation showing earlier ATR activation in MGMT- cells with temozolomide treatment. (A) IP with various concentrations of TMZ showing increased pCHK1 levels at 4h in MGMT- compared to MGMT+ cells. (B) Whole cell lysate showing MGMT status.

3.3. Discussion

Validating the cell lines and recapitulating the phenotype seen previously is valuable before proceeding further with experiments, as it also confirms the legitimacy of newer work. In this chapter, I authenticated the LN229 MGMT- and MGMT+ cells through many techniques including short-term cell viability assays and the clonogenic survival assay. From this, I confirmed that the MGMT- cells are sensitive to TMZ compared to the MGMT+ cells. Additionally, I recapitulated the phenotype that the MGMT- cells have earlier ATR activation seen through pCHK1 levels upon TMZ treatment compared to the MGMT+ cells in an immunoprecipitation.

For most of my research, I focus on using LN229 glioblastoma cells although there are other options for glioblastoma cell line models. These cell lines include U87 glioblastoma cells, T98G glioblastoma cells, and U251 glioblastoma cells (though these cells are later used briefly in **Chapter 5**).

U87 cells are a hypodiploid cell line, with most cells containing about 44 chromosomes as opposed to the 46 chromosomes found in healthy human cells. This cell line forms tumors in nude mice, making it a suitable option for our *in vivo* studies. However, the origin of this cell line has not been fully confirmed as glioblastoma and has been deemed to be “likely” from glioblastoma of the central nervous system origin¹¹⁷. Though this cell line has been used extensively in the literature presumed as glioblastoma cells, I preferred to use a glioblastoma cell line that had had its origin confirmed prior.

T98G cells contain a hyperpentaploid chromosome count, meaning most cells have between 128 and 132 chromosomes. Additionally, these cells exhibit stationary G₁ arrest *in vitro* making them a poor candidate for cell cycle studies, which will be a technique

employed later in **Chapter 6**¹¹⁸. These cells are also not tumorigenic in nude mice, proving difficult for potential *in vivo* studies. T98G cells express high levels of the MGMT enzyme at baseline, which means that MGMT must be silenced to create an isogenic cell line pair as a model system¹¹⁹. Though O⁶-benzylguanine has been used to silence MGMT in cells, it is a transient silencing method and would not be applicable for long-term experiments or in the clinic³⁰. It would be possible to complete a CRISPR knockout of the MGMT enzyme, but this poses more challenges with potential off-target effects from the guide RNA. Thus, using the isogenic LN229 pair with the MGMT+ overexpression cell line would prove to be more suitable for the experiments proposed going forward.

Finally, the U251 cell line is thought to be derived from a glioblastoma. However, controversy arose when there were similarities between the U251 cell line and the U373 cell line, both originating from the same laboratory in Uppsala, Sweden¹²⁰. Because of the confusion in identity between cell these lines, I chose not to use the U251 cell line as the first choice for a glioblastoma cell line model. Because of these reasons listed, the LN229 cells were the best option to proceed for further investigation and mechanistic studies.

One thing to consider is that the original paper from our laboratory shows ATR activation in MGMT- cells; however, ATR activation is still present in the MGMT+ cells at later time points as seen from the western blot (**Figure 1.9**). This suggests that the ATR pathway could be activated in the MGMT+ cells, given increasing pCHK1 levels after 48 hours, or that the cells could be suffering from other toxicity and damage leading to ATR activation¹²¹. However, this is broad speculation and further studies to probe the kinetics of ATR activation depending on MGMT-status are required. The increase in pCHK1 levels were also seen in the immunoprecipitations that I optimized. Interestingly, it seems that

different concentrations of TMZ affect ATR signaling through pCHK1 levels over time. For example, it appears that the higher concentrations of TMZ at 50 μ M and 100 μ M induce greater ATR activation earlier in the MGMT- cells over time, and the MGMT+ cells never reach the same pCHK1 levels. This data prompts additional experiments to see how TMZ concentration can affect ATR activation in MGMT- vs. MGMT+ cells and would shed light on optimal dosing concentrations for enhanced therapeutic gain in glioblastoma patients.

Overall, this chapter covered the validation of the LN229 MGMT- and MGMT+ cell lines and provided rationale for using these cell lines over other models. In future parts of this dissertation, I will continue with the LN229 cell line model which will be key in creating the MMR knockdown cell lines as discussed in **Chapter 4**.

4. Chapter 4: Creation of shRNA mismatch repair knockdown cell lines

4.1. Introduction

As mentioned previously, using the correct cell line model is fundamental when looking to characterize the role of a specific protein. Because I am interested in understanding the role of individual MMR proteins in ATR activation, I needed to create controlled isogenic cell lines with knockdowns for the individual MMR proteins in both the *MGMT*- and *MGMT*+ setting. This will allow me to study how the specific knocked-down MMR protein may play a role in ATR activation upon TMZ-induced damage, and whether *MGMT*-promoter methylation is involved in this intricate pathway as well.

To this end, I focused on creating the shMMR cell lines in the LN229 glioblastoma cells. MMR mutations are commonly found in cancers ranging from glioblastoma to colorectal cancer and ovarian cancer; however, treatment with TMZ has been largely confined to glioblastoma, making the LN229 glioblastoma cells a perfect model in which to study the role of MMR. I chose to use the short hairpin RNA (shRNA system), which is based on creating a protein knockdown. This means that there would be reduced protein expression, compared to the CRISPR/Cas9 system which would be used to create a total protein knockout. Glioblastoma patients who present with MMR-mutations often show reduced expression of the MMR protein and not complete ablation of protein expression, making the shRNA system better than CRISPR/Cas9 for my purposes⁸⁹.

The shRNA system is based upon the discovery of RNA interference (RNAi), which is a powerful tool to study the roles of protein and gene function. shRNAs are

artificially engineered RNA molecules consisting of a tight hairpin turn that is used to silence gene expression and thus reduce protein expression^{122,123}. There are two main types of shRNAs available for use, including single stem-loop and microRNA (miR)-adapted shRNA. The shRNA constructs used in this study to create the knockdown cell lines are miR-adapted shRNA with the pGIPZ lentiviral vector. These shRNA constructs are expressed as miRNA-30 primary transcripts, which allows for a Drosha processing site in the hairpin construct to increase the efficiency of gene silencing. The specific shRNAs I am using consist of a hairpin stem with 22 nucleotides (nt) of a double strand RNA (dsRNA) and a 19 nt loop from miR-30. To increase both Drosha and Dicer processing, the hairpin contains the miR-30 loop and 125 nt of miR-30 flanking sequence. Increasing Drosha and Dicer processing allows for shRNA production and higher chance of expressing the hairpins for gene silencing (Technical Manual GIPZ Lentiviral shRNA from Horizon Dharmacon).

Drosha and Dicer are the required processing enzymes involved in shRNA knockdowns. Typically, in the cytoplasm, Dicer cleaves large double stranded structures, such as the dsRNA from our shRNA construct, into shorter fragments^{122,123}. The dsRNA fragments are then split into single strand fragments and bind the RNA-induced silencing complex (RISC). These fragments guide the RISC complex to a specific gene of interest, where the single stranded RNA binds to the mRNA of the gene of interest, resulting in its cleavage. Similarly, in the nucleus the miR processing enzyme is known as Drosha. After processing by Drosha, the miRNA is translocated from the nucleus to the cytoplasm, where it is processed by Dicer and ultimately results in translational inhibition of protein expression.

The shRNA pGIPZ lentiviral vector acquired from Horizon Dharmacon is shown in **Figure 4.1**. A key feature of this plasmid is the Amp^R marker, or ampicillin resistance marker. This marker is important during the initial steps of plasmid preparation from the glycerol stock, to know that I can perform the miniprep and midiprep in the presence of ampicillin and that bacteria that do not have the construct will die due to lack of the Amp^R marker. Some additional important features to point out in this vector are the turboGFP (tGFP) tag and the puromycin resistance (Puro^R) marker. The tGFP will be key in visualizing whether the cells have taken up the plasmid under the fluorescence microscope. Additionally, I can select the cells with puromycin and cells that do not have the construct will die from lack of the Puro^R marker. A more detailed vector map is shown in **Figure 4.2**.

In this chapter, I describe how I created shRNA knockdowns of human MSH2, MSH3, MSH6, MLH1, and PMS2 in the LN229 MGMT- and MGMT+ cells. I performed successful plasmid preparation of all the shRNA glycerol stocks, isolated plasmid DNA with midiprep, produced lentiviral particles in HEK293T cells, and performed viral transfection in LN229 MGMT- and MGMT+ cells. Then, I confirmed the polyclonal populations through western blot before a single cell limiting dilution for the monoclonal cell population and confirmed protein expression of single cell clones through western blot once again. Ultimately, I created isogenic MMR-deficient cell lines in the MGMT- and MGMT+ contexts which can be used as a valuable resource for studying the individual roles of these MMR proteins in this study and many going forward.

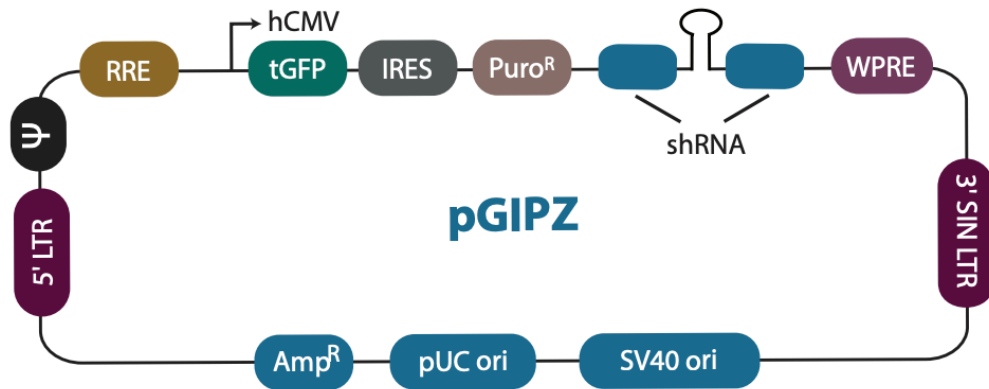


Figure 4.1. pGIPZ lentiviral vector purchased from Horizon Dharmacon.

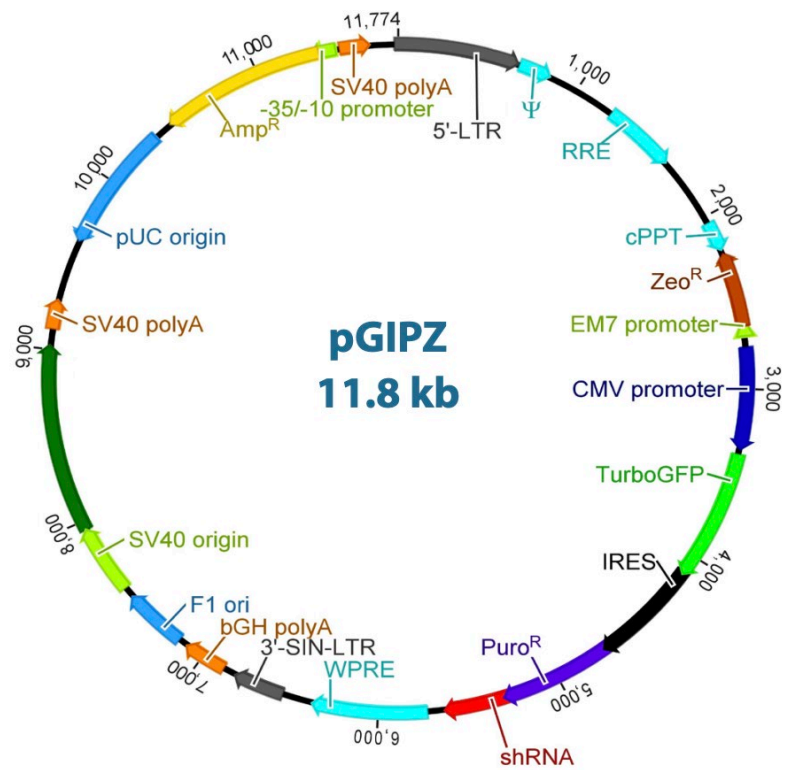


Figure 4.2. Detailed vector map of pGIPZ lentiviral vector purchased from Horizon Dharmacon.

4.2. Results

4.2.1. Plasmid preparation and restriction digest

To first create the MMR knockdowns, I acquired pGIPZ shRNA lentiviral vectors in the form of a glycerol stock for the MMR proteins of interest except for MSH2, of which was already available in the lab (**Table 2**). I thawed the glycerol stocks from the -80C and vortexed the tubes to resuspend any *E. coli* that may have settled to the bottom of the tube. I inoculated 10 μ L of each individual glycerol stock into 4 mL of Luria broth (LB) containing 100 μ g/mL of ampicillin. I incubated the cultures at 37C overnight with vigorous shaking. The next morning, I pelleted the cultures and performed a miniprep (Qiagen QIAprep Spin Miniprep Kit, 27104) to isolate the plasmid DNA from the bacteria. Then, I quantified the DNA isolated from each sample with a nanodrop spectrophotometer.

For the restriction digest, I added the compounds listed in **Table 4** in the order stated to a sterile PCR tube and mixed gently to avoid bubbles. I placed the PCR tubes at 37C for 15 minutes before loading on a gel along with undigested sample for comparison. The SacII digest should produce bands at 7927 bp, 2502 bp, and 1345 bp. After confirming the plasmid through restriction digest, I performed a transformation onto ampicillin plates using the successful minipreps, picked colonies to inoculate a starter culture, and then scaled up for a midiprep to obtain a higher concentration of DNA. I ran a SacII restriction digest on the DNA samples from midiprep and confirmed effective plasmid preparation (**Figure 4.3**).

Table 4. Restriction digest components to confirm shMMR plasmid preparation.

Component	Amount
Water, nuclease free	Up to 12.5 μ L
10X CutSmart Buffer	2 μ L
DNA sample in water	X μ L
6X loading dye	2 μ L
FastDigest Enzyme SacII	1 μ L

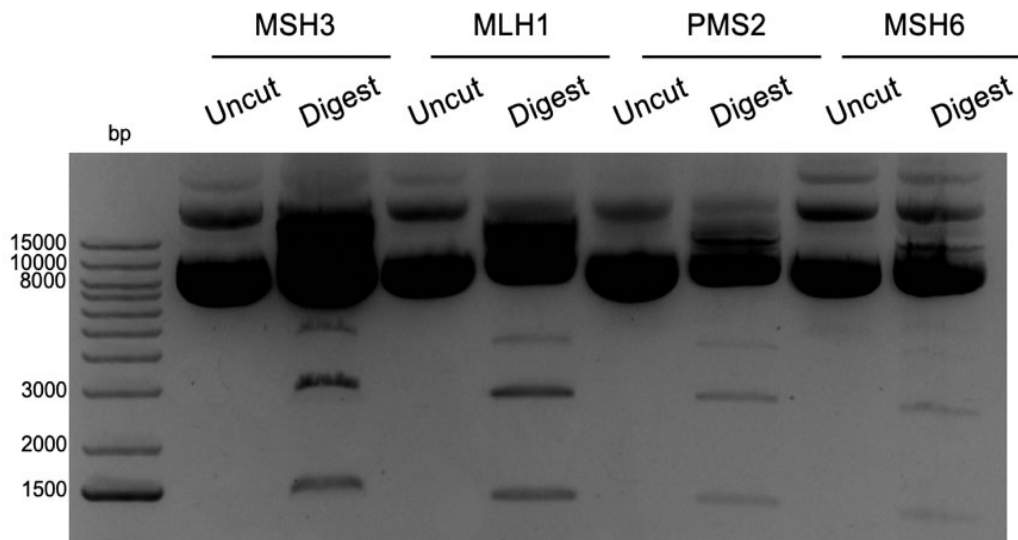


Figure 4.3. Successful restriction digest of shMMR plasmids with SacII after midiprep. After midiprep, the concentrations of DNA were 4.467 μ g/ μ L of MSH3, 2.719 μ g/ μ L of MLH1, 4.426 μ g/ μ L of PMS2, and 1.861 μ g/ μ L of MSH6. I loaded 2.5 μ g of DNA of each sample onto the 1% agarose gel containing ethidium bromide. In lanes that are digested, there are 3 bands indicating effective SacII digest of the plasmid.

4.2.2. Viral production and transfection

With the confirmed shRNA plasmid DNA for each MMR protein, I then proceeded with viral production in the HEK293T cells expressing the oncogenic SV40 large T-antigen¹²⁴. These cells have improved capacity for replication and expression of transfected plasmids, especially those containing the SV40 origin of replication, which all of the pGIPZ shRNA plasmids that I am using contain¹²⁵.

To produce lentiviral particles in 10 cm dishes of HEK293T cells, I proceeded with a reverse transfection, seeding cells prior to the transfection. I gathered two tubes: Tube A containing 2 µg of VSVG envelop plasmid, 18 µg of psPAX2 packaging plasmid, 20 µg of the shRNA plasmid DNA, 10 µL of P3000 buffer from the Lipofectamine 3000 kit and 500 µL of OptiMEM media, and Tube B containing 15 µL of Lipofectamine 3000 and 500 µL of OptiMEM media. I thoroughly mixed the components of Tube A and Tube B at a 1:1 ratio for a total volume of 1 mL and allowed the reaction to incubate for 15m at room temperature. Then, I added the 1 mL to the DMEM media with HEK293T cells and allowed cells to incubate at 37C for 48 to 72 hours, harvesting the viral media at both of those time points to ensure maximum viral production (**Figure 4.4**).

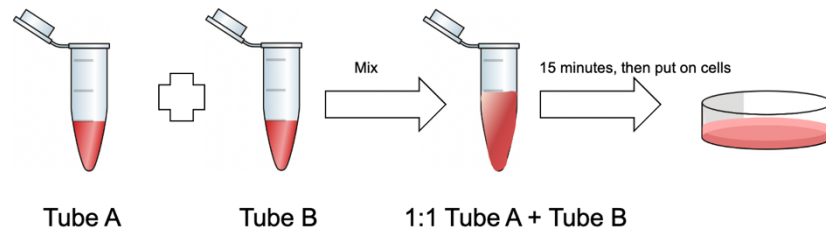


Figure 4.4. Schematic for lentiviral production with the Lipofectamine 3000 kit.

I mixed 500 μL of viral media with 500 μL of DMEM media and 8 $\mu\text{g}/\text{mL}$ of polybrene (which amounts to 0.8 μL) and transfected into 6-well dishes pre-seeded with MGMT- and MGMT+ cells with the shRNA MMR knockdown of interest. After 48 hours, I selected cells with 1 $\mu\text{g}/\text{mL}$ of puromycin for 3 to 4 days before confirming successful viral transfection of the polyclonal population by green fluorescence under the EVOS microscope due to the turboGFP vector found in the transfected shRNA plasmids (**Figure 4.5**). I performed western blotting to confirm the polyclonal population before proceeding with a single cell limiting dilution into 96-well plates. Single cell clones were not cultured in puromycin selection.

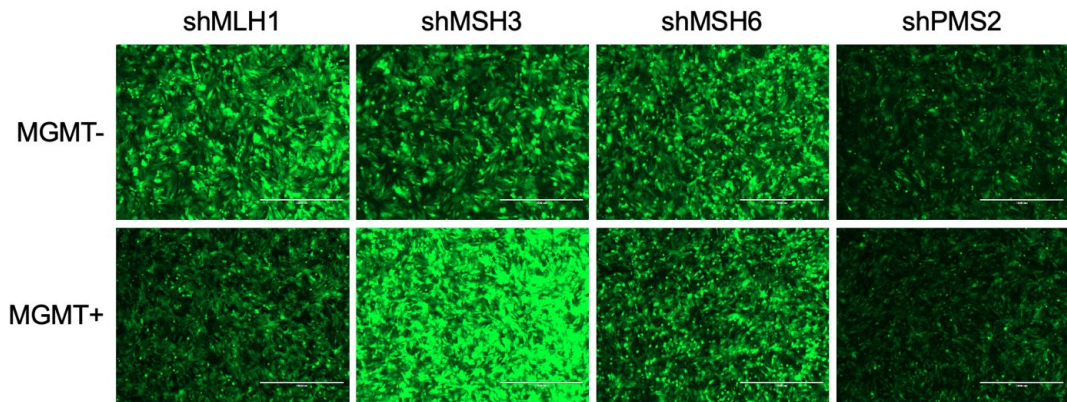


Figure 4.5. Images of polyclonal populations of LN229 cells with shRNA knockdown of interest. Images were taken with EVOS fluorescent microscope. Cells have taken up the shRNA plasmids of interest to varying degrees as indicated by the intensity of the green found in each image.

4.2.3. Screening of monoclonal shRNA knockdown cell line clones

After confirming the knockdown of the shRNA of interest in the polyclonal populations, I performed a limiting single cell limiting dilution where I attempted to seed 1 cell per well of a 96-well plate. The purpose of a single cell limiting dilution is to isolate a monoclonal cell population from one cell. This one cell will form its own colony of cells from the initial parent cell. This colony of cells is likely to be a homogenous population with the same genetic characteristics versus a more heterogeneous population of cells from the polyclonal population. After 1 week of seeding single cells, I began to screen the formation of colonies for green fluorescence under the EVOS microscope to look for clones that had successfully grown and taken up the shRNA plasmid of interest. After moving clones from 96-well plates to 24-well plates, to 6-well plates, I performed western blotting analysis to confirm the knockdown of the protein of interest from multiple monoclonal cell populations. An image of one of these western blots for the MGMT+ shMSH2 screen from various monoclonal cell populations is shown in **Figure 4.6**. The long exposure in the western blot is to be sure that the protein of interest is knocked down. Finally, I had created isogenic cell line models with MGMT- and MGMT+ for shRNA of MSH2^{*}, MSH3, MSH6, PMS2, and MLH1 cells (**Figure 4.7**).

*MGMT- shMSH2 cells were created previously in the lab by Christopher Jackson.

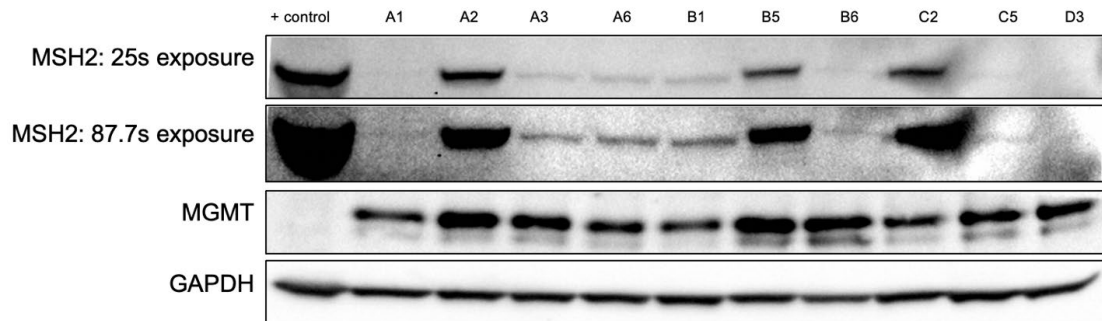


Figure 4.6. MGMT+ shMSH2 clone screening through western blot. This blot is a representation of the extensive screening process required to confirm each shRNA knockdown monoclonal cell population, taken with multiple exposures to ensure clean knock down and decrease in protein expression.

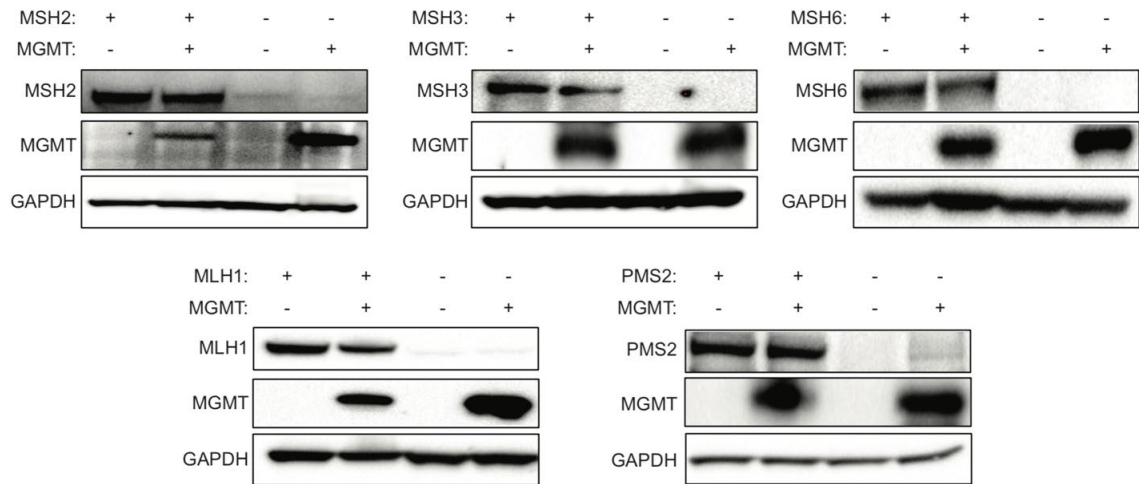


Figure 4.7. Western blot of shRNA mismatch repair cell line models. Each of these blots exhibit the parental LN229 MGMT- and MGMT+ cells in the left two lanes containing the functional MMR protein of interest. The right two lanes in all these blots contain the MMR protein knockdown of MSH2, MSH3, MSH6 (top panel, left to right), MLH1 and PMS2 (bottom panel, left to right).

It has not been described previously if mismatch repair protein knockdown would affect the stability of its heterodimeric partner. To this end, I ran a western blot on whole cell lysates of all the shMMR cell lines and probed for MSH2, MSH6, and MSH3 along with MLH1 and PMS2. I observed reduced levels of MSH2 protein in the shMSH6 cells similar to the levels seen in the shMSH2 cells, and reduced levels of MSH6 in shMSH2 cells. There was slight reduction of MSH2 in the shMSH3 cells as well (**Figure 4.8A**). These data suggest that MSH2-MSH6 is unstable when one of the heterodimeric components is knocked down, but the MSH2-MSH3 heterodimer remains somewhat stable. Additionally, knocking down MLH1 did not seem to affect the expression of PMS2 as much, indicating that this heterodimer may be functional even when the expression of its partner is knocked down (**Figure 4.8B**).

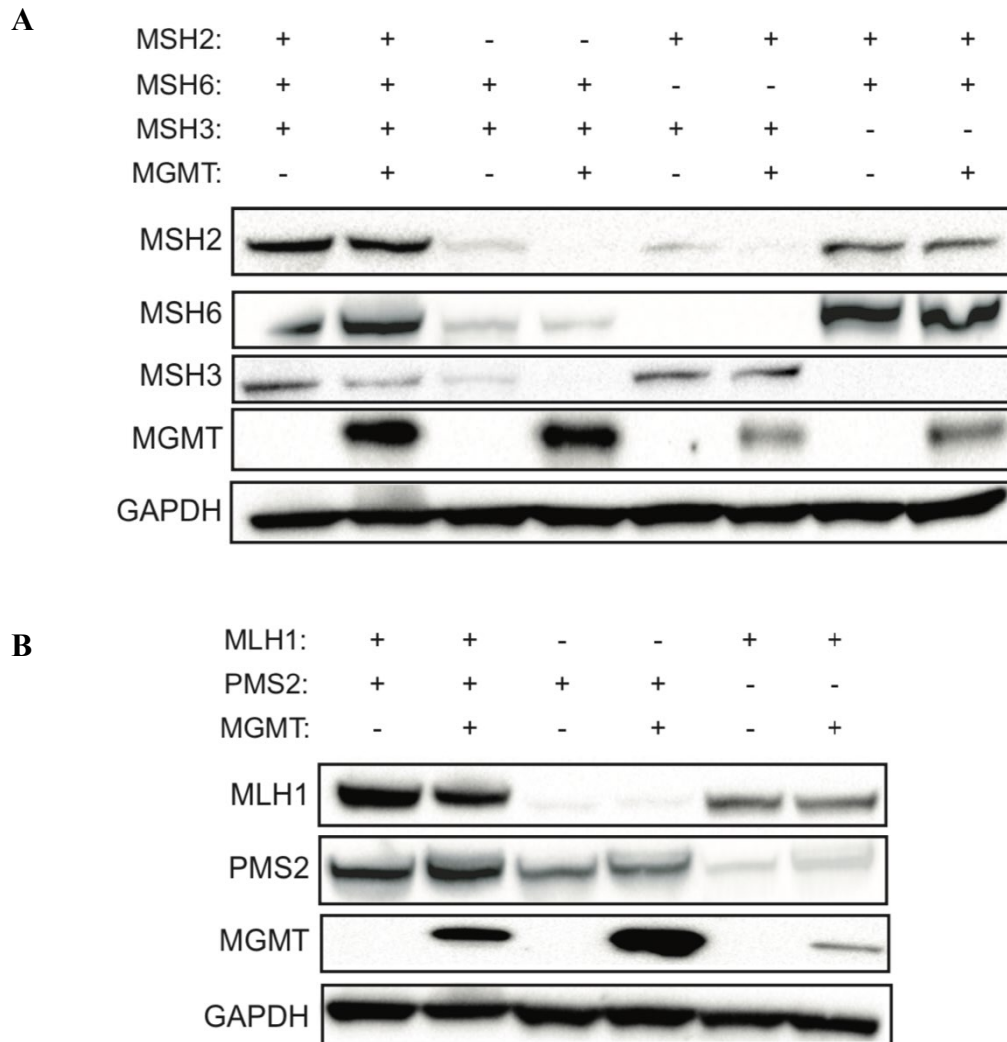


Figure 4.8. Western blot of stability of shMMR proteins and their heterodimeric partner(s). (A) shMSH2 and shMSH6 cells are more affected by each other's knockdown than the shMSH3 cells, but not the shMSH3 knockdown affects MSH2 and MSH6 levels. (B) shMLH1 and shPMS2 are only slightly reduced in levels upon knockdown of their heterodimeric partner.

4.3. Discussion

In this chapter, I detailed the creation of the ten isogenic LN229 shMMR cell lines in the MGMT- and MGMT+ context. I showed the validation of the successful plasmid preparation through a restriction digest on a 1% agarose gel, the images of the pooled cell populations under the fluorescent microscope to show transfection efficiency, and the western blots of the monoclonal populations of all the shMMR cells. The creation of these cell lines will allow me to study the role of individual MMR proteins as it relates to ATR activation upon TMZ-induced damage in the MGMT- and MGMT+ settings.

Though the western blots of the monoclonal populations show clean bands, the process to validate the antibodies for the MMR proteins was arduous. Before creating the shMMR cell lines, I had begun by creating transient siRNA knockdowns of the MMR proteins for siMSH2, siMSH3, siMSH6, siMLH1, and siPMS2, to confirm the antibodies for these proteins before proceeding with the laborious and lengthier process to create the shMMR cells. There were numerous times where I proceeded with the western blot as normal and the antibodies I had previously confirmed did not work. Specifically, I had difficulty with MLH1 since I was able to confirm the MLH1 antibody in the siMLH1 cells, but it took additional time to confirm the shMLH1 cells due to the antibody not working as it had done prior. MSH6 also provided great difficulty, where I attempted six different antibodies with various blocking buffer conditions and was not met with great success. Finally, after many attempts I was able to optimize and validate all the antibodies used to confirm the shMMR cells at the correct molecular weights. The information for these antibodies can be found in **Table 3**.

Lentiviral production in the HEK293T cells has been widely used for its ability to create high titer virus stocks for viral transfection into the cells of interest. I did not perform multiplicity of infection (MOI) calculations on the virus created for all the shMMR cells. MOI is a measure of the ratio how many viral particles are present to infect the number of host cells. For example, an MOI of 1 means that there is 1 viral particle to infect 1 cell. The higher MOI number indicates a higher ratio of viral particles to host cells, suggesting a higher level of transfection efficiency. There could have been repercussions by not calculating the MOI in that the viral titer was not high enough to effectively knock down the protein of interest. The lack of concentrating the virus could have also reduced the efficiency of the protein knock down. In the future, it is vital to create a concentrated high titer virus and keep track of the MOI to be confident in the potential transfection efficiency.

There are advantages and disadvantages to creating and using monoclonal populations instead of using the polyclonal population for experiments. Using a monoclonal population can be considered riskier due to any genetic aberrations that may be specific to that one clone compared to a more heterogeneous polyclonal population of cells. A good example of this is looking at the levels of MGMT in the western blots for the shMMR MGMT⁺ clones as seen in **Figure 4.6**. Through the selection of single cells that grow into a population of new cells, the levels of MGMT vary between clones and compared to the LN229 MGMT⁺ MMR-proficient cells. This was commonly seen as I screened dozens of clones. In many cases, I purposely chose to use the clones that contained very high expression of MGMT, since I did not want any confusion of whether there was MGMT expression or not. To avoid biasing the selection of monoclonal cells populations, the polyclonal population may be used instead.

The selection and screening of dozens of clones through western blotting can be thought of as an inefficient process. There are other screening methods that could expedite this process. One of these ways is through using a 96-well plate reverse transcription PCR (RT-PCR) to measure the levels of RNA in the cells. If the shRNA knockdown was successful, then there should be reduced levels of the mRNA from that MMR gene in the cells. The 96-well plate format would allow the screening of many clones at once in replicates and would allow us to see whether the RNA levels are lower in the shMMR cells versus the controls. Another option for screening the monoclonal cells takes advantage of the tGFP construct found in the shRNA lentiviral vector. The tGFP construct allows cells that have taken up the shRNA to fluoresce green. These cells can be sorted through fluorescence activated cell sorting (FACS) for GFP. This system can be employed at large scale in 96-well plates and can screen hundreds of clones much faster than collecting cell pellets for western blotting. There are new technologies such as the WOLF cell sorter from nanocollect that would allow for the rapid sorting of GFP+ cells at high efficiency in either 96-well plates or even 384-well plates. Though these are some additional options for expediting monoclonal population screening, ultimately visualizing and quantifying protein expression with western blotting is considered the best readout to see if the shRNA knockdown was successful.

Overall, this chapter comprehensively covered the creation of the shMMR cell lines. In future chapters of this dissertation, these cell lines will be used heavily and thoroughly investigated for the role of individual MMR proteins in ATR activation upon TMZ treatment. Further, these cell lines can be used in other applications to study the role of MMR proteins upon treatment with other drugs and in other relevant pathways.

5. Chapter 5: Response of mismatch repair knockdown cells to temozolomide and ATR inhibitor

5.1. Introduction

With the newly created the shMMR cell line models in the MGMT- and MGMT+ context, I wanted to begin to test the function of individual MMR proteins upon TMZ-induced damage and see how MGMT-status plays a role if any. Understanding how these cells respond to the treatment of TMZ is imperative in learning how to treat these MMR mutations in patients. Additionally, about 50% of cancers have a methylated *MGMT* promoter so investigating the role of MGMT-status along with MMR-status can provide us with novel information that may be useful in the clinic. Finally, MMR mutations are common in recurrent glioblastoma where patients have been shown to be resistant to TMZ; thus, learning about the intricacies of the MMR mutations can be beneficial to create more targeted therapies or new biomarkers for patients with cancer^{87,88}.

To identify how cells are responding to drug treatment, the first experiment to perform is a short-term cell viability assay, or growth delay assay, in which one assesses the growth of the cells upon varying concentrations of drug treatment. In this assay, between 500 and 2000 cells are plated in each well of a 96-well plate in triplicate before drugging with 10 concentrations of a monotherapy drug of choice, in a serial dilution from highest to lowest concentrations. A serial dilution allows for testing of a large concentration range of drugs. After three to six days of treatment, the cells are fixed, stained, and imaged. Short-term cell viability assays are a good first measure of gauging working concentrations for drugs in a variety of cell lines. Because different cell lines will respond differently to

drug treatment, it is imperative to begin with this assay in all the shMMR cell lines before proceeding with other assays.

After performing short-term cell viability assays to obtain a working concentration of drugs as monotherapy, it is important to use this data for performing 2-drug synergy assays. This assay allows for the experimentation of two different drugs for maximum cell kill. Synergy assays are like short-term cell viability assays in that they are setup in a 96-well plate format. However, each plate of a synergy assay is its own replicate, so it is necessary to set up triplicate plates. From the 2 drugs used for synergy assays, one will have the opportunity to test up to 10 different concentrations in a serial dilution, and the other drug can be tested with up to 6 different concentrations. The goal of the synergy assay for my purposes is to see whether the shMMR cells affect synergy between TMZ and ATR inhibitor. If the knockdown of one MMR protein abrogates the synergy seen in the wild-type cells, then it suggests that the knocked down MMR protein is required for the synergy between the two drugs. This would then allow us to probe the mechanism behind the synergy.

Finally, the response of MMR deficiency to temozolomide and ATR inhibitor can be assayed using a clonogenic survival assay (CSA)¹¹⁶. To build up to the CSA, it is imperative that the short-term cell viability assays and synergy assays are completed to understand the optimal concentrations to use. Because a CSA is long-term assay, the concentrations of drug treatment are usually lower than what would be taken from the short-term cell viability assay or synergy assay; however, understanding the concentration range from those assays will be the deciding factor in the dosing regimen for the CSA. A CSA is considered the gold standard of assessing the efficacy of a drug treatment or

combination of drug treatment over the course of 10-16 days, compared to the shorter timeline for a synergy assay. For a CSA, cells are seeded in 6-well plates in triplicate over a range of concentrations, from 9,000 cells per well to 33 cells per well. This assay tests the ability of cells to undergo unlimited cell division and form colonies upon drug treatment. Because theoretically these cells can undergo unlimited cell division, the lack of cell colonies in an effective drug treatment condition suggests that the possibility for the tumor cells to be eradicated.

In this chapter, I employ the shMMR cell lines I created to test them for their sensitivity to TMZ as a monotherapy, sensitivity to TMZ and ATR inhibitors in synergy assays, and sensitivity to TMZ an ATR inhibitor in CSAs. Though these experiments may feel redundant between all the shMMR cell lines, it is important that I thoroughly investigate the role of individual MMR proteins for their role in TMZ-induced ATR signaling.

5.2. Results

5.2.1. shMMR cells response to TMZ and ATR inhibitor as monotherapy

I sought to investigate each MMR protein individually for its sensitivity to TMZ and ATR inhibitor. Thus, I began by performing short-term cell viability assays with the parental LN229 MGMT- cells and the LN229 MGMT- MMR-knockdown cells. I observed that the LN229 MGMT- cells are sensitive to TMZ as a monotherapy, as expected (**Figure 5.1**). Upon increasing doses of TMZ over a 6-day treatment, the MGMT- cells are sensitive and do not survive at high concentrations of the drug, whereas the shMSH2, shMSH6, shMLH1, and shPMS2 cells are resistant to TMZ treatment even at the highest concentrations. Interestingly, the shMSH3 cells are sensitive to TMZ as a monotherapy like the MGMT- parental cell line. Further, all cell lines regardless of MMR status are sensitive to the treatment of the ATR inhibitor BAY-1895344 as seen from single agent dose-response curves data taken from the Combobenefit synergy plots (**Figure 5.2**).

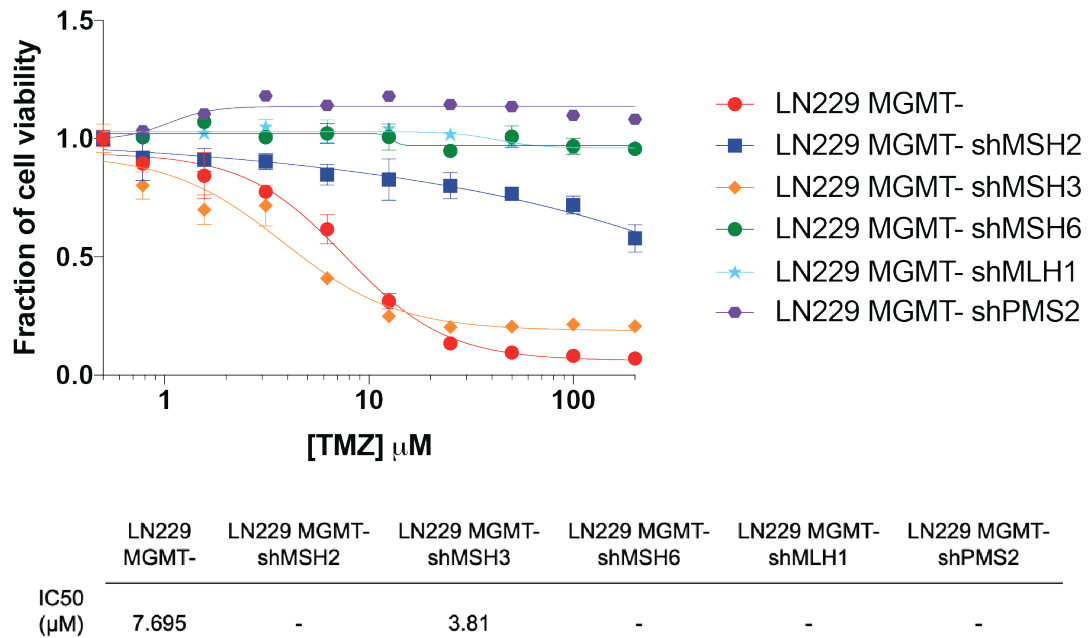
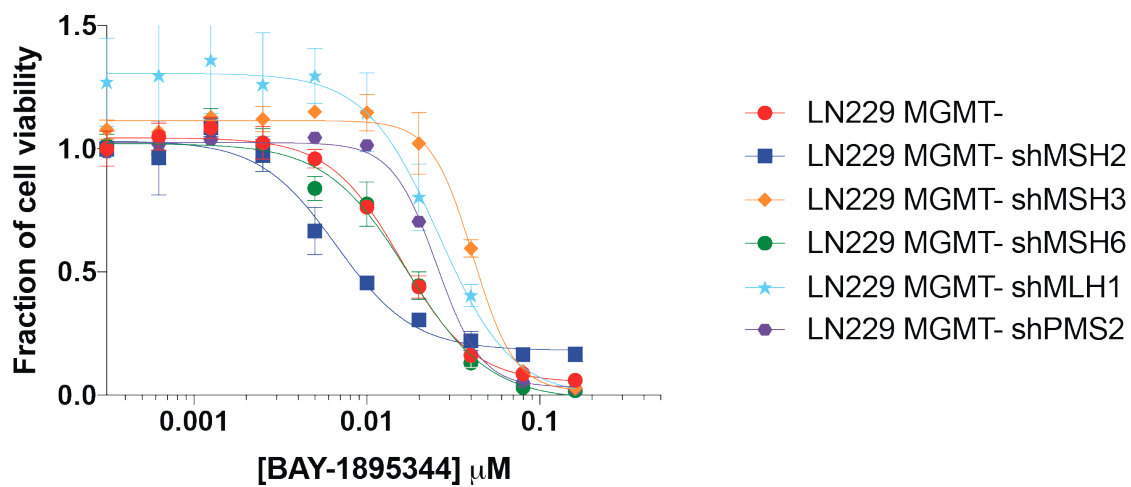


Figure 5.1. Short-term cell viability assay with temozolomide in MGMT- shMMR cells. shMSH2, shMSH6, shMLH1, and shPMS2 MGMT- cells are resistant to the treatment of temozolomide as a monotherapy at increasingly higher concentrations, and shMSH3 MGMT- cells are sensitive to temozolomide treatment like the MGMT- cells.



	LN229 MGMT-	LN229 MGMT- shMSH2	LN229 MGMT- shMSH3	LN229 MGMT- shMSH6	LN229 MGMT- shMLH1	LN229 MGMT- shPMS2
IC50 (μM)	0.01582	0.006655	0.04106	0.01717	0.026	0.02534

Figure 5.2. Short-term cell viability assay with BAY-1895344 in MGMT- shMMR cells.

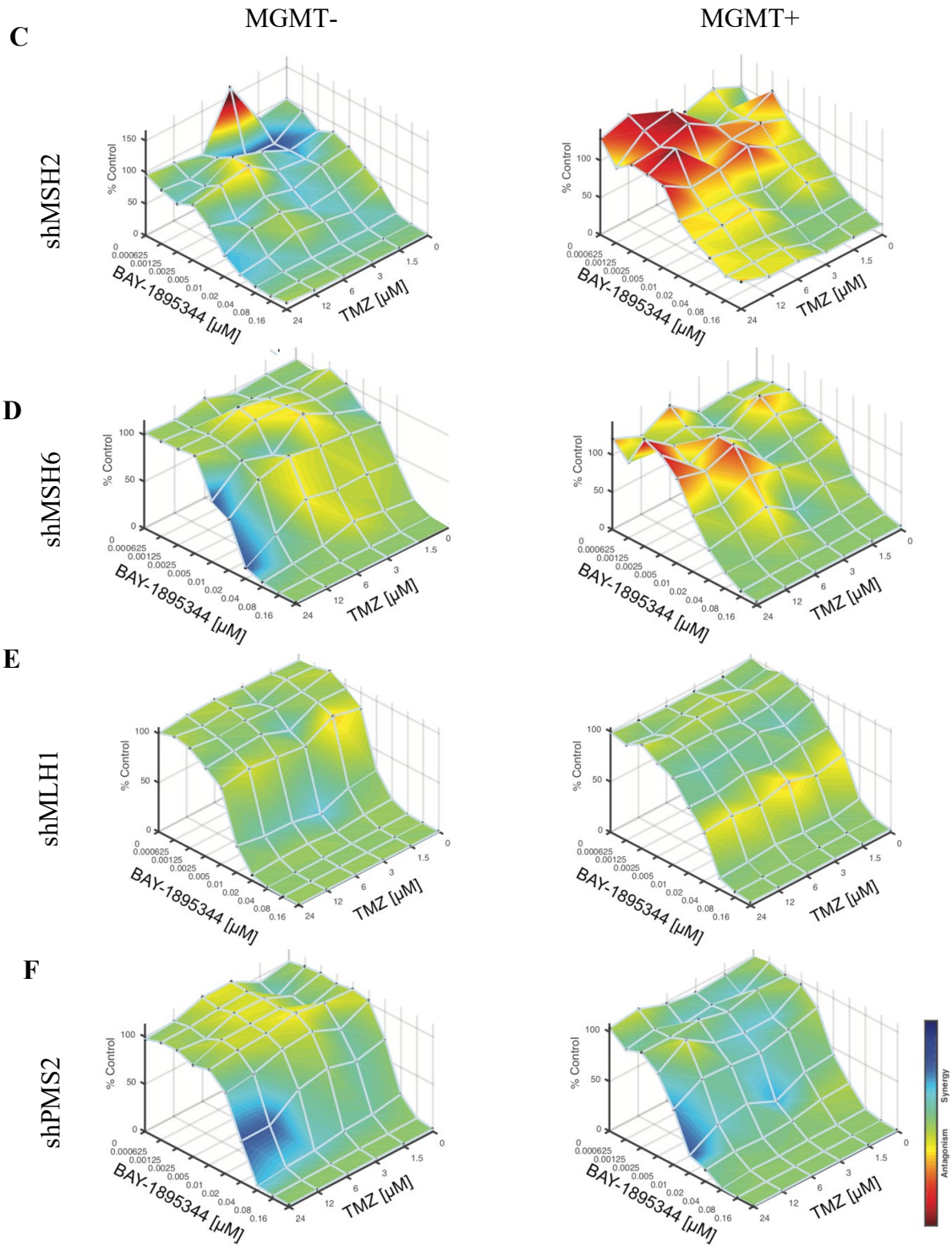
There is no significant difference in sensitivity between any of these cell lines.

5.2.2. Functional MMR is required for synergy between TMZ and ATR inhibitors

As our previously published findings have demonstrated, TMZ sensitizes MGMT-tumor cells to ATR inhibitors¹⁰⁹; however, it is unknown whether mismatch repair plays a role in this synergistic interaction. I tested if mismatch repair-deficient TMZ-resistant cells would be sensitized to the combination of TMZ and ATR inhibitor. As seen previously, I observe exquisite synergy in LN229 MGMT- cells when treated with TMZ and the ATR inhibitor BAY-1895344 which is not seen in LN229 MGMT+ cells (**Figure 5.3A**). I also observe synergy between TMZ and this ATR inhibitor in the MSH3-deficient cells (**Figure 5.3B**). However, cells with the mismatch repair deficiencies of MSH2, MSH6, MLH1, and PMS2, do not synergize with TMZ and BAY-1895344 (**Figure 5.3C-F**). This data suggests that the MSH2-MSH6 and MLH1-PMS2 heterodimers are responsible for attending to TMZ-induced mismatch lesions, as opposed to the MSH2-MSH3 heterodimer. Cells that are mismatch repair deficient and MGMT+ also do not exhibit synergy, indicating that *MGMT*-promoter methylation status and mismatch repair status are equally important for determining whether there are synergistic interactions between TMZ and ATR inhibitors.

I tested the synergistic combination of TMZ with another structurally unique ATR inhibitor, AZ-20. Once again, I observe that MSH2, MSH6, MLH1, and PMS2 are required for synergy between TMZ and this ATR inhibitor, whereas MSH3 is not (**Figure 5.4**).

Figure 5.3 continued from the previous page.



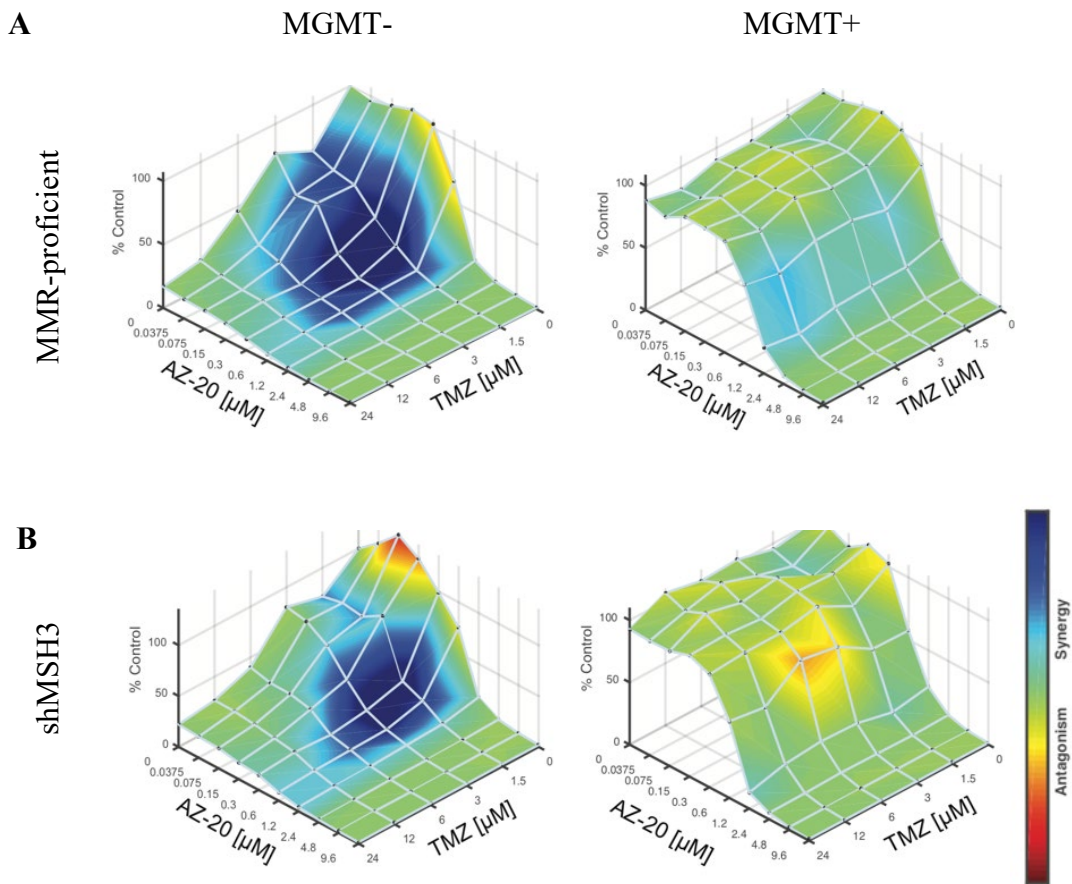
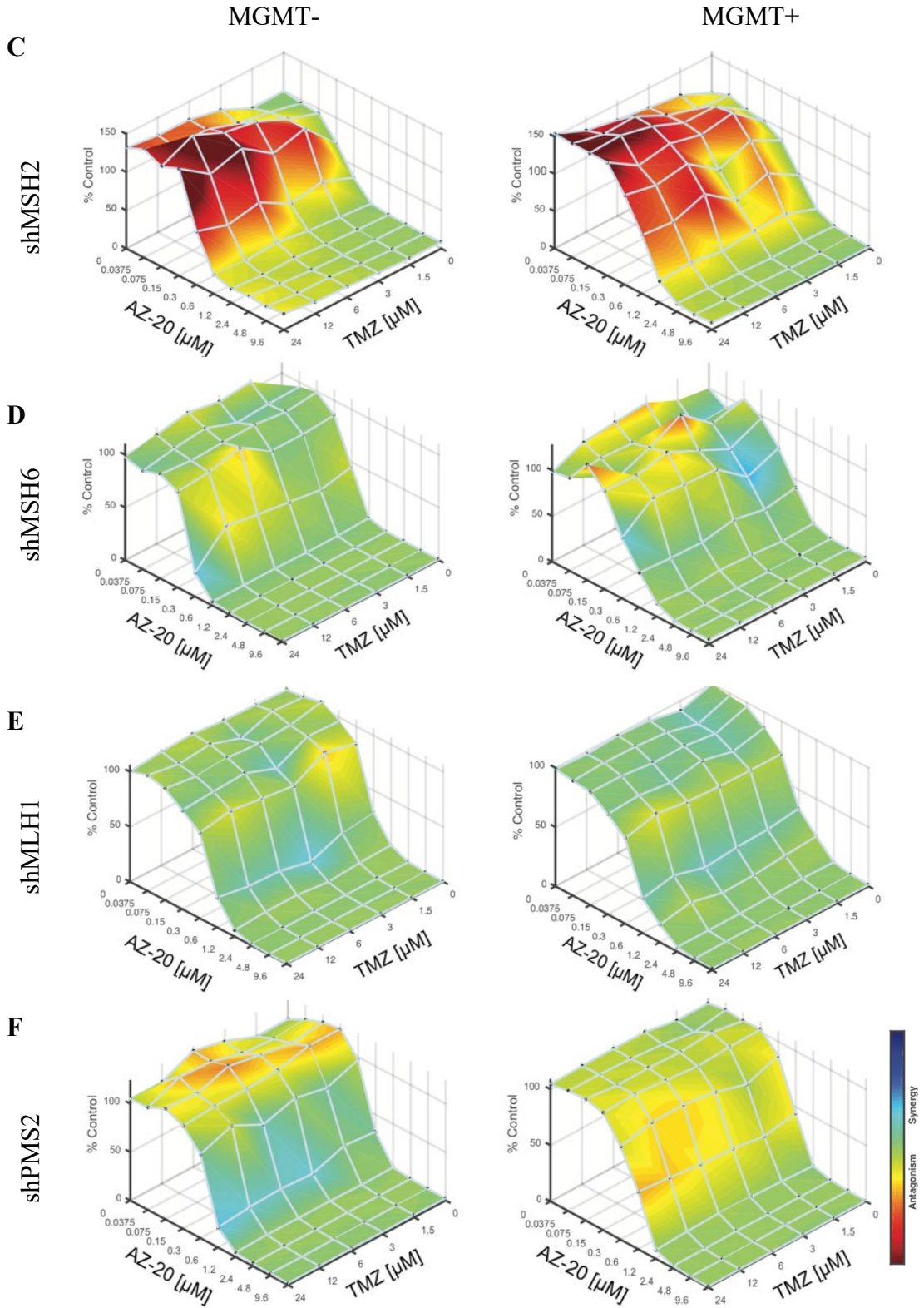


Figure 5.4. Synergy plots of shMMR cells with temozolomide and AZ-20. (A) MMR-proficient MGMT- cells and **(B)** shMSH3 MGMT- cells exhibit synergy when treated with the combination of temozolomide and AZ-20.

Continued on the next page:

(C) shMSH2, **(D)** shMSH6, **(E)** shMLH1, and **(F)** shPMS2 cells do not exhibit synergy when treated with the combination of temozolomide and AZ-20, regardless of MGMT-status.

Figure 5.4 continued from the previous page.



Further, I tested the synergistic combination of TMZ with a CHK1 inhibitor, as CHK1 is a direct downstream substrate of ATR. I observe synergy in the MGMT- cells and MGMT- shMSH3 cells but not in other MGMT- shMMR cells, suggesting that MMR proteins, besides MSH3, are implicated in the entire ATR/CHK1 signaling axis upon TMZ treatment (**Figure 5.5**).

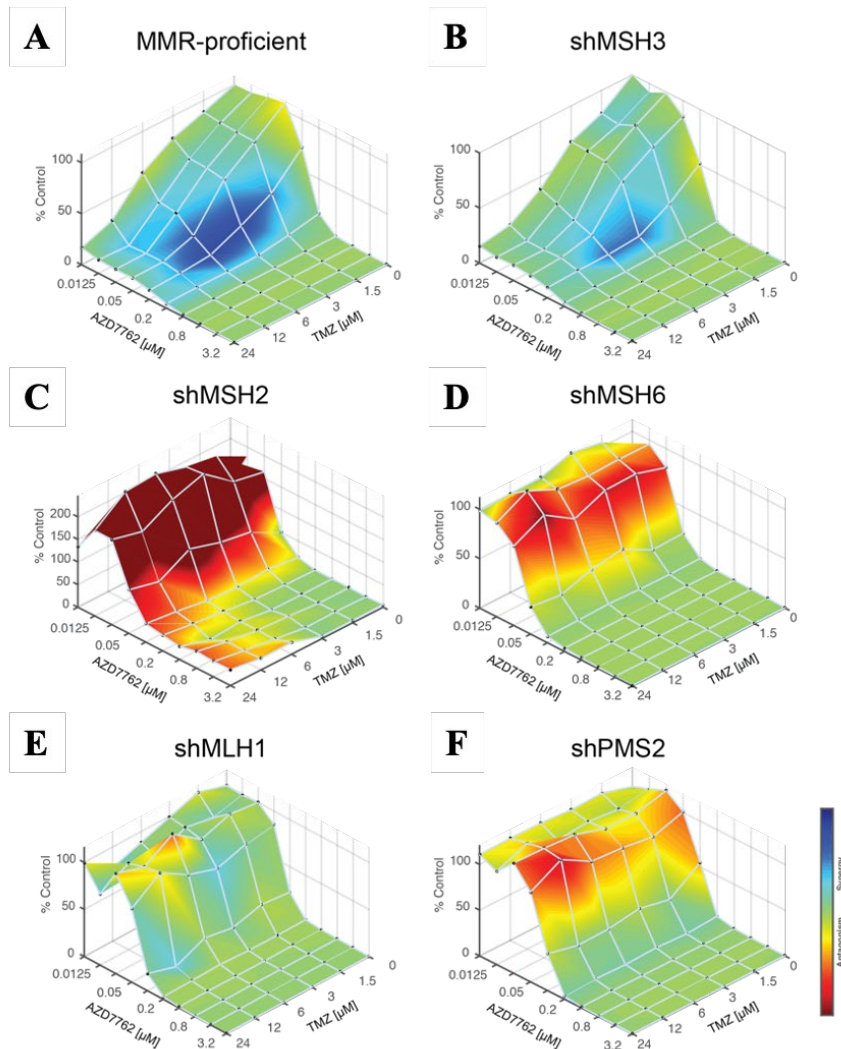


Figure 5.5. Synergy plots of shMMR cells with temozolomide and CHK1 inhibitor AZD7762. Synergy is abrogated in shMMR cells except for the **(B)** shMSH3 cells, indicating involvement of MMR in the entire ATR/CHK1 signaling axis.

I performed clonogenic survival assays using TMZ and the ATR inhibitor BAY-1895344. The LN229 MGMT- cells show sensitivity to TMZ alone, and I see increased sensitivity to the combination of TMZ and BAY-1895344. As expected from the synergy assays, the LN229 MGMT- shMSH3 cells were sensitive to TMZ and to the combination of TMZ and ATR inhibitor (**Figure 5.6A**). The LN229 MGMT- shMSH2, shMSH6, shMLH1, and shPMS2 cells are all resistant to treatment with TMZ, and furthermore, did not respond to the combination treatment of TMZ and ATR inhibitor (**Figure 5.6B-E**).

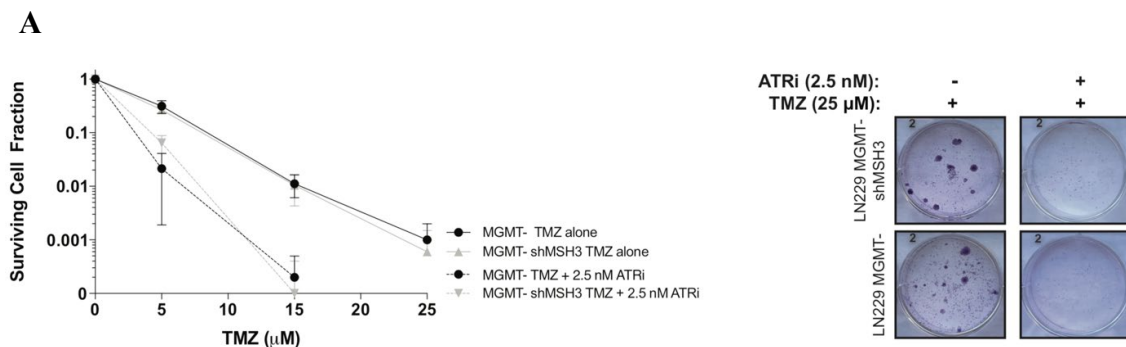
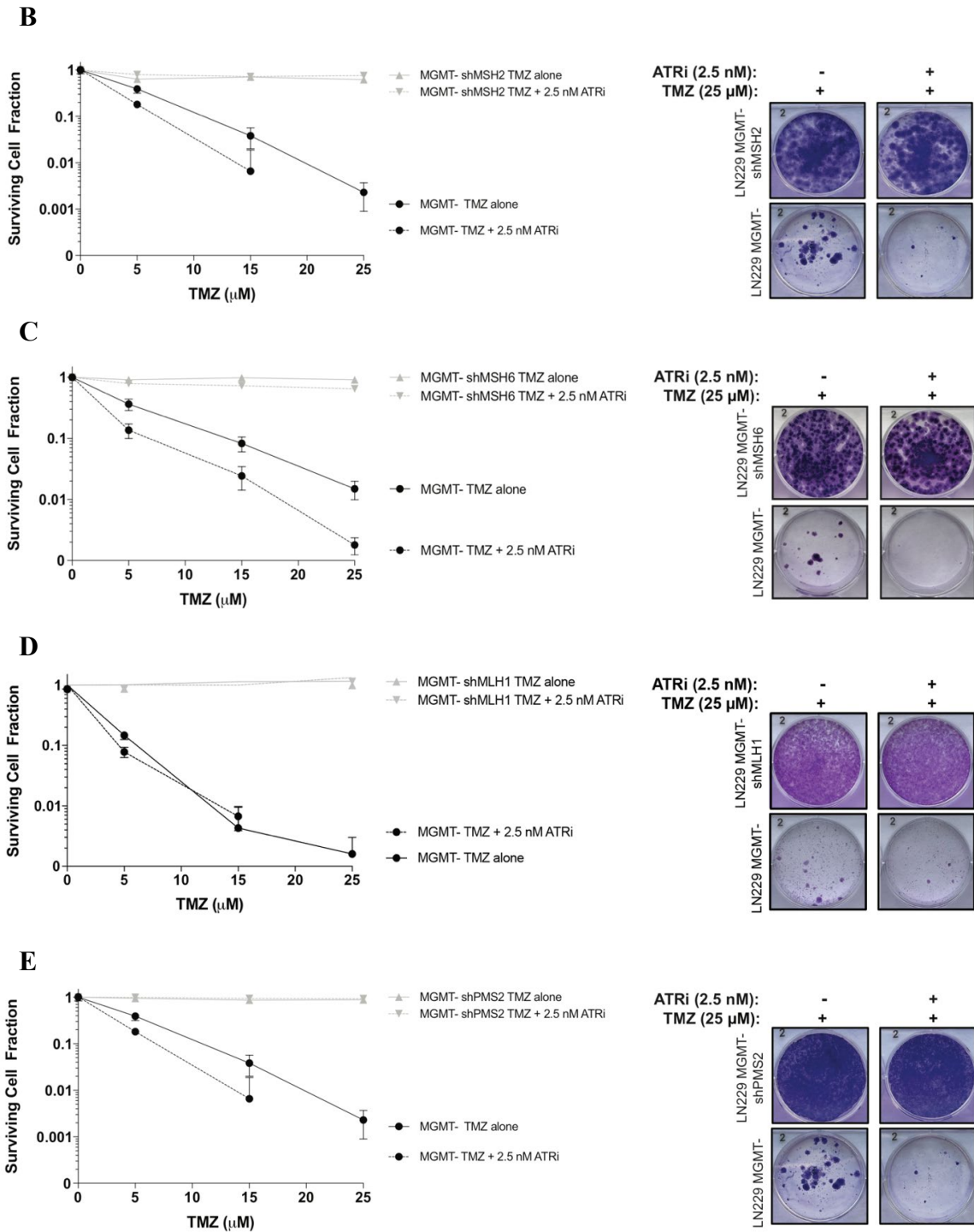


Figure 5.6. Clonogenic survival assay of shMMR cells with temozolomide and BAY-1895344. (A) shMSH3 MGMT- cells are sensitive to temozolomide treatment alone like the MGMT- MMR-proficient cells, and both the MGMT- and MGMT- shMSH3 cells are even more sensitive to the combination of temozolomide and BAY-1895344.

Continued on the next page:

(B) shMSH2, (C) shMSH6, (D) shMLH1, and (E) shPMS2 are not sensitive to temozolomide alone or the combination of temozolomide and BAY-1895344 in clonogenic survival assay.

Figure 5.6 continued from the previous page.



I wanted to know whether MMR would be required for the synergistic interaction between TMZ and other phosphatidylinositol 3- kinase (PI3K) inhibitors, or if this synergy is confined to ATR⁹². Thus, I tested whether mismatch repair proteins would be required in pathways with kinases similar to ATR, such as ATM and DNA-PK. Unlike with ATR inhibitor, ATM inhibitor AZD0156 and DNA-PK inhibitor AZD7648 did not display marked specificity for synergy in the LN229 MGMT- or LN229 MGMT- shMSH2 cells with TMZ (**Figure 5.7**). This suggests that mismatch repair proteins, like MSH2, are only implicated in the ATR pathway and not necessarily the ATM or DNA-PK pathways.

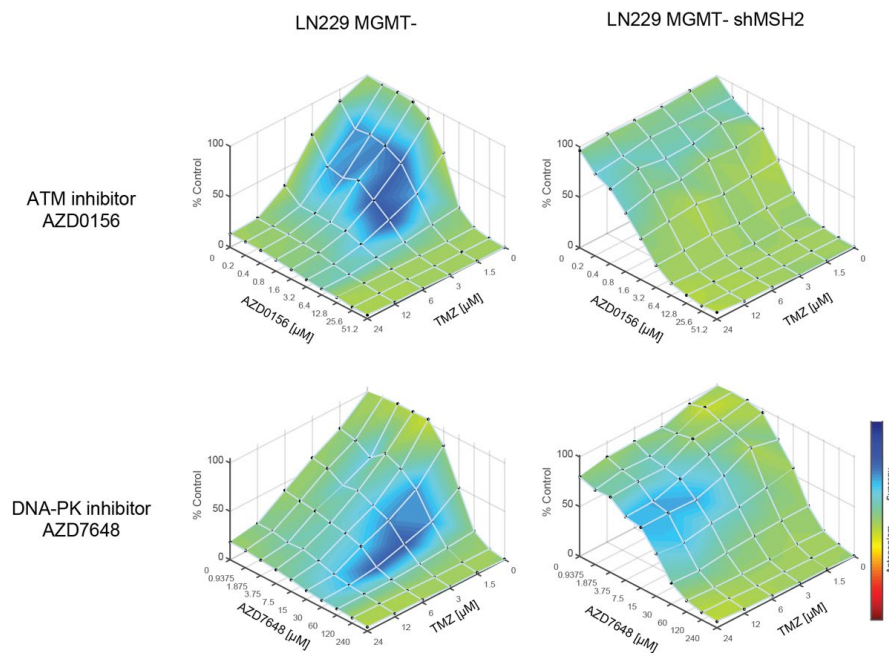


Figure 5.7. Synergy plots of MGMT- and MGMT- shMSH2 cells with temozolomide and ATM inhibitor or DNA-PK inhibitor. Cells do not display exquisite synergy between temozolomide and these other inhibitors as they did for ATR inhibitor.

Further, I recapitulated the mismatch repair deficiency phenotype observed in the LN229 MGMT- cells using another glioma cell line. I tested the combination of ATR inhibitor and TMZ in an isogenic glioma cell line model using U251 wild-type cells and U251 shMSH2 cells, which are both MGMT- (**Figure 5.8A**). As seen with the LN229 MGMT- shMSH2 cells, the U251 shMSH2 cells are also resistant to TMZ as a monotherapy (**Figure 5.8B**). Additionally, they do not exhibit synergy when treated with TMZ and ATR inhibitors and are resistant to TMZ with the combination of ATR inhibitor in a clonogenic survival assay (**Figure 5.9**). Collectively, these data suggest that mismatch repair is required for the synergistic interaction between TMZ and ATR inhibitors, and that mismatch repair could be involved in TMZ induced-ATR repair.

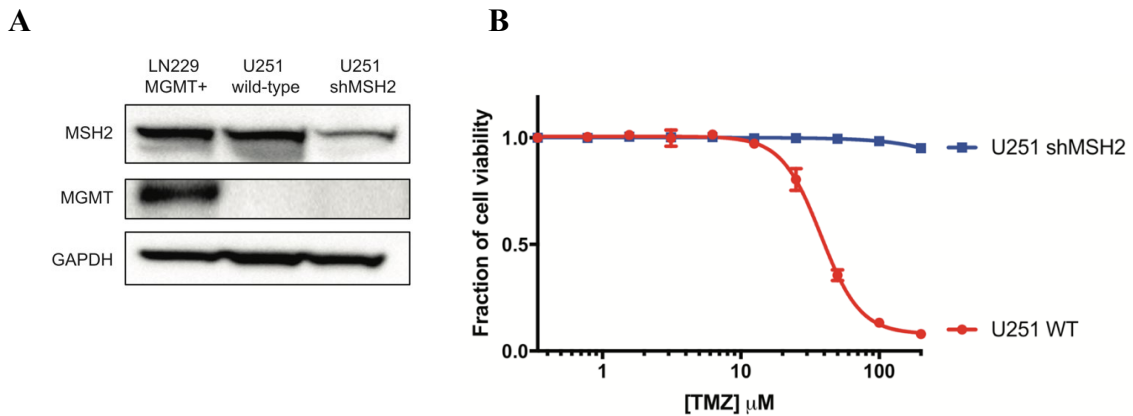
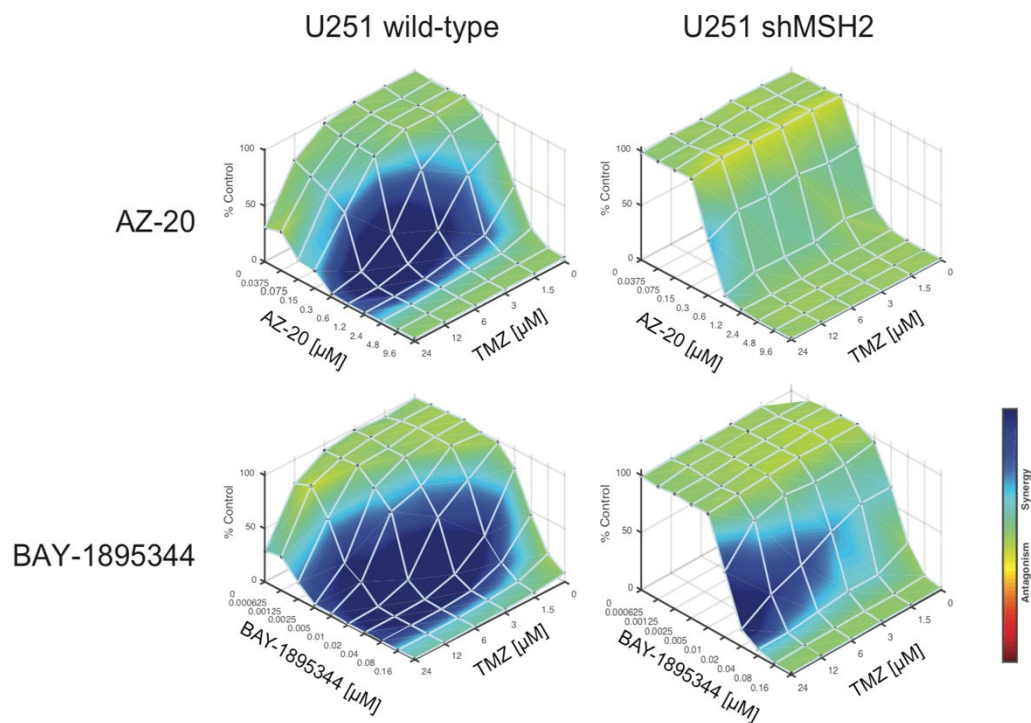


Figure 5.8. U251 shMSH2 glioblastoma cells behave similarly to LN229 MGMT-shMSH2 cells. (A) Western blot of U251 cells used in this study, showing MSH2 levels and lack of MGMT compared to LN229 MGMT+ MSH2-proficient cells. **(B)** Short-term cell viability assay showing that U251 shMSH2 cells are resistant to treatment with temozolomide compared to the U251 wild-type cells.

A



B

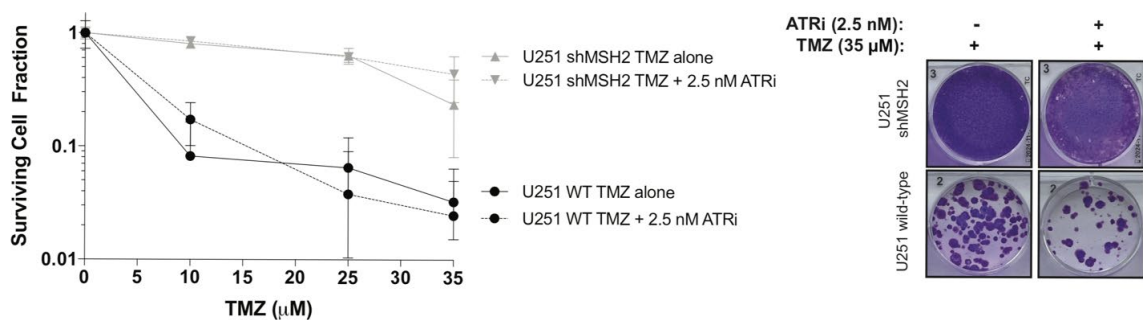


Figure 5.9. U251 shMSH2 cells are resistant to the combination of temozolomide and ATR inhibitor. (A) Lack of synergy in U251 shMSH2 cells with temozolomide and two different ATR inhibitors, BAY-1895344 and AZ-20 compared to U251 wild-type cells. (B) Clonogenic survival assay shows resistance to temozolomide or the combination of temozolomide and ATR inhibitor in the U251 shMSH2 cells compared to U251 wild-type cells.

5.3. Discussion

I began testing how MMR knockdowns would affect TMZ sensitivity and ATR inhibitor sensitivity, using the shMMR cells that I generated. In this chapter, I showed that all MMR knockdowns except for MSH3 are sensitive to TMZ as a monotherapy in short-term cell viability assays, though all shMMR knockdown cells are sensitive to ATR inhibitor as a monotherapy. Furthermore, I went to show that the knockdown of MSH2, MSH6, MLH1, and PMS2 abrogate the synergy seen between TMZ and ATR inhibitor in the MMR-proficient cells and the shMSH3 MGMT- cells. The data also suggests a dependence on MGMT-status as well, since the shMSH3 MGMT+ cells had an abrogation of synergy compared to the shMSH3 MGMT- cells. The shMMR MGMT- cells besides shMSH3 also had an abrogation of synergy upon treatment with TMZ and a CHK1 inhibitor, indicating a role for MMR proteins in the entire ATR/CHK1 signaling axis. Clonogenic survival assays corroborated the findings of the synergy assays as well. Overall, I showed that each MMR protein may have an individual role in ATR signaling.

The sensitivity of the shMMR cells to the ATR inhibitor alone may beg the question of why I would test synergistic combinations with TMZ. There has been minimal data showing the effect of ATR inhibitors in the MMR-deficient setting, so the data presented here is novel and had not been investigated previously¹¹⁰. Additionally, data previously published from our lab showed that TMZ sensitizes MGMT- cells to ATR inhibitors, yet the role of MMR in this interaction remained unclear until further investigation¹⁰⁹. It is interesting that even though the shMMR cells are sensitive to ATR inhibitor alone, the combination of TMZ and ATR inhibitor is not synergistic. This suggests that functional MMR is required for synergistic combination, and that ATR inhibitor is not potent enough

to overcome TMZ resistance in the MMR-deficient setting. Also, since I realized that the shMMR cells were all equally sensitive to ATR inhibitor, I did not attempt a condition in the CSAs with ATR inhibitor alone. I assumed the ATR inhibitor monotherapy in the CSA would have caused cell death and lack of colony formation in all the shMMR cells, as well as the MMR-proficient cells.

In addition to testing TMZ in combination with ATR inhibitors, I was also interested in seeing whether MMR plays a role in other PI3K pathways. There is slight synergy seen with both the ATM and DNA-PK inhibitors in the wild-type MMR-proficient cells, which is abrogated in the MSH2-deficient cells. This suggests some crosstalk between the PI3K pathways. However, the concentrations of these inhibitors used was much higher than what is physiologically applicable, thus further investigation into a better concentration range of these inhibitors in combination with TMZ would provide more accurate data regarding whether MMR is involved or not. Additionally, there are many commercially available ATM inhibitors and DNA-PK inhibitors which I could have continued to test, to confirm that MMR does not play a role in the activation of these kinases. I also only tested the TMZ with ATM/DNA-PK inhibitor combination in the shMSH2 MGMT- cells, which means other MMR proteins could be implicated in these pathways that I did not fully and thoroughly examine.

One may be considering why I did not use MMR-inhibitors in this study instead of knocking down cell lines and treating with TMZ and ATR inhibitors, as this would still allow me to study the role of MMR upon TMZ-induced alkylation damage and its role in the ATR pathway. However, there is little to no information on commercially available MMR inhibitors. The lack of MMR inhibitors is rational, as cancer patients usually present

with MMR-deficiencies and would need to reconstitute MMR function instead of inhibiting it. Though there have been some documented cases of MMR-overexpression, these are rare and do not usually affect genomic stability to a great extent¹²⁶.

Though I detailed my choice of the LN229 cells in **Chapter 3**, I performed a similar set of assays on an isogenic pair of U251 cells. I wanted to confirm that the phenotype seen in the LN229 shMSH2 cells were not confined specifically to that one cell line, to generalize the findings that MMR is required for synergy between ATR inhibitors and TMZ regardless of cell line. To be more thorough with the generalization of these findings, I should continue these experiments in other isogenic cell lines with various MMR-deficiencies. For example, our lab has a normal human astrocyte cell line with an isogenic pair containing an MLH1 knockout. In the future, I could use this cell line pair to test whether the MLH1 deficiency has similar effects across multiple cell lines. Additional studies performed in patient-derived xenograft (PDX) cell lines with an MMR-deficiency could also help to bolster the results of this study. If the findings repeat in these cell lines, then I can be confident that the MMR-deficient phenotype is generalizable and will perform in a predictable manner clinically.

The synergy plots shown here were calculated from a program known as Combobenefit, which allows for the synergy output in 3 different ways: the Loewe model, the Bliss model, and the highest single agent (HSA) model¹¹¹. This means that there are often inconsistencies when calculating and presenting synergy data because of the various options to choose from. Because the HSA model was used in the previously published paper from our lab, I chose to use this model to keep the results of my data consistent. The HSA approach is also known as the cooperative effect and is defined as synergy when the

effect of a drug combination is greater than the effect of the single drug components. This means that if the effect of drug A is arbitrarily “2” and the effect of drug B is arbitrarily “1”, synergy is defined as any combination that has a value greater than drug A, or “2”. This method uses the highest number from the effect of a single agent as a threshold instead of an additive effect which would prove to be of greater synergistic significance. In my opinion, the Bliss model is the better model for use in calculating synergy plots. The Bliss model states that if the effect of drug A is “2” and the effect of drug B is “1”, then synergy is defined as any drug combination that has a value greater than “3.” This method uses a higher threshold to calculate synergy, making the synergy seen more accurate and dependable compared to the HSA model.

Overall, this chapter began to explore the role of individual MMR proteins upon treatment with TMZ and ATR inhibitors through numerous, diverse assays. I found that MSH2, MSH6, MLH1, and PMS2 are likely involved in the ATR pathway but that MSH3 is not. This segues well into the next chapter of this dissertation, which begins to mechanistically probe the role of these MMR proteins as it relates to ATR upon TMZ-induced alkylation.

6. Chapter 6: Mechanism of DNA repair in mismatch repair knockdown cell lines

6.1. Introduction

After having created the MMR-deficient cell lines of interest and testing their response to TMZ and ATR inhibitors, I was interested in understanding the underlying mechanism of DNA repair. Often to identify the mechanisms of DNA repair, elucidating the proteins and components involved in signaling is essential.

Cell cycle analysis through propidium iodide (PI) staining can be used to measure the proportion of cells in each cell cycle upon various treatments and time points¹²⁷. The PI stain is stoichiometric and will bind in proportion to the amount of DNA present in the cell. This means that cells that are in S phase will have more DNA than cells that are in G₁, and thus will absorb more dye proportionally and fluoresce more brightly than the G₁ cells. The variation in intensity of the PI allows for the quantification of cell cycle stages. PI is the most commonly used dye in cell cycle analysis and it intercalates into the major groove of double stranded DNA¹²⁸. Typically, cells that are stained with PI produce a fluorescent signal when excited at 488 nm and a maximum wavelength at 617 nm. Even though the shMMR cells have the tGFP construct that can also be excited at 488 nm, the emissions of the PI and tGFP are at different wavelengths, reassuring us that there will be little to no interference between the PI staining and tGFP in the shMMR cells (**Figure 6.1**). PI staining can provide data to see whether treatment with TMZ is causing MMR-deficient cells to be arrested during a certain cell cycle stage. This data can then be used to investigate the DNA repair pathways more closely.

Immunofluorescence can be used to recognize specific proteins involved in DNA repair, as DNA damage will cause the recruitment of many of these repair factors in the form of foci. Each focus is meant to represent one protein at the site of damage; thus, quantifying the number of foci over time should be an indicator of the amount of DNA repair that is occurring¹²⁹.

There are two main repair factors that I am interested in studying, γ H2AX and pRPA32 serine 33 (pRPA32 S33). γ H2AX foci is a result of the histone H2 variant H2AX being phosphorylated at residue serine 139 by either ATR, ATM, or DNA-PK^{130,131}. These kinases will phosphorylate H2AX to signal a double strand DNA break. γ H2AX foci arrive quickly at break sites, making this marker an effective way to study how many DNA breaks are occurring throughout the genome¹³². Additionally, the γ H2AX foci serves to recruit other DNA repair factors such as proteins involved in homologous recombination or nonhomologous end joining for the repair of the DNA damage^{104,130}. In the field, the phosphorylation of γ H2AX is widely accepted as an early sign of DNA damage. Quantifying γ H2AX foci upon various treatment conditions and timepoints can be used as a direct readout for the accumulation of genomic damage.

Another repair factor that I am interested in studying is pRPA32 S33. Replication protein A (RPA) has three subunits: a 70 kilodalton (kDa) subunit, 32 kDa subunit, and 14 kDa subunit, sometimes also referred to as RPA1, RPA2, and RPA3 respectively¹³³. The phosphorylation of RPA32 at the serine 33 site is performed exclusively by ATR, so studying this phosphor-site specifically can provide valuable information about ATR activation in the shMMR cells¹³⁴. This phosphorylation occurs primarily in the late S and G₂ phases of the cell cycle, most likely where there are stalled DNA replication forks.

Moreover, pRPA32 S33 serves as a sign of replication stress, coating single-stranded DNA at stalled or collapsed replication forks¹³⁵. Mechanistically, studying pRPA32 S33 foci is reasonable and can provide insight into whether MMR-deficiencies potentially cause increased replication stress, increased stalled DNA replication forks, and ATR activation upon TMZ damage.

Finally, *in vivo* studies can be used to uncover the underlying mechanisms of various disease processes and to assess the potential safety and efficacy of new treatments¹³⁶. Here, I was interested in seeing whether the MMR-deficiencies affect the treatment of mice with TMZ or ATR inhibitor (or in combination). *In vivo* studies are seen as a middle ground between *in vitro* experiments and human trials. Thus, replicating my *in vitro* data to an *in vivo* model system provides greater impact of the entire study, and the findings here could potentially be translated to the clinic as a new biomarker for treatment.

In this chapter, I discuss experiments performed for cell cycle flow cytometry studies, immunofluorescence studies, and *in vivo* studies. The data from these experiments can be used to begin to piece together the mechanism of DNA repair in the shMMR cell lines.

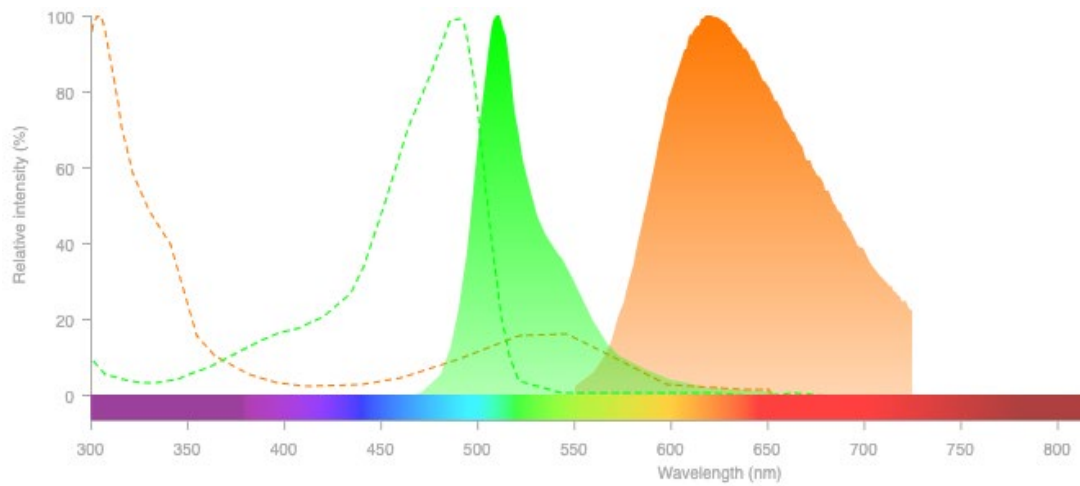


Figure 6.1. Fluorescence spectra viewer showing minimal overlap between GFP (green curve) and PI (orange curve). Image acquired from ThermoFisher.com.

6.2. Results

6.2.1. shMMR cells exhibit dysregulated cell cycling

I went on to probe the mechanism of distinct responses of MMR protein deficiencies upon TMZ-mediated damage. MGMT- cells treated with TMZ undergo G₂/M arrest in the cell cycle, which is thought to be due to ATR activation and CHK1 phosphorylation. I sought to understand whether mismatch repair deficiency would affect cell cycle progression and phase distribution. After treating cells with TMZ over the course of 48 hours, I stained the cells with propidium-iodide for cell cycle analysis using flow cytometry with the help of Dr. Amrita Sule. As seen previously from our lab's published findings, I observe an increase in G₂/M arrest in the MGMT- cells after 48 hours of TMZ treatment (**Figure 6.2A**). The MGMT- shMSH3 cells are arrested in G₂/M after 48 hours of TMZ treatment like the MGMT- cells (**Figure 6.2B**). The MGMT- shMSH2 cells do not exhibit G₂/M arrest, suggesting reduced ATR activation in these cells (**Figure 6.2C**). The MGMT- shMSH6 and shPMS2 and shMLH1 cells also do not appear to be arrested in G₂/M, but rather remain mostly in G₁ even after 48 hours of TMZ treatment (**Figure 6.2D-F**). This suggests that the knockdown of these MMR proteins (MSH2, MSH6, MLH1, and PMS2) does not activate ATR, leading to an abrogation of G₂/M arrest and a resumption of normal cell cycling. Another way of saying this is that these MMR proteins are required for ATR activation and G₂/M arrest.

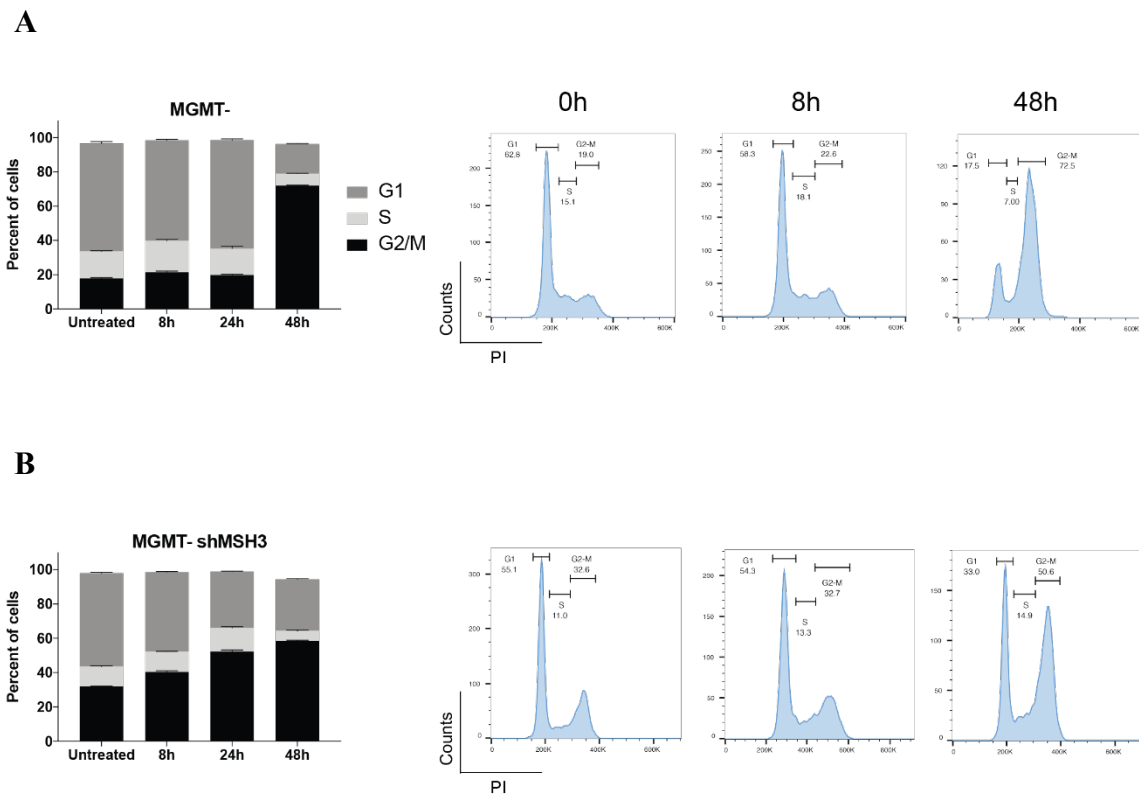


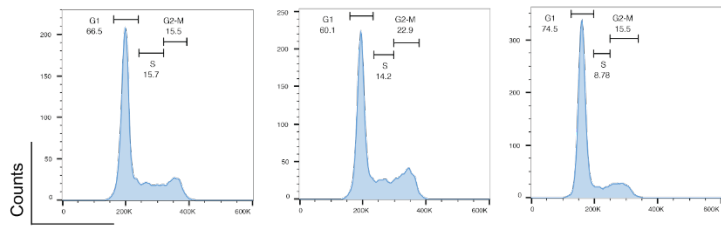
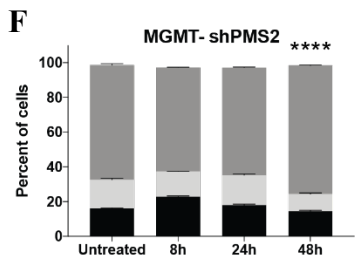
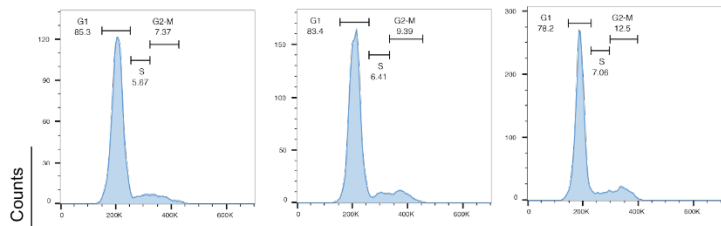
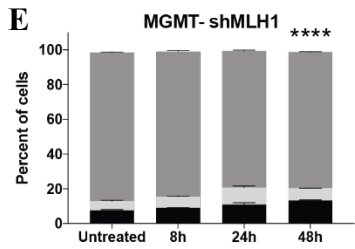
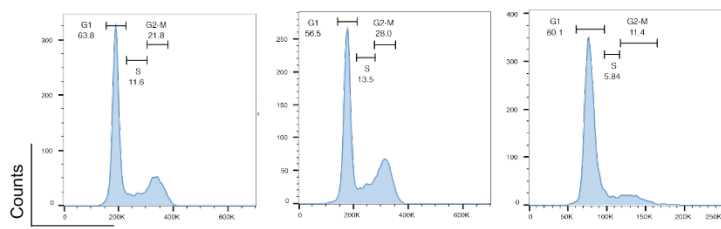
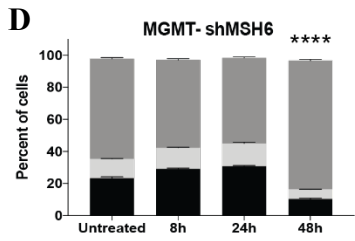
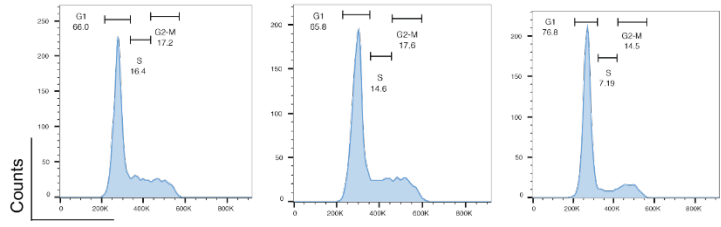
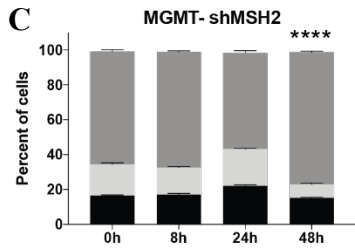
Figure 6.2. Flow cytometry plots of shMMR cells after treatment with temozolomide. (A) MGMT MMR-proficient cells and (B) shMSH3 MGMT- cells all exhibit elevated levels of G2/M after 48 hours of temozolomide treatment.

Continued on the next page:

(C) shMSH2, (D) shMSH6, (E) shMLH1, and (F) shPMS2 MGMT- cells all exhibit normal cycling compared to the untreated controls after 48 hours of temozolomide treatment.

Where indicated, **** $p < 0.0001$ comparing 48h G₂/M of MGMT- cells with others.

Figure 6.2 continued from the previous page.



6.2.2. shMMR cells exhibit increased DNA replication stress

Given that I observe dysregulation of cell cycle in MMR-deficient cells, I wanted to know if these cells had increased levels of replication stress. This can provide us with insight into why the TMZ/ATR inhibitor synergy is abrogated in several MMR-deficient cell lines. ATR phosphorylates RPA at serine 33, which serves as a sign of replication stress and can be observed through immunofluorescence. I also assessed the MMR-deficient cells for increased double-stranded DNA breaks over time with TMZ treatment, seen through γ H2AX immunofluorescence. In the MGMT- cells, there are low and steady levels of pRPA foci over time, suggesting that there is not much replication stress upon TMZ treatment (**Figure 6.3A**). However, I see an increase in γ H2AX over time, suggesting increased double strand breaks, consistent with previously published data (**Figure 6.3A**). MLH1 and PMS2 which comprise the MutL α heterodimer show increased pRPA and γ H2AX foci over time over 24 hours of TMZ treatment (**Figure 6.3B-C**).

The MGMT- shMSH2 cells showed increases in both pRPA and γ H2AX foci over time, though there was only a slight increase (**Figure 6.3D**). This indicates that there is a baseline elevated level of replication stress and double-stranded breaks in the MSH2 knockdown cells which stays consistent over time, compared to the MGMT-cells. MSH6 also shows baseline elevated levels of pRPA and γ H2AX. The pRPA levels decrease over 24 hours, indicating some resolution of replication stress (**Figure 6.3E**). In contrast, MSH3 which also partners with MSH2 sees increasing levels of pRPA and γ H2AX (**Figure 6.3F**).

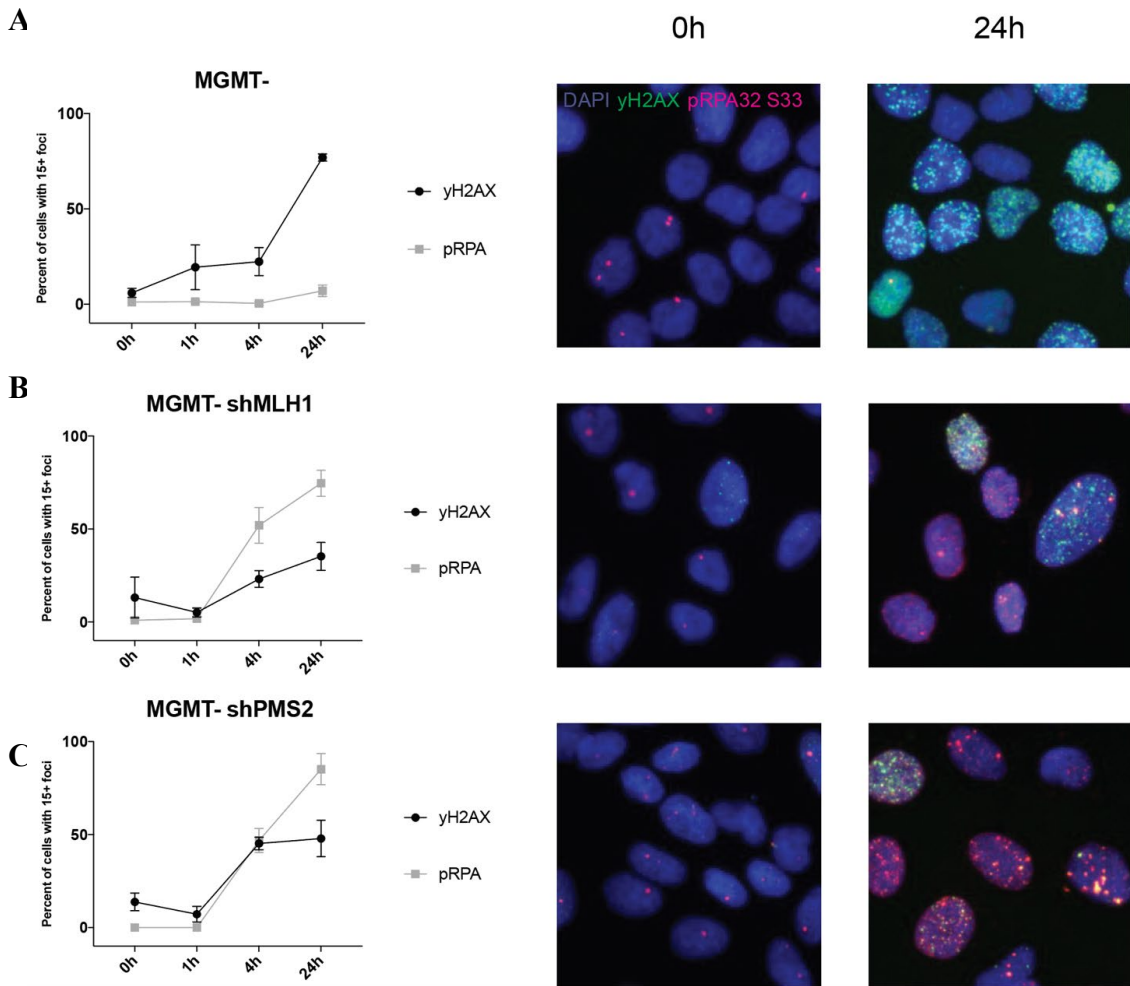
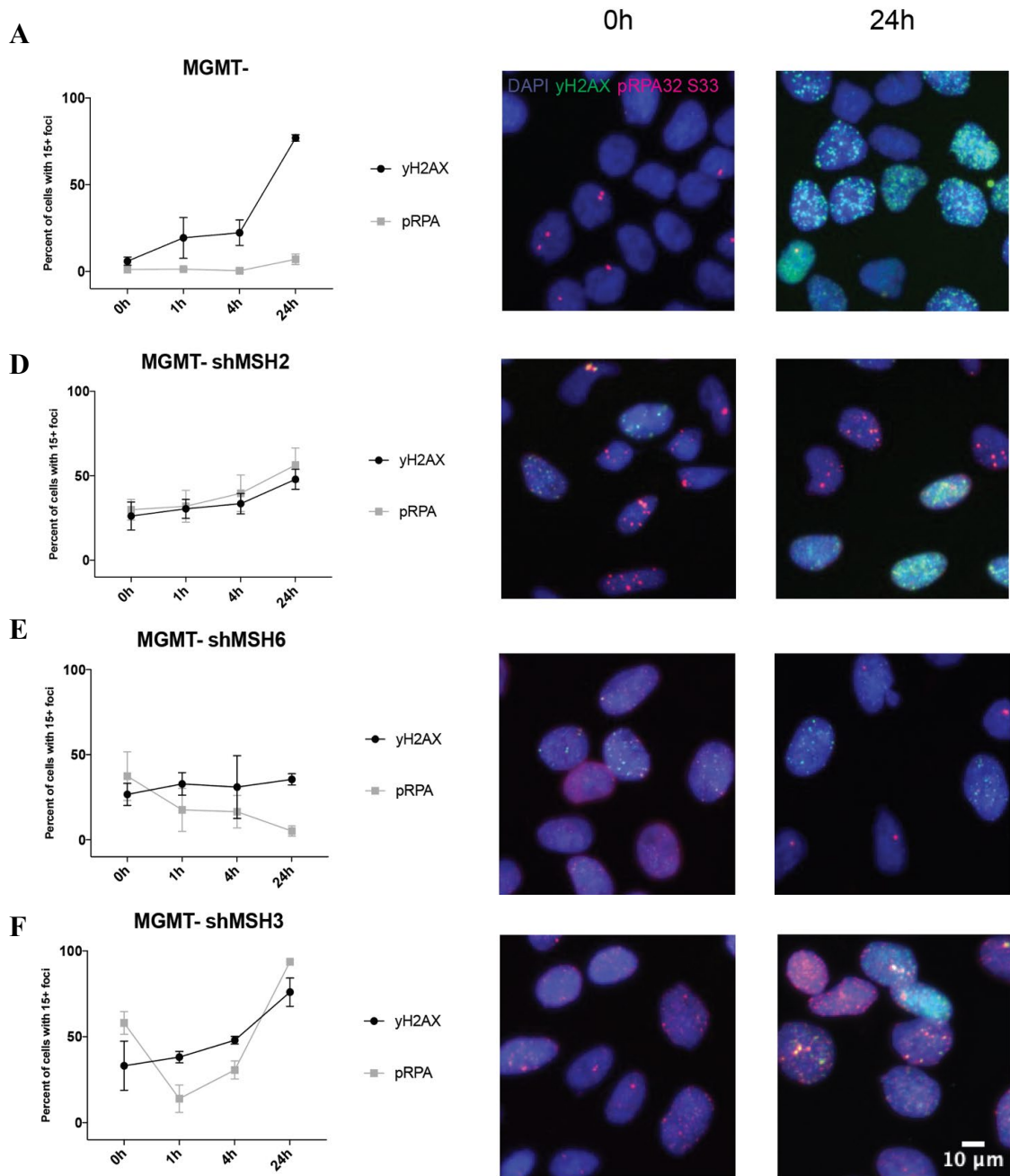


Figure 6.3. Immunofluorescence of pRPA and γ H2AX over time in shMMR cells after temozolomide treatment. (A) MGMT-, (B) shMLH1, and (C) shPMS2 MGMT-cells show increases in γ H2AX foci over time.

Continued on the next page:

(D) shMSH2, (E) shMSH6, and (F) shMSH3 MGMT- cells have increased baseline levels of pRPA and γ H2AX foci.

Figure 6.3 continued from the previous page.



6.2.3. *In vivo*, MMR is required for synergy between TMZ and ATR inhibitors

Finally, I tested the combination of TMZ and ATR inhibitor, VX-970, with *in vivo* flank tumor models using LN229 MGMT- and LN229 MGMT- shMSH6 cells with the help of Dr. Ranjini Sundaram. After 28 days of tumor growth, Dr. Ranjini Sundaram and I measured the tumor volumes of the mice and randomized them into four groups with similar mean starting tumor volume. Average tumor volume per group before beginning treatment was $81.0 \text{ mm}^3 \pm 1.36 \text{ mm}^3$ for LN229 MGMT-, and $89.6 \text{ mm}^3 \pm 1.31 \text{ mm}^3$ for LN229 MGMT- shMSH6. The treatment schedule was 4 days on/3 days off for a total of 21 days before a 14-day washout period. In those 4 treatment days, days 1 and 3 were reserved for TMZ treatment and tumor and weight measurements. Days 2 and 4 were reserved for VX-970 and vehicle treatment (cyclodextrin). After 21 days of treating mice (3 cycles of treatment), we continued to measure mice for 2 weeks post-treatment. I saw that this combination treatment regimen of TMZ and VX-970 significantly delayed tumor growth in LN229 MGMT- flank tumors relative to TMZ or VX-970 alone (**Figure 6.4A**). In mice bearing LN229 MGMT- shMSH6 flank tumors, there was tumor growth even after the combination of TMZ and ATR inhibitor, without reducing body weight significantly (**Figure 6.4B-C**). Statistical significance between combination treatment and vehicle is marked with an asterisk after performing a 2-way ANOVA, where *** $P \leq 0.001$, **** $P \leq 0.0001$.

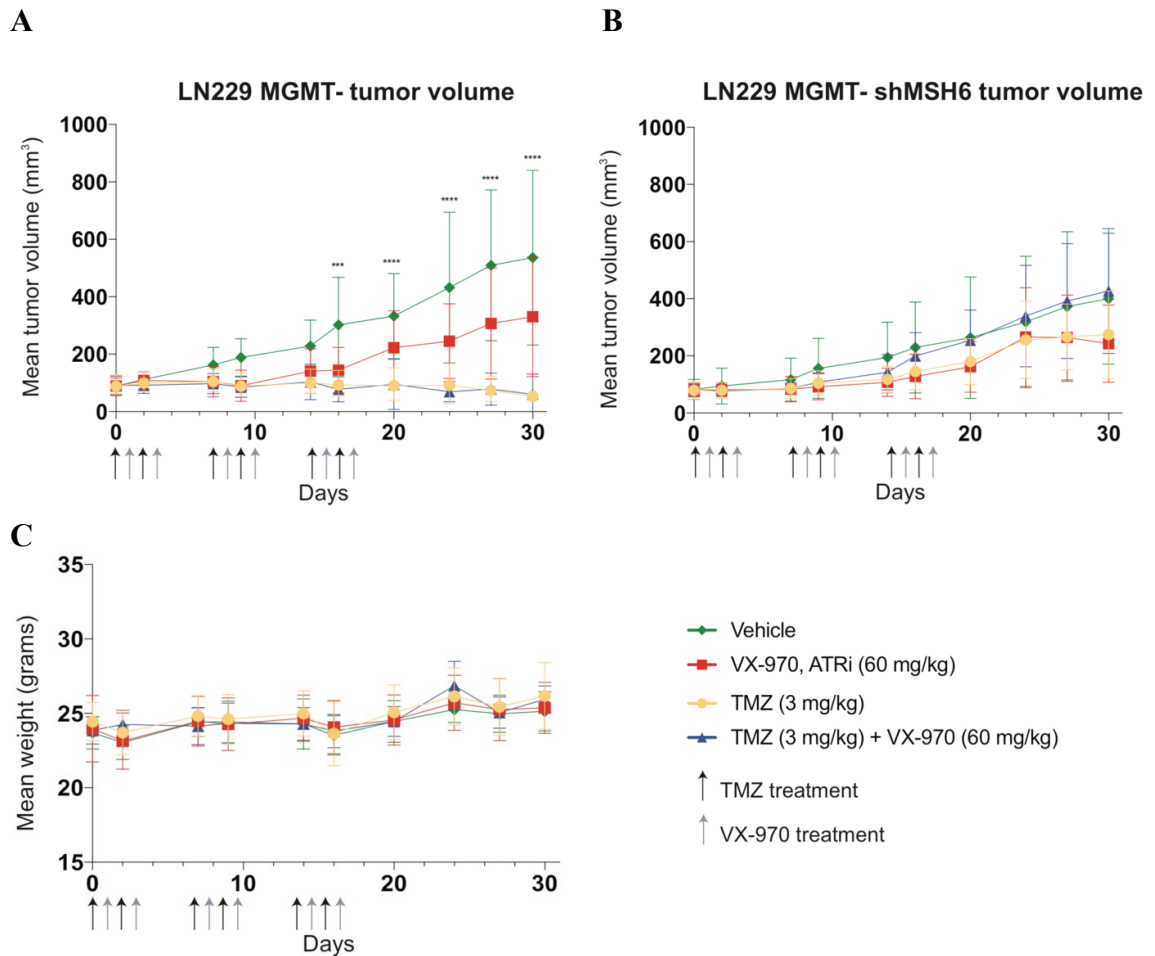


Figure 6.4. *In vivo* shMSH6 MGMT- tumors do not respond to treatment with temozolomide and ATR inhibitor VX-970. (A) Mean tumor volume for mice with MGMT- tumor, where there is a significant difference between the vehicle treated group and the combination of temozolomide and VX-970 group. **(B)** Mean tumor volume for mice with MGMT- shMSH6 tumor, with no significant difference between treatment groups. **(C)** Mean weight of mice showing treatment does not cause significant toxicity over time. *** $p \leq 0.001$, **** $p \leq 0.0001$.

6.3. Discussion

In this chapter, I began to elucidate the underlying mechanisms of DNA repair as it relates to MMR-mediated ATR activation upon TMZ-induced damage. Having used a variety of techniques including immunofluorescence, cell cycle analysis, and *in vivo* studies, I am only just beginning to understand the intricacies of how MMR knockdowns can affect DNA repair pathways.

The data from the flow cytometry cell cycle analysis suggests that MMR pathways are involved in causing G₂/M arrest upon 48 hours of TMZ treatment, as seen in the MMR-proficient cell line. The shMSH2, shMSH6, shMLH1, and shPMS2 cell lines all displayed normal cycling, meaning that the knockdown of these proteins abrogated the G₂/M arrest phenotype seen in the MMR-proficient cells. G₂/M arrest is a sign of ATR activation; thus the lack of G₂/M arrest in the MMR-deficient cells suggests that these MMR proteins are involved in the activation of ATR, as the synergy data shown previously indicated. Additionally, flow cytometry cell cycle experiments comparing the shMMR MGMT- and MGMT+ lines would also provide insight into how *MGMT*-promoter methylation affects cell cycle progression. Finally, experiments where the MMR-deficient cells are treated with TMZ and ATR inhibitor in combination could shed key information into whether the TMZ-induced MMR-deficient cell cycling is truly related to ATR activation. It would be beneficial to proceed with more mechanistic studies to see which proteins are specifically involved in this signaling cascade, from ATR activation to checkpoint signaling.

The immunofluorescence data seemingly matches the flow cytometry data. In the MGMT- cells, I see an increase in γ H2AX over time, suggesting increased double stranded DNA breaks, consistent with previously published data. This alludes to the futile cycling

model, where overtime the TMZ-induced damage with functional MMR leads to single-stranded DNA breaks and ultimately double-stranded DNA breaks. Though I showed destabilization of MSH6 upon MSH2-loss in **Figure 4.8**, the MSH6-deficient cells showed differences in pRPA and γ H2AX levels versus the MSH2-cells, indicating a unique role for each protein in the dimer separately. Unlike the MSH2-MSH6 heterodimer, MSH2-MSH3 is known for repairing larger lesions, which is a possibility for why we see an increase in γ H2AX foci over time and increased G₂/M arrest in the shMSH3 cells. The MSH6-deficient cells showed decreasing pRPA levels over time, indicating a mitigation of replication stress which could also explain how the cells seem to be cycling normally after 48h of TMZ treatment. Given that the shMLH1 and shPMS2 cells cycle normally like the shMSH2 and shMSH6 cells but exhibit increased pRPA and γ H2AX over time, I speculate that these proteins may use different pathway regulators for repairing damage.

In these studies, I used pRPA32 S33 for immunofluorescence studies instead of RPA in its unphosphorylated form. RPA is upstream of ATR and will coat single-stranded DNA to prevent it from re-annealing onto itself. RPA commonly serves as a marker for single-stranded DNA breaks. I was more interested in looking at pRPA as it is directly phosphorylated by ATR, which would indicate ATR activation. It also indicates replication stress, which would allow me to delve into the DNA repair mechanisms surrounding the role of MMR proteins in TMZ-induced ATR activation. Furthermore, I could have tested 53BP1, which is also commonly studied for double-stranded breaks in addition to γ H2AX for its recruitment of proteins involved in nonhomologous end joining¹³⁷. Thus, understanding whether there are increased single-stranded breaks with RPA and staining for 53BP1 can provide an additional layer of mechanistic insight.

Though the synergy assays were in ATR inhibitors other than VX-970, I used VX-970 for its relevant use in current and ongoing clinical trials versus the other inhibitors. I wanted to see whether the mechanism of MMR-deficient resistance to TMZ and ATR inhibitor would hold true *in vivo*. I chose to use MSH6-deficient cells as MSH6 is thought to be the most mutated MMR protein in cancers, and this study would provide novel insight into whether these tumors respond to treatment with TMZ and ATR inhibitor. Further, there is not much of a difference between TMZ monotherapy and TMZ + ATR inhibitor combination in the MGMT- cells. This is unlike what we have seen and published before¹⁰⁹. There should ideally be a larger difference between those two data points.

Additionally, patients with recurrent GBM who are TMZ-resistant after initial chemotherapy tend to develop this resistance due to newly acquired MSH6 mutations⁸⁷. Thus, understanding whether MSH6-deficient cancer cells can be treated with the combination of TMZ and ATR inhibitor *in vivo* could shed light on valuable information for detecting new biomarker therapies for these patients.

Overall, this study begins to elucidate a novel mechanism for the individual roles of MMR proteins in ATR activation upon TMZ treatment in *MGMT*-promoter methylated cancer cells. Our data suggest that MMR proteins besides MSH3 are required for ATR signaling, and that each distinct MMR protein serves a unique function.

7. Chapter 7: Discussion

7.1. Conclusions

In this study, I was first interested in recapitulating a phenotype seen in previously published work from our laboratory to prove that MGMT-status affects ATR signaling upon TMZ treatment. After successfully developing an IP protocol and seeing that pCHK1 levels were different in MGMT- cells vs. MGMT+ cells, I myself was able to demonstrate that MGMT- status affects ATR activation. Then, I began to hypothesize that perhaps ATR activation is linked to the MMR system, given that there have been numerous studies linking the mechanism of TMZ toxicity to MMR futile cycling in MGMT- cells, and that TMZ causes ATR activation in MGMT- cells. Thus, I was interested in understanding whether and how the DNA MMR pathway plays a role in ATR activation upon TMZ treatment, if any. To study my research question, I created 10 isogenic cell lines in the MGMT- and MGMT+ settings that had shRNA knockdowns of the 5 main human MMR proteins: MSH2, MSH3, MSH6, MLH1, and PMS2. Using these shMMR cells, I performed short-term cell viability assays, synergy assays, clonogenic survival assays, and even an *in vivo* experiment to show which MMR proteins are involved in ATR activation. I further went on to attempt studying the intricate mechanisms of MMR in ATR activation through cell cycle analysis with flow cytometry, and immunofluorescence.

My work here shows that MSH2, MSH6, MLH1, and PMS2 are likely implicated in ATR activation upon TMZ treatment in MGMT- cells but MSH3 is not. This work provides significant clinical insight into potential prognostic biomarkers for treating patients. Many glioblastoma patients with MGMT- tumors develop resistance to TMZ, and

though our lab's previously published work shows that these tumors can be sensitized to ATR inhibitors in combination with TMZ, it may not be as straight-forward as we thought. Checking the MMR status of these tumors can help distinguish whether TMZ and ATR inhibitor combinations would be beneficial, as it turns out that tumors with mutations in MSH2, MSH6, MLH1, and PMS2 likely will not respond to this combination therapy. Additionally, these cell lines that I have created have the potential to be used in future studies to find new therapies for patients that can specifically target the MMR-deficiency.

7.2. Further exploration of mechanism

Though I determined which MMR proteins are required for ATR activation and began to delve into mechanistic studies, there is a lot more work to be done here. Flow cytometry data allowed me to visualize cell cycle effects in the shMMR cells, showing that MLH1, PMS2, and MSH6 are responsible for ATR activation as lack of these proteins leads to normal cycling instead of the ATR-activated G₂/M arrest. Immunofluorescence allowed me to track the presence of replication stress and double strand breaks over time, shedding light on the dynamic kinetics of these proteins and other potential pathways and proteins that could be involved in MMR-induced ATR activation. However, these mechanistic studies only begin to scratch the surface and there is more work to be done which would allow me to really understand how MMR is activating ATR. Some of these additional studies that can be used include western blotting, comet assays, and fiber combing assays to understand how TMZ affects MGMT- cells in the MMR-deficient setting.

Western blotting for pCHK1 upon TMZ treatment in the shMMR cells could be another useful metric to visualize if ATR activation is ablated without functional MMR. I performed a western blot seen in the MGMT- cells and shMSH2 MGMT- cells with TMZ over 24 hours and saw that there is a lack of increased ATR in the shMSH2 MGMT- cells over time, and rather a constant level of pCHK1 that remains elevated even upon no treatment (**Figure 7.1**). Further experiments such as this western blot with the other shMMR cell lines could allow me to visualize the effects of ATR activation as it relates to pCHK1 signaling. Additional western blots with a TMZ time course in the MGMT- vs. MGMT- shMMR cells could probe for other proteins known to be implicated in the ATR

pathway such as pRPA. To be confident that the MMR-knockdowns only affect ATR signaling, I could also perform a western blot probing for pCHK2 or pKAP1 which are substrates of ATM; thus if there is no difference in the levels of these phosphorylated proteins over time, one can assume that MMR is only implicated in ATR signaling and not ATM signaling.

Comet assays are typically used to understand whether there are DNA breaks occurring in single cells¹³⁸. Because the immunofluorescence for γ H2AX can show whether there are double-stranded breaks, this assay would be more of a verification that the foci data are reputable. Furthermore, one can use fiber combing for mechanistic studies at the DNA level. DNA fiber combing allows DNA from cells to be stretched evenly on a silane coated glass after 5-Iodo-2'-deoxyuridine (IdU) and 5-chloro-2'-deoxyuridine (CldU) incorporation, which are both thymidine analogs that are incorporated into newly synthesized DNA¹³⁹. This method allows for the visualization and quantification of DNA damage such as replication stress, replication fork progression rate, fork stability, or origin firing. Looking at the mechanisms of MMR in ATR activation with these techniques would provide more insight into how the DNA is being damaged upon TMZ treatment and could offer new perspectives on treatment regimens for MMR-deficient cancer patients.

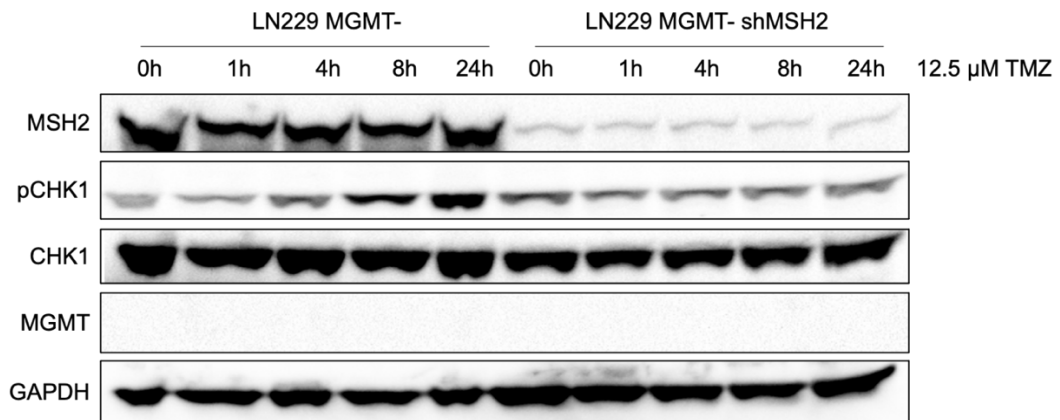


Figure 7.1. Western blot of MGMT- and MGMT- shMSH2 cells upon temozolomide treatment. MGMT- shMSH2 cells have an abrogation of pCHK1 signal over time compared to the MGMT- MMR-proficient cells.

7.3. Other ATR inhibitors, alkylators, and combination therapies

The study here focused mainly on the use of 3 distinct ATR inhibitors: BAY-1895344, AZ-20, and VX-970; however, there are a plethora of other ATR inhibitors available for use. The reason I chose these inhibitors was for their commercial availability and for their successful use in our lab previously. These inhibitors were also used in the previously published paper from our lab that led to the conception of this project, thus I wanted to be certain that these ATR inhibitors would work potently in the LN229 cell lines. To reaffirm the findings from this study, I could have also used AZD6738, as is used widely throughout the literature. AZD6738 is an analog of AZ-20, but is orally bioavailable, which is preferable in the clinic. This ATR inhibitor is strongly selective for ATR compared to the other PI3-like kinases such as ATM or DNA-PK, making it an excellent candidate for use. Moreover, AZD6738 has been shown to work as a monotherapy in certain tumor backgrounds and even in combination with carboplatin, bendamustine, cyclophosphamide, and PARP inhibitors⁹⁹. Because of its ability to synergize with bendamustine, an alkylator, there are higher chances for synergy with temozolomide as well.

Temozolomide was used as the alkylating agent in this study since our group found that it can sensitize MGMT- cells to the combination treatment with ATR inhibitor. However, further studies can be completed using other alkylating agents, both monofunctional and bifunctional, to understand how the MMR pathway is involved upon these various types of damage. For example, in addition to TMZ as a monofunctional alkylator, dacarbazine and procarbazine, and streptozotocin could be tested too³⁴. Bifunctional alkylators such as cyclophosphamide and bendamustine were shown to synergize with the ATR inhibitor AZD6738 and could be studied for the types of damage

they cause, what pathways are activated upon that DNA damage, and whether MMR is involved.

I mainly focused my dissertation research on the combination of TMZ and ATR inhibitors. In the future, understanding the role of DNA damage by other alkylators and DNA repair inhibitors in the context of MGMT-status can help solve the perplexing mysteries of targeted therapies for MMR-deficient tumors.

7.4. Future directions

Here, I unraveled the role of MMR proteins in ATR activation upon TMZ-induced damage. However, this work is not completed and has only just begun. I found that certain MMR proteins are required for ATR signaling, though the brunt of this work shows that ATR inhibitors and TMZ are not a suitable combination in MMR-deficient cancers. The next step is finding a therapy that can treat tumors with MMR-deficiencies.

Ongoing work from our laboratory has led to the development of a new alkylating agent created by student Kingson Lin. This alkylating agent has shown promising data regarding overcoming TMZ alkylator resistance in the MMR-deficient background as a monotherapy. Preliminary data shows that this agent is safe to use *in vivo* as well, with significant tumor reduction in the MMR-deficient tumors compared to TMZ alone. This is an exciting avenue of research that may soon enter clinical trials to potentially provide a new chemotherapy for MMR-deficient cancer patients.

Chapter 8. References

1. Olsson, M. & Lindahl, T. Repair of alkylated DNA in *Escherichia coli*. Methyl group transfer from O6-methylguanine to a protein cysteine residue. *J. Biol. Chem.* **255**, 10569–10571 (1980).
2. Oh, H. K. *et al.* Conformational change in human DNA repair enzyme O6-methylguanine-DNA methyltransferase upon alkylation of its active site by SN1 (indirect-acting) and SN2 (direct-acting) alkylating agents: Breaking a ‘salt-link’? *Biochemistry* **35**, 12259–12266 (1996).
3. Srivenugopal, K. S., Yuan, X.-H., Friedman, H. S. & Ali-Osman, F. *Ubiquitination-Dependent Proteolysis of O 6-Methylguanine-DNA Methyltransferase in Human and Murine Tumor Cells following Inactivation with O 6-Benzylguanine or 1,3-Bis(2-chloroethyl)-1-nitrosourea †.* (1996).
4. Daniels, D. S. *et al.* DNA binding and nucleotide flipping by the human DNA repair protein AGT. *Nat. Struct. Mol. Biol.* **11**, 714–720 (2004).
5. Pegg, A. E., Dolan, M. E. & Moschel, R. C. Structure, Function, and Inhibition of O6-Alkylguanine-DNA Alkyltransferase. *Prog. Nucleic Acid Res. Mol. Biol.* **51**, 167–223 (1995).
6. Weller, M. *et al.* MGMT promoter methylation in malignant gliomas: Ready for personalized medicine? *Nature Reviews Neurology* **6**, 39–51 (2010).
7. Gardiner-Garden, M. & Frommer, M. CpG Islands in vertebrate genomes. *J. Mol. Biol.* **196**, 261–282 (1987).
8. Nakagawachi, T. *et al.* Silencing effect of CpG island hypermethylation and histone modifications on O6-methylguanine-DNA methyltransferase (MGMT) gene expression in human cancer. *Oncogene* **22**, 8835–8844 (2003).

9. Everhard, S. *et al.* Identification of regions correlating MGMT promoter methylation and gene expression in glioblastomas. *Neuro. Oncol.* **11**, 348–356 (2009).
10. Jaeckle, K. A. *et al.* Correlation of tumor O6 methylguanine-DNA methyltransferase levels with survival of malignant astrocytoma patients treated with bis- chloroethylnitrosourea: A Southwest Oncology Group study. *J. Clin. Oncol.* **16**, 3310–3315 (1998).
11. Belanich, M. *et al.* Retrospective study of the correlation between the DNA repair protein alkyltransferase and survival of brain tumor patients treated with carmustine. *Cancer Res.* **56**, 783–788 (1996).
12. Preusser, M. *et al.* Anti-O6-methylguanine-methyltransferase (MGMT) immunohistochemistry in glioblastoma multiforme: Observer variability and lack of association with patient survival impede its use as clinical biomarker. *Brain Pathol.* **18**, 520–532 (2008).
13. Rodriguez, F. J. *et al.* MGMT immunohistochemical expression and promoter methylation in human glioblastoma. *Appl. Immunohistochem. Mol. Morphol.* **16**, 59–65 (2008).
14. Lavon, I. *et al.* Longitudinal assessment of genetic and epigenetic markers in oligodendrogliomas. *Clin. Cancer Res.* **13**, 1429–1437 (2007).
15. Grasbon-Frodl, E. M. *et al.* Intratumoral homogeneity of MGMT promoter hypermethylation as demonstrated in serial stereotactic specimens from anaplastic astrocytomas and glioblastomas. *Int. J. Cancer* **121**, 2458–2464 (2007).
16. Herman, J. G., Graff, J. R., Myöhänen, S., Nelkin, B. D. & Baylin, S. B. Methylation-specific PCR: A novel PCR assay for methylation status of CpG islands. *Proc. Natl. Acad. Sci. U. S. A.* **93**, 9821–9826 (1996).

17. Esteller, M., Hamilton, S. R., Burger, P. C., Baylin, S. B. & Herman, J. G. Inactivation of the DNA repair gene O(6)-methylguanine-DNA methyltransferase by promoter hypermethylation is a common event in primary human neoplasia. *Cancer Res.* **59**, 793–797 (1999).
18. Ogino, S. *et al.* Precision and performance characteristics of bisulfite conversion and real-time PCR (MethyLight) for quantitative DNA methylation analysis. *J. Mol. Diagnostics* **8**, 209–217 (2006).
19. Gerson, S. L. MGMT: Its role in cancer aetiology and cancer therapeutics. *Nature Reviews Cancer* **4**, 296–307 (2004).
20. Hegi, M. E. *et al.* Clinical Trial Substantiates the Predictive Value of O-6-Methylguanine-DNA Methyltransferase Promoter Methylation in Glioblastoma Patients Treated with Temozolomide. *Clin. Cancer Res.* **10**, 1871–1874 (2004).
21. Herrlinger, U. *et al.* Phase II trial of lomustine plus temozolomide chemotherapy in addition to radiotherapy in newly diagnosed glioblastoma: UKT-03. *J. Clin. Oncol.* **24**, 4412–4417 (2006).
22. Crinière, E. *et al.* MGMT prognostic impact on glioblastoma is dependent on therapeutic modalities. *J. Neurooncol.* **83**, 173–179 (2007).
23. Reifenberger, G. *et al.* Predictive impact of MGMT promoter methylation in glioblastoma of the elderly. *Int. J. Cancer* **131**, 1342–1350 (2012).
24. Hegi, M. E. *et al.* MGMT Gene Silencing and Benefit from Temozolomide in Glioblastoma. *N. Engl. J. Med.* (2005). doi:10.1056/nejmoa043331
25. Malmström, A. *et al.* Temozolomide versus standard 6-week radiotherapy versus hypofractionated radiotherapy in patients older than 60 years with glioblastoma: The Nordic randomised, phase 3 trial. *Lancet Oncol.* **13**, 916–926 (2012).
26. Wick, W. *et al.* Temozolomide chemotherapy alone versus radiotherapy alone for malignant astrocytoma in the elderly: The NOA-08 randomised, phase 3 trial. *Lancet Oncol.* **13**, 707–715 (2012).

27. Van Den Bent, M. J. *et al.* MGMT promoter methylation is prognostic but not predictive for outcome to adjuvant PCV chemotherapy in anaplastic oligodendroglial tumors: A report from EORTC brain tumor group study 26951. *J. Clin. Oncol.* **27**, 5881–5886 (2009).
28. Yu, W., Zhang, L., Wei, Q. & Shao, A. O6-Methylguanine-DNA Methyltransferase (MGMT): Challenges and New Opportunities in Glioma Chemotherapy. *Frontiers in Oncology* **9**, 1547 (2020).
29. Schold, S. C. *et al.* O6-benzylguanine suppression of O6-alkylguanine-DNA alkyltransferase in anaplastic gliomas. *Neuro. Oncol.* **6**, 28–32 (2004).
30. Koch, D., Hundsberger, T., Boor, S. & Kaina, B. Local intracerebral administration of O6-benzylguanine combined with systemic chemotherapy with temozolomide of a patient suffering from a recurrent glioblastoma. *J. Neurooncol.* **82**, 85–89 (2007).
31. Ranson, M. *et al.* Lomeguatrib, a potent inhibitor of O6-alkylguanine-DNA-alkyltransferase: Phase I safety, pharmacodynamic, and pharmacokinetic trial and evaluation in combination with temozolomide in patients with advanced solid tumors. *Clin. Cancer Res.* **12**, 1577–1584 (2006).
32. Brookes, P. The early history of the biological alkylating agents, 1918-1968. *Mutat. Res. - Fundam. Mol. Mech. Mutagen.* **233**, 3–14 (1990).
33. Khalife, O., Muhammad, M., Kenj, M. & Salamoon, M. Alkylating Agents. in *Cyclophosphamide: Clinical Pharmacology, Uses and Potential Adverse Effects* 1–19 (National Institute of Diabetes and Digestive and Kidney Diseases, 2015). doi:10.1201/b16867-6
34. Fu, D., Calvo, J. A. & Samson, L. D. Balancing repair and tolerance of DNA damage caused by alkylating agents. *Nature Reviews Cancer* **12**, 104–120 (2012).
35. Colvin, M. Alkylating agents. *Holland-Frei Cancer Medicine. 6th edition.* **15**, 317–324 (2002).

36. Goodman, L. S. *et al.* Nitrogen mustard therapy: Use of Methyl-Bis(Beta-Chloroethyl)amine Hydrochloride and Tris(Beta-Chloroethyl)amine Hydrochloride for Hodgkin's Disease, Lymphosarcoma, Leukemia and Certain Allied and Miscellaneous Disorders. *J. Am. Med. Assoc.* **132**, 126–132 (1946).
37. Ballschmiter, K. Pattern and sources of naturally produced organohalogens in the marine environment: Biogenic formation of organohalogens. in *Chemosphere* **52**, 313–324 (Chemosphere, 2003).
38. Hecht, S. S. DNA adduct formation from tobacco-specific N-nitrosamines. *Mutat. Res. - Fundam. Mol. Mech. Mutagen.* **424**, 127–142 (1999).
39. Hamilton, J. T. G., McRoberts, W. C., Keppler, F., Kalin, R. M. & Harper, D. B. Chloride methylation by plant pectin: An efficient environmentally significant process. *Science (80-.)*. **301**, 206–209 (2003).
40. Rydberg, B. & Lindahl, T. Nonenzymatic methylation of DNA by the intracellular methyl group donor S-adenosyl-L-methionine is a potentially mutagenic reaction. *EMBO J.* **1**, 211–216 (1982).
41. Taverna, P. & Sedgwick, B. Generation of an endogenous DNA-methylating agent by nitrosation in *Escherichia coli*. *J. Bacteriol.* **178**, 5105–5111 (1996).
42. Kufe, D. W. *et al.* Holland-Frei Cancer Medicine, 6th edition. (2003).
43. Newlands, E. S., Stevens, M. F. G., Wedge, S. R., Wheelhouse, R. T. & Brock, C. Temozolomide: A review of its discovery, chemical properties, pre-clinical development and clinical trials. *Cancer Treat. Rev.* **23**, 35–61 (1997).
44. Singh, N., Miner, A., Hennis, L. & Mittal, S. Mechanisms of temozolomide resistance in glioblastoma - a comprehensive review. *Cancer Drug Resistance* **4**, 17–43 (2021).
45. Arora, A. & Somasundaram, K. Glioblastoma vs temozolomide: can the red queen race be won? *Cancer Biology and Therapy* **20**, 1083–1090 (2019).

46. Stupp, R., Brada, M., van den Bent, M. J., Tonn, J. C. & Pentheroudakis, G. High-grade glioma: ESMO clinical practice guidelines for diagnosis, treatment and follow-up. *Ann. Oncol.* **25**, 93–101 (2014).
47. Mohammad, S. N. & Hopfinger, A. J. Chemical reactivity of a methyldiazonium ion with nucleophilic centers of DNA bases. *J. Theor. Biol.* **87**, 401–419 (1980).
48. Friedman, H. S., Kerby, T. & Calvert, H. Temozolomide and treatment of malignant glioma. *Clinical Cancer Research* **6**, 2585–2597 (2000).
49. Stupp, R. *et al.* Radiotherapy plus Concomitant and Adjuvant Temozolomide for Glioblastoma. *N. Engl. J. Med.* **352**, 987–996 (2005).
50. Zhang, L. *et al.* Inactivation of DNA repair gene O6-methylguanine-DNA methyltransferase by promoter hypermethylation and its relation to p53 mutations in esophageal squamous cell carcinoma. *Carcinogenesis* **24**, 1039–1044 (2003).
51. Thomas, A. *et al.* Temozolomide in the Era of Precision Medicine. (2017). doi:10.1158/0008-5472.CAN-16-2983
52. Wick, W. & Platten, M. Understanding and targeting alkylator resistance in glioblastoma. *Cancer Discov.* **4**, 1120–1122 (2014).
53. Xie, Q., Mittal, S. & Berens, M. E. Targeting adaptive glioblastoma: An overview of proliferation and invasion. *Neuro-Oncology* **16**, 1575–1584 (2014).
54. Giglia-Mari, G., Zotter, A. & Vermeulen, W. DNA damage response. *Cold Spring Harb. Perspect. Biol.* **3**, 1–19 (2011).
55. Lindahl, T. Instability and decay of the primary structure of DNA. *Nature* (1993). doi:10.1038/362709a0
56. Weber, S. Light-driven enzymatic catalysis of DNA repair: A review of recent biophysical studies on photolyase. *Biochimica et Biophysica Acta - Bioenergetics* **1707**, 1–23 (2005).

57. Almeida, K. H. & Sobol, R. W. A unified view of base excision repair: Lesion-dependent protein complexes regulated by post-translational modification. *DNA Repair* **6**, 695–711 (2007).
58. Hegde, M. L., Hazra, T. K. & Mitra, S. Early steps in the DNA base excision/single-strand interruption repair pathway in mammalian cells. *Cell Research* **18**, 27–47 (2008).
59. Caldecott, K. W. Mammalian single-strand break repair: Mechanisms and links with chromatin. *DNA Repair (Amst)*. **6**, 443–453 (2007).
60. El-Khamisy, S. F. *et al.* Synergistic decrease of DNA single-strand break repair rates in mouse neural cells lacking both Tdp1 and aprataxin. *DNA Repair (Amst)*. **8**, 760–766 (2009).
61. Gueven, N. *et al.* Aprataxin, a novel protein that protects against genotoxic stress. *Hum. Mol. Genet.* **13**, 1081–1093 (2004).
62. Hoeijmakers, J. H. J. Nucleotide excision repair II: from yeast to mammals. *Trends in Genetics* **9**, 211–217 (1993).
63. Gillet, L. C. J. & Schärer, O. D. Molecular mechanisms of mammalian global genome nucleotide excision repair. *Chemical Reviews* **106**, 253–276 (2006).
64. Ogi, T. *et al.* Three DNA Polymerases, Recruited by Different Mechanisms, Carry Out NER Repair Synthesis in Human Cells. *Mol. Cell* **37**, 714–727 (2010).
65. Moser, J. *et al.* Sealing of Chromosomal DNA Nicks during Nucleotide Excision Repair Requires XRCC1 and DNA Ligase III α in a Cell-Cycle-Specific Manner. *Mol. Cell* **27**, 311–323 (2007).
66. Helleday, T., Lo, J., van Gent, D. C. & Engelward, B. P. DNA double-strand break repair: From mechanistic understanding to cancer treatment. *DNA Repair (Amst)*. **6**, 923–935 (2007).
67. Wyman, C. & Kanaar, R. DNA double-strand break repair: All's well that ends well. *Annual Review of Genetics* **40**, 363–383 (2006).

68. Cahill, D., Connor, B. & Carney, J. P. Mechanisms of eukaryotic DNA double strand break repair. *Frontiers in Bioscience* **11**, 1958–1976 (2006).
69. Li, G. M. Mechanisms and functions of DNA mismatch repair. *Cell Research* **18**, 85–98 (2008).
70. Prolla, T. A., Christie, D. M. & Liskay, R. M. Dual requirement in yeast DNA mismatch repair for MLH1 and PMS1, two homologs of the bacterial mutL gene. *Mol. Cell. Biol.* **14**, 407–415 (1994).
71. Li, G. M. & Modrich, P. Restoration of mismatch repair to nuclear extracts of H6 colorectal tumor cells by a heterodimer of human MutL homologs. *Proc. Natl. Acad. Sci. U. S. A.* **92**, 1950–1954 (1995).
72. Drummond, J. T., Li, G. M., Longley, M. J. & Modrich, P. Isolation of an hMSH2-p160 heterodimer that restores DNA mismatch repair to tumor cells. *Science* (80-). **268**, 1909–1912 (1995).
73. Acharya, S. *et al.* hMSH2 forms specific mispair-binding complexes with hMSH3 and hMSH6. *Proc. Natl. Acad. Sci. U. S. A.* **93**, 13629–13634 (1996).
74. Hsieh, P. & Zhang, Y. The Devil is in the details for DNA mismatch repair. *Proceedings of the National Academy of Sciences of the United States of America* **114**, 3552–3554 (2017).
75. Hombauer, H., Campbell, C. S., Smith, C. E., Desai, A. & Kolodner, R. D. Visualization of eukaryotic DNA mismatch repair reveals distinct recognition and repair intermediates. *Cell* **147**, 1040–1053 (2011).
76. Zhang, Y. *et al.* Reconstitution of 5'-directed human mismatch repair in a purified system. *Cell* **122**, 693–705 (2005).
77. Goellner, E. M., Putnam, C. D. & Kolodner, R. D. Exonuclease 1-dependent and independent mismatch repair. *DNA Repair (Amst)*. **32**, 24–32 (2015).

78. Pluciennik, A. *et al.* PCNA function in the activation and strand direction of MutL α endonuclease in mismatch repair. *Proc. Natl. Acad. Sci. U. S. A.* **107**, 16066–16071 (2010).
79. Wang, J. Y. J. & Edelmann, W. Mismatch repair proteins as sensors of alkylation DNA damage. *Cancer Cell* **9**, 417–418 (2006).
80. Nowosielska, A. & Marinus, M. G. DNA mismatch repair-induced double-strand breaks. *DNA Repair (Amst)*. **7**, 48–56 (2008).
81. Tuna, M. & Amos, C. I. Genomic sequencing in cancer. *Cancer Letters* **340**, 161–170 (2013).
82. Atkin, N. B. Microsatellite instability. *Cytogenet. Cell Genet.* **92**, 177–181 (2001).
83. Boland, C. R. & Goel, A. Microsatellite Instability in Colorectal Cancer. *Gastroenterology* **138**, 2073 (2010).
84. Popat, S., Hubner, R. & Houlston, R. S. Systematic review of microsatellite instability and colorectal cancer prognosis. *Journal of Clinical Oncology* **23**, 609–618 (2005).
85. Kastrinos, F. *et al.* Risk of pancreatic cancer in families with Lynch syndrome. *JAMA - J. Am. Med. Assoc.* **302**, 1790–1795 (2009).
86. Buecher, B. *et al.* Role of microsatellite instability in the management of colorectal cancers. *Digestive and Liver Disease* **45**, 441–449 (2013).
87. McCarthy, A. J. *et al.* Heterogenous loss of mismatch repair (MMR) protein expression: a challenge for immunohistochemical interpretation and microsatellite instability (MSI) evaluation. *J. Pathol. Clin. Res.* **5**, 115–129 (2019).
88. McFaline-Figueroa, J. L. *et al.* Minor changes in expression of the mismatch repair protein MSH2 exert a major impact on glioblastoma response to temozolomide. *Cancer Res.* **75**, 3127–3138 (2015).

89. Ericson, K. M., Isinger, A. P., Isfoss, B. L. & Nilbert, M. C. Low frequency of defective mismatch repair in a population-based series of upper urothelial carcinoma. *BMC Cancer* **5**, (2005).
90. Ciccica, A. & Elledge, S. J. The DNA Damage Response: Making It Safe to Play with Knives. *Molecular Cell* **40**, 179–204 (2010).
91. Flynn, R. L. & Zou, L. ATR: A master conductor of cellular responses to DNA replication stress. *Trends in Biochemical Sciences* **36**, 133–140 (2011).
92. Cimprich, K. A. & Cortez, D. ATR: An essential regulator of genome integrity. *Nature Reviews Molecular Cell Biology* **9**, 616–627 (2008).
93. Shiotani, B. *et al.* Two Distinct Modes of ATR Activation Orchestrated by Rad17 and Nbs1. *Cell Rep.* **3**, 1651–1662 (2013).
94. Zou, L. & Elledge, S. J. Sensing DNA damage through ATRIP recognition of RPA-ssDNA complexes. *Science (80-.)*. **300**, 1542–1548 (2003).
95. Kumagai, A., Lee, J., Yoo, H. Y. & Dunphy, W. G. TopBP1 activates the ATR-ATRIP complex. *Cell* **124**, 943–955 (2006).
96. Navadgi-Patil, V. M. & Burgers, P. M. The Unstructured C-Terminal Tail of the 9-1-1 Clamp Subunit Ddc1 Activates Mec1/ATR via Two Distinct Mechanisms. *Mol. Cell* **36**, 743–753 (2009).
97. Zou, L., Cortez, D. & Elledge, S. J. Regulation of ATR substrate selection by Rad17-dependent loading of Rad9 complexes onto chromatin. *Genes Dev.* **16**, 198–208 (2002).
98. Leung-Pineda, V., Ryan, C. E. & Piwnicka-Worms, H. Phosphorylation of Chk1 by ATR Is Antagonized by a Chk1-Regulated Protein Phosphatase 2A Circuit. *Mol. Cell. Biol.* **26**, 7529–7538 (2006).
99. Karnitz, L. M. & Zou, L. Molecular pathways: Targeting ATR in cancer therapy. *Clin. Cancer Res.* **21**, 4780–4785 (2015).

100. Shiotani, B. & Zou, L. ATR signaling at a glance. *J. Cell Sci.* **122**, 301–304 (2009).
101. Lyer, R. R., Pluciennik, A., Burdett, V. & Modrich, P. L. DNA mismatch repair: Functions and mechanisms. *Chemical Reviews* **106**, 302–323 (2006).
102. Sarkaria, J. N. *et al.* Inhibition of ATM and ATR kinase activities by the radiosensitizing agent, caffeine. *Cancer Res.* **59**, 4375–4382 (1999).
103. Charrier, J. D. *et al.* Discovery of Potent and Selective Inhibitors of Ataxia Telangiectasia Mutated and Rad3 Related (ATR) Protein Kinase as Potential Anticancer Agents. *J. Med. Chem.* **54**, 2320–2330 (2011).
104. Fokas, E. *et al.* Targeting ATR in DNA damage response and cancer therapeutics. *Cancer Treatment Reviews* **40**, 109–117 (2014).
105. Foote, K. M. *et al.* Discovery of 4-{4-[(3R)-3-methylmorpholin-4-yl]-6-[1-(methylsulfonyl) cyclopropyl]pyrimidin-2-yl}-1H-indole (AZ20): A potent and selective inhibitor of ATR protein kinase with monotherapy in vivo antitumor activity. *J. Med. Chem.* **56**, 2125–2138 (2013).
106. Wengner, A. M. *et al.* The novel ATR inhibitor BAY 1895344 is efficacious as monotherapy and combined with DNA damage-inducing or repair-compromising therapies in preclinical cancer models. *Mol. Cancer Ther.* **19**, 26–38 (2020).
107. Xiao, Y. *et al.* Identification of preferred chemotherapeutics for combining with a CHK1 Inhibitor. *Mol. Cancer Ther.* **12**, 2285–2295 (2013).
108. Huntoon, C. J. *et al.* ATR inhibition broadly sensitizes ovarian cancer cells to chemotherapy independent of BRCA status. *Cancer Res.* **73**, 3683–3691 (2013).
109. Jackson, C. B. *et al.* Temozolomide sensitizes MGMT-deficient tumor cells to ATR inhibitors. *Cancer Res.* canres.3394.2018 (2019). doi:10.1158/0008-5472.CAN-18-3394.

110. Yoshioka, K. ichi, Yoshioka, Y. & Hsieh, P. ATR Kinase Activation Mediated by MutSa and MutLa in Response to Cytotoxic O6-Methylguanine Adducts. *Mol. Cell* **22**, 501–510 (2006).
111. Di Veroli, G. Y. *et al.* Combenefit: An interactive platform for the analysis and visualization of drug combinations. *Bioinformatics* **32**, 2866–2868 (2016).
112. Oeck, S. *et al.* The Focinator v2-0-Graphical Interface, Four Channels, Colocalization Analysis and Cell Phase Identification. *Radiat. Res.* **188**, 114–120 (2017).
113. Ishii, N. *et al.* Frequent Co-alterations of TP53, p16/CDKN2A, p14(ARF), PTEN tumor suppressor genes in human glioma cell lines. *Brain Pathol.* **9**, 469–479 (1999).
114. Bernd, K., Fritz, G., Mitra, S. & Coquerelle, T. Transfection and expression of human O6-methylguanine-DNA methyltransferase (MGMT) cDNA in chinese hamster cells: The role of MGMT in protection against the genotoxic effects of alkylating agents. *Carcinogenesis* **12**, 1857–1867 (1991).
115. D’Atri, S. *et al.* Involvement of the mismatch repair system in temozolomide-induced apoptosis. *Mol. Pharmacol.* **54**, 334–341 (1998).
116. Franken, N. A. P., Rodermond, H. M., Stap, J., Haveman, J. & van Bree, C. Clonogenic assay of cells in vitro. *Nat. Protoc.* *2006 15* **1**, 2315–2319 (2006).
117. Allen, M., Bjerke, M., Edlund, H., Nelander, S. & Westermarck, B. Origin of the U87MG glioma cell line: Good news and bad news. *Sci. Transl. Med.* **8**, (2016).
118. Stein, G. H. T98G: An anchorage-independent human tumor cell line that exhibits stationary phase G1 arrest in vitro. *J. Cell. Physiol.* **99**, 43–54 (1979).
119. Lee, S. Y. Temozolomide resistance in glioblastoma multiforme. *Genes and Diseases* **3**, 198–210 (2016).
120. Torsvik, A. *et al.* U-251 revisited: Genetic drift and phenotypic consequences of long-term cultures of glioblastoma cells. *Cancer Med.* **3**, 812–824 (2014).

121. Caporali, S. *et al.* DNA damage induced by temozolomide signals to both ATM and ATR: Role of the mismatch repair system. *Mol. Pharmacol.* **66**, 478–491 (2004).
122. Paddison, P. J., Caudy, A. A., Bernstein, E., Hannon, G. J. & Conklin, D. S. Short hairpin RNAs (shRNAs) induce sequence-specific silencing in mammalian cells. *Genes Dev.* **16**, 948–958 (2002).
123. Brummelkamp, T. R., Bernards, R. & Agami, R. A system for stable expression of short interfering RNAs in mammalian cells. *Science (80-.)*. **296**, 550–553 (2002).
124. Bae, D. H. *et al.* Design and Testing of Vector-Producing HEK293T Cells Bearing a Genomic Deletion of the SV40 T Antigen Coding Region. *Mol. Ther. - Methods Clin. Dev.* **18**, 631–638 (2020).
125. Wang, X. & McManus, M. Lentivirus production. *J. Vis. Exp.* **32**, 1499 (2009).
126. Chakraborty, U., Dinh, T. A. & Alani, E. Genomic instability promoted by overexpression of mismatch repair factors in yeast: A model for understanding cancer progression. *Genetics* **209**, 439–456 (2018).
127. Kim, K. H. & Sederstrom, J. M. Assaying cell cycle status using flow cytometry. *Curr. Protoc. Mol. Biol.* **2015**, 28.6.1-28.6.11 (2015).
128. Shen, Y., Vignali, P. & Wang, R. Rapid Profiling Cell Cycle by Flow Cytometry Using Concurrent Staining of DNA and Mitotic Markers. *BIO-PROTOCOL* **7**, (2017).
129. Im, K., Mareninov, S., Diaz, M. F. P. & Yong, W. H. An introduction to performing immunofluorescence staining. in *Methods in Molecular Biology* **1897**, 299–311 (NIH Public Access, 2019).
130. Kuo Linda J. & Yang Li-Xi. γ H2AX - A Novel Biomarker for DNA Double-strand Breaks. *In Vivo (Brooklyn)*. **22**, 305–310 (2008).
131. Paull, T. T. *et al.* A critical role for histone H2AX in recruitment of repair factors to nuclear foci after DNA damage. *Curr. Biol.* **10**, 886–895 (2000).

132. Collins, P. L. *et al.* DNA double-strand breaks induce H2Ax phosphorylation domains in a contact-dependent manner. *Nat. Commun.* **11**, 1–9 (2020).
133. Yates, L. A. *et al.* A structural and dynamic model for the assembly of Replication Protein A on single-stranded DNA. *Nat. Commun.* **9**, 1–14 (2018).
134. Murphy, A. K. *et al.* Phosphorylated RPA recruits PALB2 to stalled DNA replication forks to facilitate fork recovery. *J. Cell Biol.* **206**, 493–507 (2014).
135. Vassin, V. M., Anantha, R. W., Sokolova, E., Kanner, S. & Borowiec, J. A. Human RPA phosphorylation by ATR stimulates DNA synthesis and prevents ssDNA accumulation during DNA-replication stress. *J. Cell Sci.* **122**, 4070–4080 (2009).
136. Klein, S. The use of biorelevant dissolution media to forecast the in vivo performance of a drug. *AAPS Journal* **12**, 397–406 (2010).
137. Mirza-Aghazadeh-Attari, M. *et al.* 53BP1: A key player of DNA damage response with critical functions in cancer. *DNA Repair* **73**, 110–119 (2019).
138. Olive, P. L. & Banáth, J. P. The comet assay: A method to measure DNA damage in individual cells. *Nat. Protoc.* **1**, 23–29 (2006).
139. Kaykov, A., Taillefumier, T., Bensimon, A. & Nurse, P. Molecular Combing of Single DNA Molecules on the 10 Megabase Scale. *Sci. Rep.* **6**, 1–9 (2016).